

A decorative, classical-style column with a capital, rendered in a golden-brown color, is positioned on the left side of the slide.

Adaptive Differential Discontinuous High-Order Methods in CFD

**Z.J. Wang (zjwang.com)
Spahr Professor and Chair
Department of Aerospace Engineering
University of Kansas, Lawrence, U.S.A.**





Outline

➤ Lecture 1:

- Introduction and review
- Extending a 1st order scheme to higher-order
 - Discontinuous Galerkin
 - Spectral volume
 - Spectral difference
 - Correction procedure via reconstruction or flux reconstruction

➤ Lecture 2:

- Extension to multiple dimensions
- Extension to viscous problems



Outline (cont.)

- Lecture 3:
 - Boundary conditions
 - Shock capturing
 - Limiter
 - Artificial viscosity
- Lecture 4:
 - Solution based hp-adaptations
 - Sample demonstration problems
 - Remaining research issues



Outline

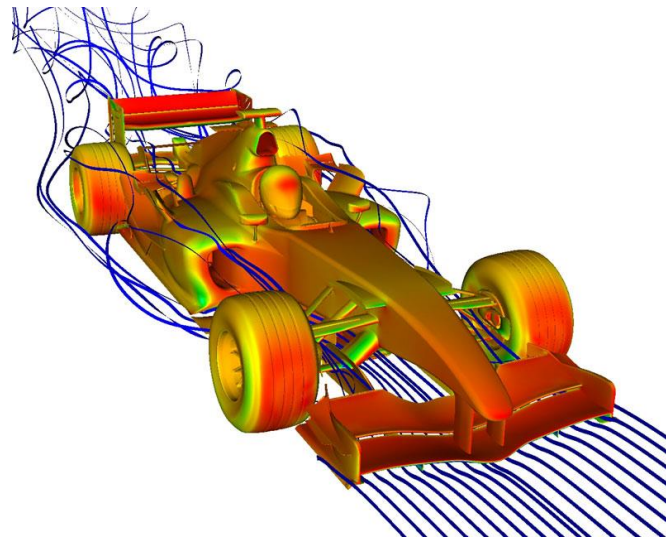
➤ Lecture 1:

- Introduction and review
- Extending a 1st order scheme to higher-order
 - Discontinuous Galerkin
 - Spectral volume
 - Spectral difference
 - Correction procedure via reconstruction or flux reconstruction



My Philosophy

- To present key ideas in 1D, not dwell on implementation details
- To show how these ideas were developed so you can develop new ones
- Highlight the similarities and differences, pros and cons wherever possible





Introduction



Navier-Stokes Equations 3 - dimensional - unsteady

Glenn
Research
Center

Coordinates: (x,y,z)	Time: t	Pressure: p	Heat Flux: q
Velocity Components: (u,v,w)	Density: ρ	Stress: τ	Reynolds Number: Re
	Total Energy: Et		Prandtl Number: Pr

Continuity: $\frac{\partial \rho}{\partial t} + \frac{\partial(\rho u)}{\partial x} + \frac{\partial(\rho v)}{\partial y} + \frac{\partial(\rho w)}{\partial z} = 0$

X - Momentum: $\frac{\partial(\rho u)}{\partial t} + \frac{\partial(\rho u^2)}{\partial x} + \frac{\partial(\rho uv)}{\partial y} + \frac{\partial(\rho uw)}{\partial z} = -\frac{\partial p}{\partial x} + \frac{1}{Re_r} \left[\frac{\partial \tau_{xx}}{\partial x} + \frac{\partial \tau_{xy}}{\partial y} + \frac{\partial \tau_{xz}}{\partial z} \right]$

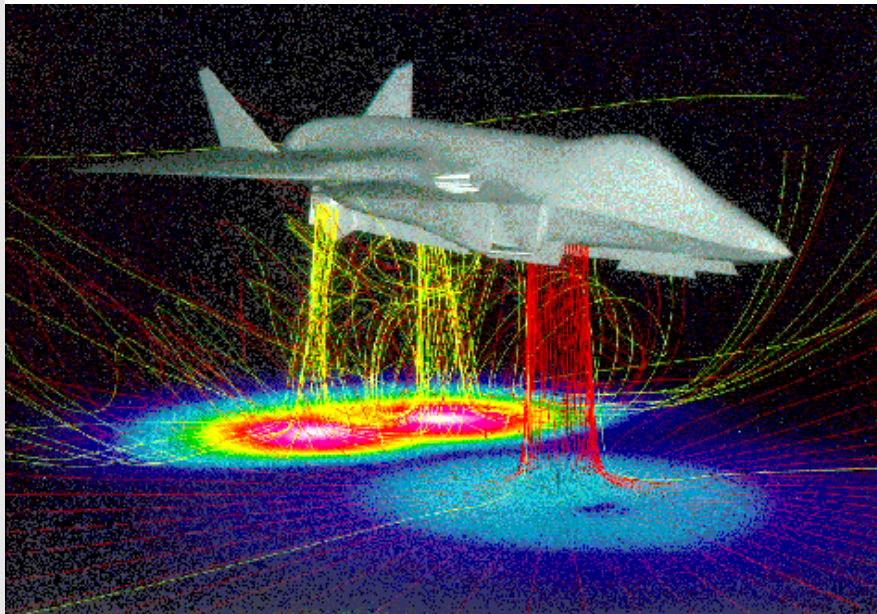
Y - Momentum: $\frac{\partial(\rho v)}{\partial t} + \frac{\partial(\rho uv)}{\partial x} + \frac{\partial(\rho v^2)}{\partial y} + \frac{\partial(\rho vw)}{\partial z} = -\frac{\partial p}{\partial y} + \frac{1}{Re_r} \left[\frac{\partial \tau_{xy}}{\partial x} + \frac{\partial \tau_{yy}}{\partial y} + \frac{\partial \tau_{yz}}{\partial z} \right]$

Z - Momentum: $\frac{\partial(\rho w)}{\partial t} + \frac{\partial(\rho uw)}{\partial x} + \frac{\partial(\rho vw)}{\partial y} + \frac{\partial(\rho w^2)}{\partial z} = -\frac{\partial p}{\partial z} + \frac{1}{Re_r} \left[\frac{\partial \tau_{xz}}{\partial x} + \frac{\partial \tau_{yz}}{\partial y} + \frac{\partial \tau_{zz}}{\partial z} \right]$

Energy: $\frac{\partial(E_t)}{\partial t} + \frac{\partial(uE_t)}{\partial x} + \frac{\partial(vE_t)}{\partial y} + \frac{\partial(wE_t)}{\partial z} = -\frac{\partial(u p)}{\partial x} - \frac{\partial(v p)}{\partial y} - \frac{\partial(w p)}{\partial z} - \frac{1}{Re_r Pr_r} \left[\frac{\partial q_x}{\partial x} + \frac{\partial q_y}{\partial y} + \frac{\partial q_z}{\partial z} \right] + \frac{1}{Re_r} \left[\frac{\partial}{\partial x} (u \tau_{xx} + v \tau_{xy} + w \tau_{xz}) + \frac{\partial}{\partial y} (u \tau_{xy} + v \tau_{yy} + w \tau_{yz}) + \frac{\partial}{\partial z} (u \tau_{xz} + v \tau_{yz} + w \tau_{zz}) \right]$



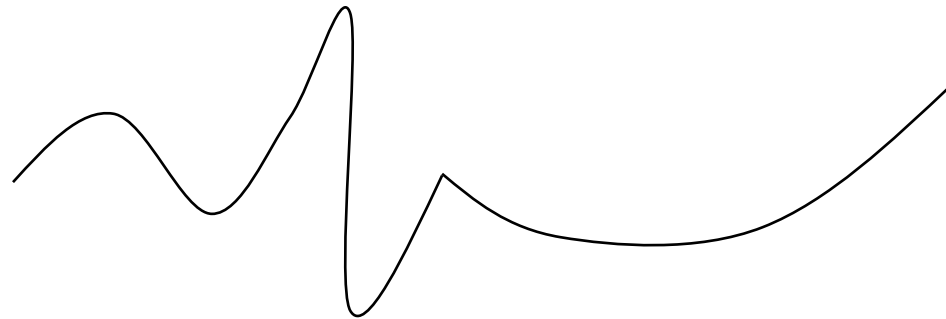
$$\frac{\partial u}{\partial t} + c \frac{\partial u}{\partial x} = 0, c > 0$$





Introduction – Approximation

- How to approximate an unknown solution with possibly infinite number of degrees of freedom (nDOFs) with a limited nDOFs



- Piece-wise polynomials (FD, FV, FE, ...)
- A global expansion composed of discrete sine and cosine functions (spectral method)
- A global high-order polynomial?
- ...



Degrees of Freedom

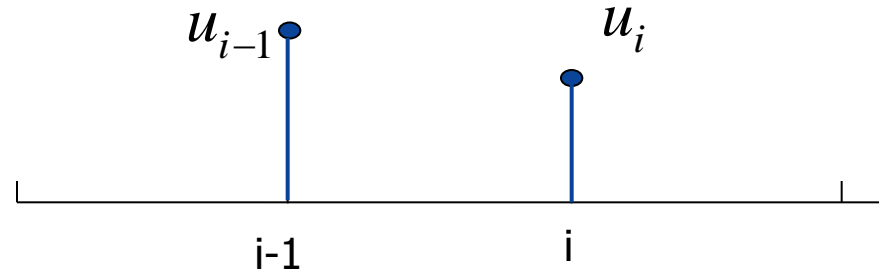
- Finite difference (FD)
 - Nodal values on a set of discrete points
 - Local polynomial approximation
 - Discontinuous?
- Finite volume (FV)
 - Control volume averages
 - Local polynomial approximation
 - Discontinuous
- Finite element (FE)
 - Nodal or modal
 - Local polynomial approximation
 - Either continuous or discontinuous



Let's Start from the Very Beginning

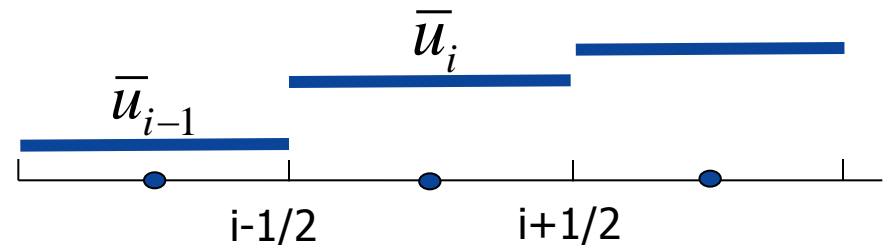
- 1st order FD upwind scheme

$$\frac{\partial u_i}{\partial t} + c \frac{(u_i - u_{i-1})}{\Delta x} = 0$$



- 1st order FV upwind scheme

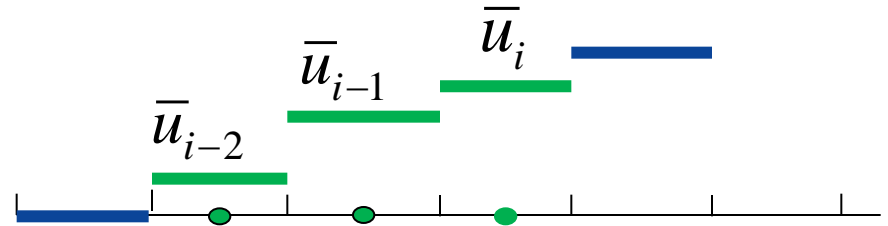
$$\frac{\partial \bar{u}_i}{\partial t} + c \frac{(\bar{u}_i - \bar{u}_{i-1})}{\Delta x} = 0$$



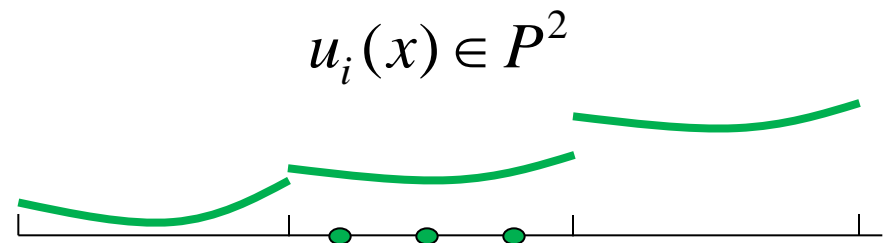


How to Extend to Higher Order

- Extend the stencil



- Add more degrees of freedom in element





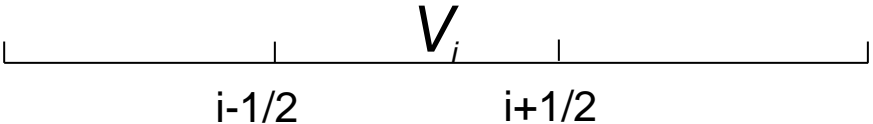
Extending Stencil vs. More Internal DOFs

- **Simple formulation and easy to understand for structured mesh**
- **Complicated boundary conditions: high-order one-sided difference on uniform grids may be unstable**
- **Not compact**
- **Boundary conditions trivial with uniform accuracy**
- **Non-uniform and unstructured grids**
 - Reconstruction universal
- **Scalable**
 - Communication through immediate neighbor



Review of the Godunov FV Method

Consider

$$\frac{\partial u}{\partial t} + \frac{\partial f(u)}{\partial x} = 0$$


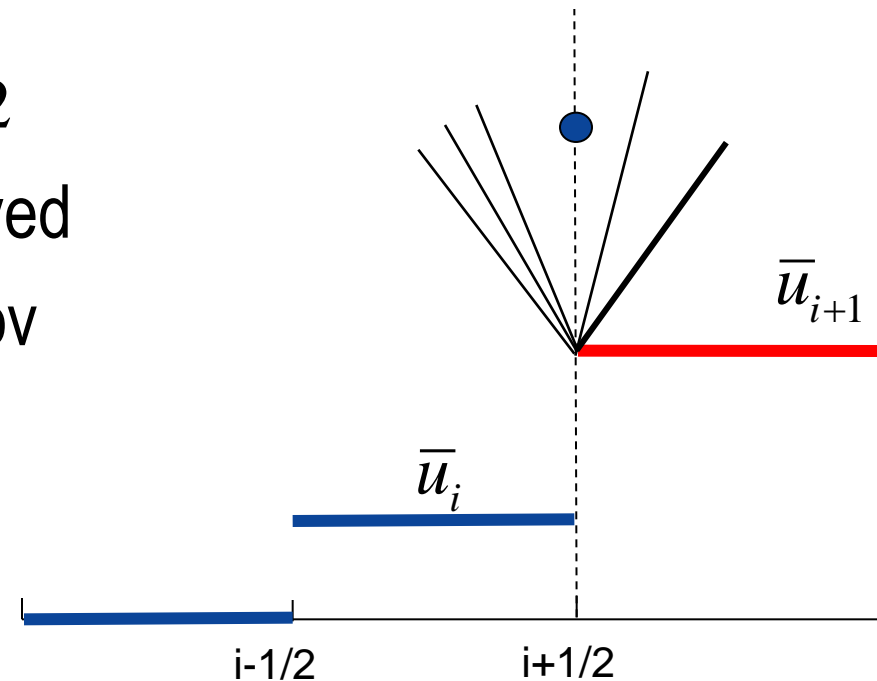
Integrate in V_i

$$\begin{aligned} \int_{V_i} \left(\frac{\partial u}{\partial t} + \frac{\partial f}{\partial x} \right) dx &= \frac{\partial \bar{u}_i}{\partial t} \Delta x_i + \int_{i-1/2}^{i+1/2} \frac{\partial f}{\partial x} dx \\ &= \frac{\partial \bar{u}_i}{\partial t} \Delta x_i + (f_{i+1/2} - f_{i-1/2}) = 0 \end{aligned}$$



Godunov FV Method (cont.)

- Assume the solution is piece-wise constant, or a degree 0 polynomial.
- However, a new problem is created. The solution is discontinuous at the interface
- How to compute the flux?
$$f_{i+1/2} = [f(\bar{u}_i) + f(\bar{u}_{i+1})]/2$$
- A “shock-tube” problem solved to obtain the flux by Godunov
- Other Riemann solvers developed for efficiency





Discontinuous Galerkin Method

- Originally developed in 1970s and popular since 1990s (Cockburn & Shu, Bassi & Rebay, ...)
- Each cell has enough DOFs so that neighboring data are not used in reconstructing a higher-degree polynomial
- Assume we choose a , b and c as the DOFs so that

$$U_i(x) = a_i + b_i x + c_i x^2, \quad x \in V_i$$



Discontinuous Galerkin Method (cont.)

- However, at each cell we need to update 3 DOFs! How?
- Finite volume update

$$\int_{V_i} 1 * \left(\frac{\partial U}{\partial t} + \frac{\partial f}{\partial x} \right) dx = 0$$

- Two more equations based on weighed residual

$$\int_{V_i} x * \left(\frac{\partial U}{\partial t} + \frac{\partial f}{\partial x} \right) dx = 0 \quad \int_{V_i} x^2 * \left(\frac{\partial U}{\partial t} + \frac{\partial f}{\partial x} \right) dx = 0$$

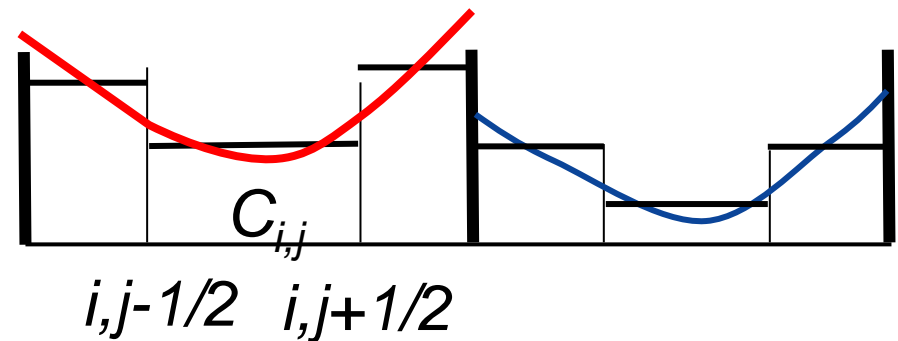
- Then

$$\int_{V_i} \varphi \left(\frac{\partial U}{\partial t} + \frac{\partial f}{\partial x} \right) dx = \int_{V_i} \varphi \frac{\partial U}{\partial t} dx + (\varphi \hat{f}_{Riem}) \Big|_{i-1/2}^{i+1/2} - \int_{V_i} f \frac{\partial \varphi}{\partial x} dx = 0$$



Spectral Volume Method

- Develop in early 2000s (Wang, Liu, ...)
- Each cell has again enough DOFs so that neighboring data are not used in reconstructing a higher-degree polynomial
- The DOFs are sub-cell averages. The number of sub-cells is $k+1$ in 1D
- The polynomial at each cell is reconstructed from the sub-cell averages



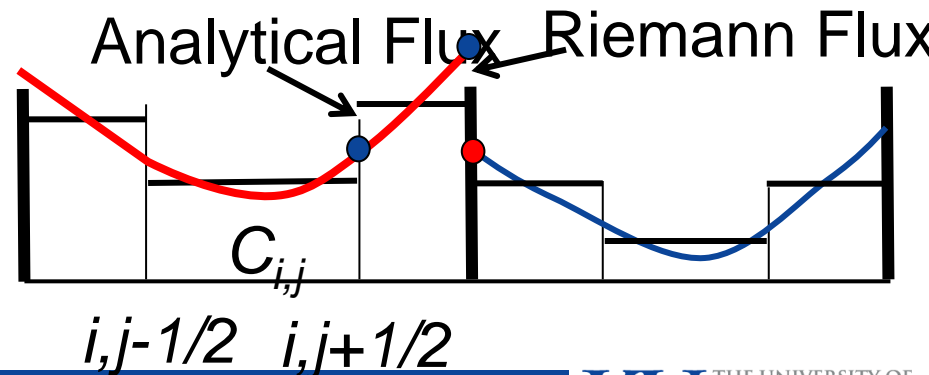


Spectral Volume Method (cont.)

- The sub-cell averages are updated using a FV method on the sub-cell

$$\frac{d\bar{u}_{i,j}}{dt} \Delta x_{i,j} + (f_{i,j+1/2} - f_{i,j-1/2}) = 0$$

- Riemann fluxes are only used across the cell interfaces
- Reconstruction universal





SD/Correction Procedure via Reconstruction

- SD developed by Y. Liu et al in 2005 and CPR Developed by Huynh in 2007 and extended to simplex by Wang & Gao in 2009, ...
- It is a differential formulation like “finite difference”

$$\frac{\partial U_i(x)}{\partial t} + \frac{\partial F_i(x)}{\partial x} = 0, \quad U_i(x) \in P^k, \quad F_i(x) \in P^{k+1}$$

- The DOFs are solutions at a set of “solution points”



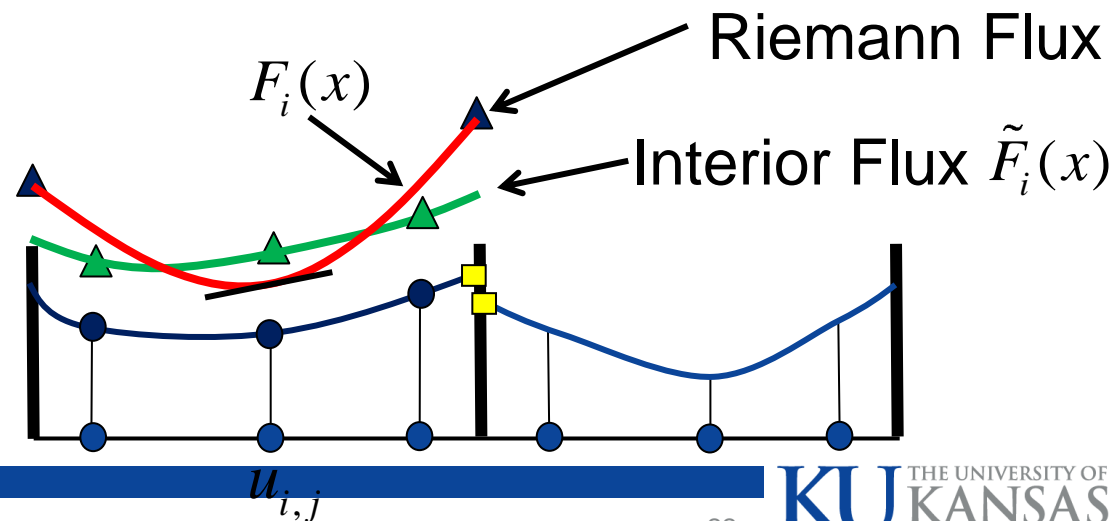
CPR (cont.)

- Find a flux polynomial $F_i(x)$ one degree higher than the solution, which minimizes

$$\|\tilde{F}_i(x) - F_i(x)\|$$

- The use the following to update the DOFs

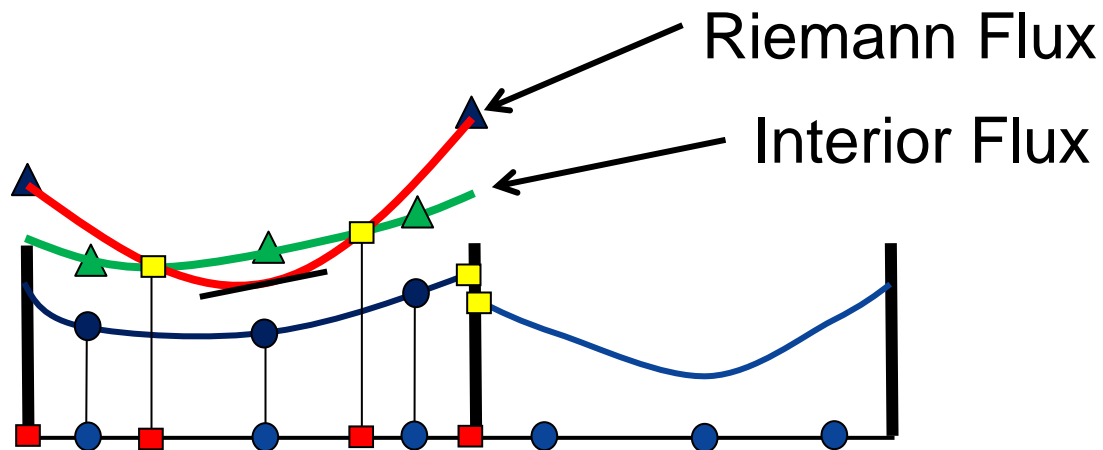
$$\frac{du_{i,j}}{dt} + \frac{dF_i(x_{i,j})}{dx} = 0$$





CPR – SD/SV

- If the new flux polynomial goes through the flux values at the flux points, the resultant scheme is spectral difference/volume





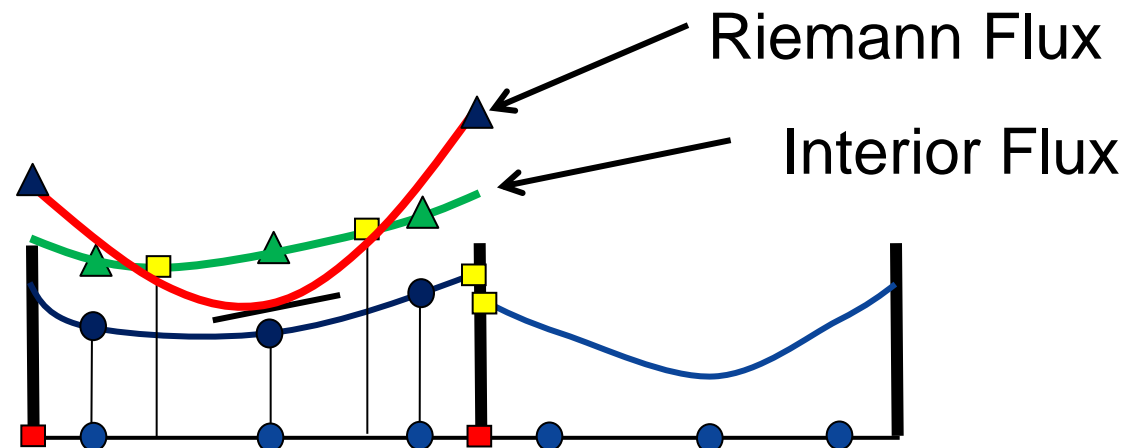
CPR – DG

- If the following equations are satisfied

$$\int_{V_i} [\tilde{F}_i(x) - F_i(x)] dx = 0$$

$$\int_{V_i} [\tilde{F}_i(x) - F_i(x)] x dx = 0$$

- The scheme is DG!





1D – P1 SV/SD and DG Schemes

$$\frac{du_{i,2}}{dt} + \frac{c}{\Delta x/2} (u_{i,2} - u_{i,1}) = 0$$

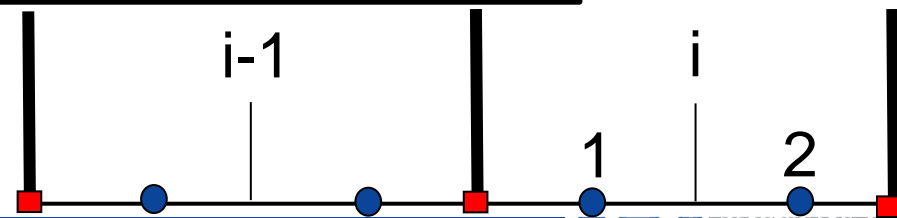
$$\frac{du_{i,1}}{dt} + \frac{c}{\Delta x} (u_{i,2} + u_{i,1} - 3u_{i-1,2} + u_{i-1,1}) = 0$$

SV/SD

$$\frac{du_{i,1}}{dt} + \frac{c}{4\Delta x} (3u_{i,2} + 7u_{i,1} - 15u_{i-1,2} + 5u_{i-1,1}) = 0$$

$$\frac{du_{i,2}}{dt} + \frac{c}{4\Delta x} (9u_{i,2} - 11u_{i,1} + 3u_{i-1,2} - 5u_{i-1,1}) = 0$$

DG





Outline

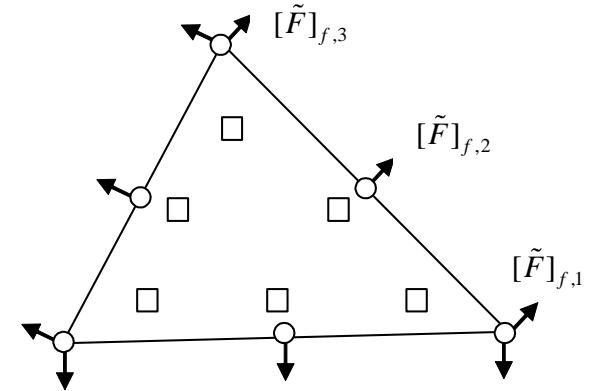
- Lecture 2:
 - Extension to multiple dimensions
 - Extension to viscous problems



CPR in 2D

Consider

$$\frac{\partial Q}{\partial t} + \nabla \cdot \vec{F}(Q) = 0$$



The weighted residual form is

$$\int_{V_i} \left(\frac{\partial Q}{\partial t} + \nabla \cdot \vec{F}(Q) \right) W dV = \int_{V_i} \frac{\partial Q}{\partial t} W dV + \int_{\partial V_i} W \vec{F}(Q) \cdot \vec{n} dS - \int_{V_i} \nabla W \cdot \vec{F}(Q) dV = 0.$$

Let Q^h be the discontinuous approximate solution in P^k .

The face flux integral replaced by a Riemann flux

$$\int_{V_i} \frac{\partial Q_i^h}{\partial t} W dV + \int_{\partial V_i} W \tilde{F}^n(Q_i^h, Q_{i+}^h, \vec{n}) dS - \int_{V_i} \nabla W \cdot \vec{F}(Q_i^h) dV = 0.$$



CPR in 2D (cont.)

Performing integration by parts to the last term

$$\int_{V_i} \frac{\partial Q_i^h}{\partial t} W dV + \int_{V_i} W \nabla \cdot \vec{F}(Q_i^h) dV + \int_{\partial V_i} W \left[\tilde{F}^n(Q_i^h, Q_{i+}^h, \vec{n}) - F^n(Q_i^h) \right] dS = 0.$$

Introduce the lifting operator

$$\int_{V_i} W \delta_i dV = \int_{\partial V_i} W [\tilde{F}] dS$$

where $\delta_i \in P^k$, $[\tilde{F}] = [\tilde{F}^n(Q_i^h, Q_{i+}^h, \vec{n}) - F^n(Q_i^h)]$ Then we have

$$\int_{V_i} \frac{\partial Q_i^h}{\partial t} W dV + \int_{V_i} W \nabla \cdot \vec{F}(Q_i^h) dV + \int_{V_i} W \delta_i dV = 0,$$



CPR in 2D (cont.)

Or

$$\int_{V_i} \left(\frac{\partial Q_i^h}{\partial t} + \nabla \cdot \vec{F}(Q_i^h) + \delta_i \right) W dV = 0,$$

which is equivalent to

$$\frac{\partial Q_i^h}{\partial t} + \nabla \cdot \vec{F}(Q_i^h) + \delta_i = 0.$$

In the new formulation, the weighting function completely disappears! Note that δ_i depends on W .



Lifting Operator – Correction Field

Obviously, the computation of δ_i is the key. From

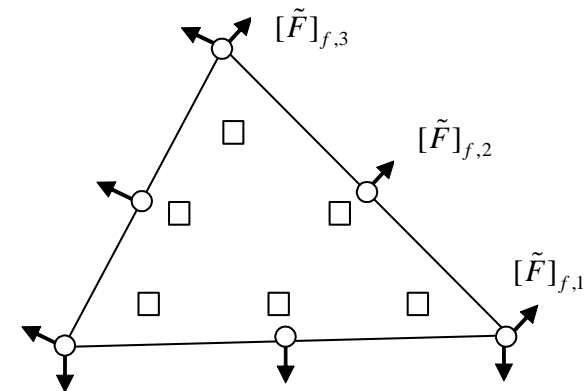
$$\int_{V_i} W \delta_i dV = \int_{\partial V_i} W [\tilde{F}] dS,$$

If $[\tilde{F}], \delta_i \in P^k$, δ_i can be computed explicitly given W . Define a set of “flux points” along the faces, and set of solution points, where the “correction field” is computed as shown.

Then

$$\delta_{i,j} = \frac{1}{|V_i|} \sum_{f \in \partial V_i} \sum_l \alpha_{j,f,l} [\tilde{F}]_{f,l} S_f,$$

$\alpha_{j,f,l}$: lifting coefficients independent of Q





CPR in 2D (cont.)

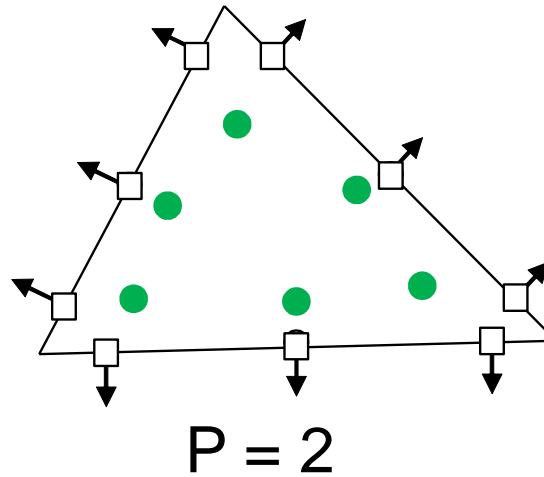
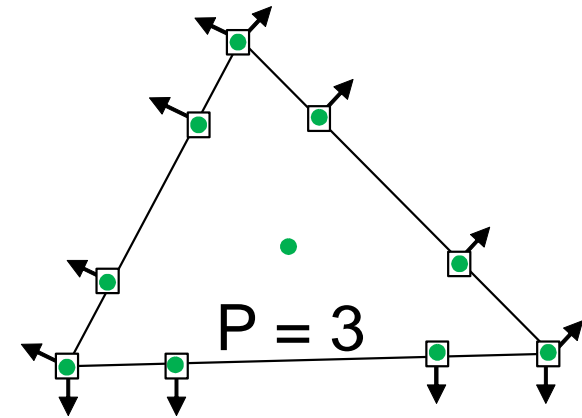
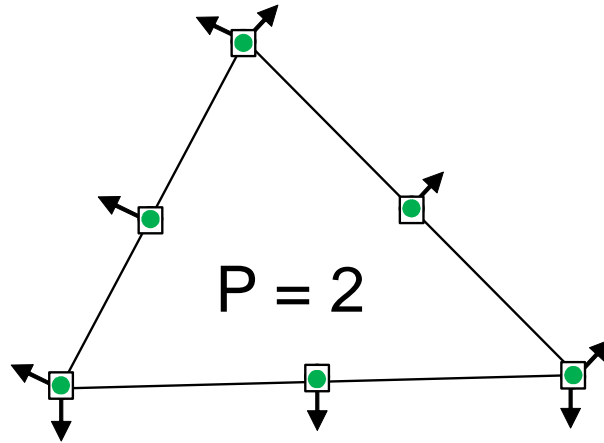
Finally the following equation is solved at the solution point j (collocation points)

$$\frac{\partial Q_{i,j}^h}{\partial t} + \nabla \cdot \vec{F}(Q_{i,j}^h) + \frac{1}{|V_i|} \sum_{f \in \partial V_i} \sum_l \alpha_{j,f,l} [\tilde{F}]_{f,l} S_f = 0.$$

The first two terms correspond to the differential equation, and the 3rd term is the correction term.



Arrangement of SPs and FPs





Extension to High-Order Elements

Transform an iso-parametric element to the standard element

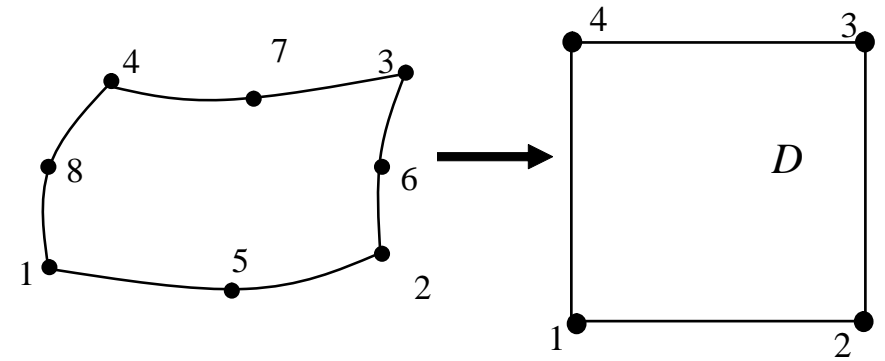
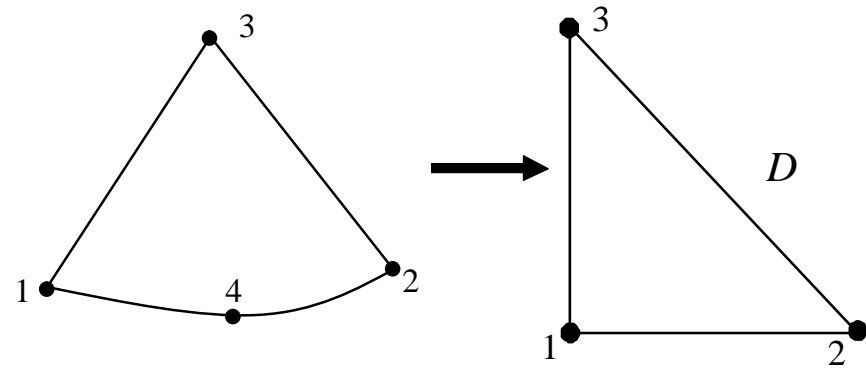
$$\mathbf{r} = \sum_{j=1}^N M_j(\xi, \eta) \mathbf{r}_j$$

Then

$$\frac{\partial Q}{\partial t} + \frac{\partial E}{\partial x} + \frac{\partial F}{\partial y} = 0$$

becomes

$$\frac{\partial \tilde{Q}}{\partial t} + \frac{\partial \tilde{E}}{\partial \xi} + \frac{\partial \tilde{F}}{\partial \eta} = 0$$





Extension to High-Order Elements (cont.)

where

$$\tilde{Q} = |J|Q$$

$$\tilde{E} = |J|(E\xi_x + F\xi_y)$$

$$\tilde{F} = |J|(E\eta_x + F\eta_y)$$

and

$$J = \frac{\partial(x, y)}{\partial(\xi, \eta)} = \begin{bmatrix} x_\xi & x_\eta \\ y_\xi & y_\eta \end{bmatrix} = \begin{bmatrix} \xi_x & \xi_y \\ \eta_x & \eta_y \end{bmatrix}^{-1}$$



Extension to High-Order Elements (cont.)

Apply CPR to the transformed equation on the standard element

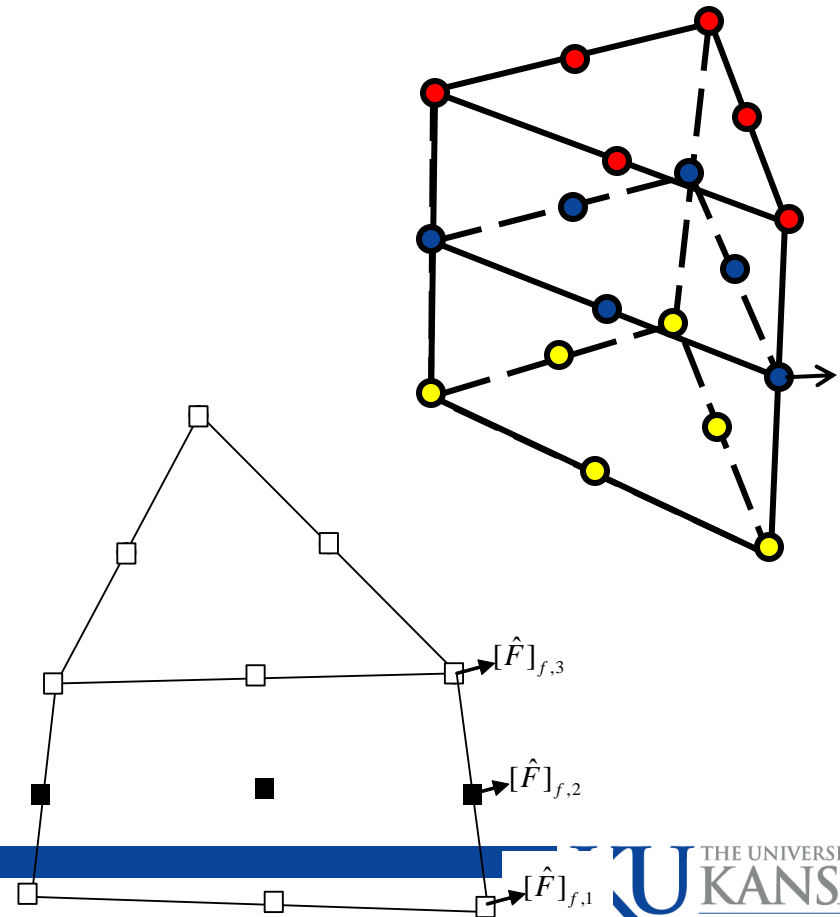
$$\frac{\partial Q_{i,j}^h}{\partial t} + \nabla \cdot \vec{F}(Q_{i,j}^h) + \frac{2}{|J_{i,j}|} \sum_{f \in \partial V_i} \sum_l \alpha_{j,f,l} [\tilde{F}]_{f,l} S_{f,l} = 0.$$

For quadrilateral element, the CPR scheme is 1D in each coordinate direction!



Mixed Grids

- In order to minimize data reconstruction and communication, solution points coincide with flux points
- For quadrilateral elements, the corrections are one-dimensional!
- Mass matrix is I for all cell-types





Extension to Viscous Flows

- How to deal with the second order derivative ?
- Second Order FV Method:
 - The solution gradients at an interface are sometimes computed by averaging the gradients of the neighboring cells sharing the face.
- High Order Method:
 - Local Discontinuous Galerkin (Cockburn and Shu), motivated by the numerical results of Bassi and Rebay
 - Internal Penalty



Simplest Case First - SV

Consider the 1D heat equation

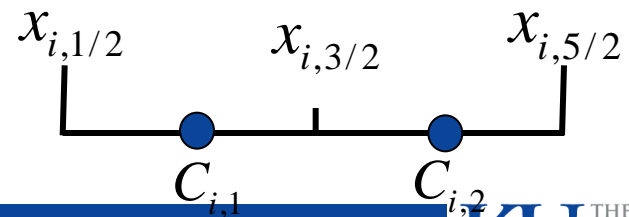
$$u_t - u_{xx} = 0, \quad x \in [0, 2\pi] \quad \text{periodic boundary condition}$$

$$u(x, 0) = \sin(x)$$

Integrating in a CV to obtain

$$\frac{d\bar{u}_{i,j}(t)}{dt} h_{i,j} - (u_x|_{i,j+1/2} - u_x|_{i,j-1/2}) = 0$$

$$\text{with } \bar{u}_{i,j}(t) = \frac{\int_{x_{i,j+1/2}}^{x_{i,j-1/2}} u(x,t) dx}{h_{i,j}}$$





Formulation for 1D Heat Equation

Because the solution is SV-wise continuous, u_x not well defined at SV boundaries. Therefore it is replaced by a “numerical flux” \hat{u}_x

$$\frac{d\bar{u}_{i,j}(t)}{dt} - \frac{1}{h_{i,j}} (\hat{u}_x|_{i,j+1/2} - \hat{u}_x|_{i,j-1/2}) \approx 0$$

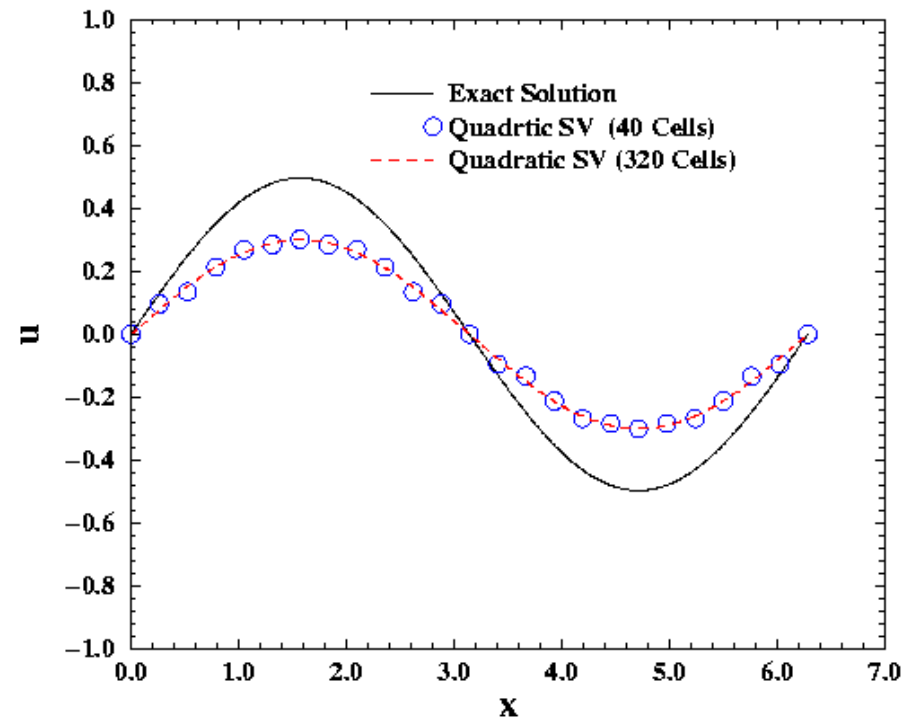
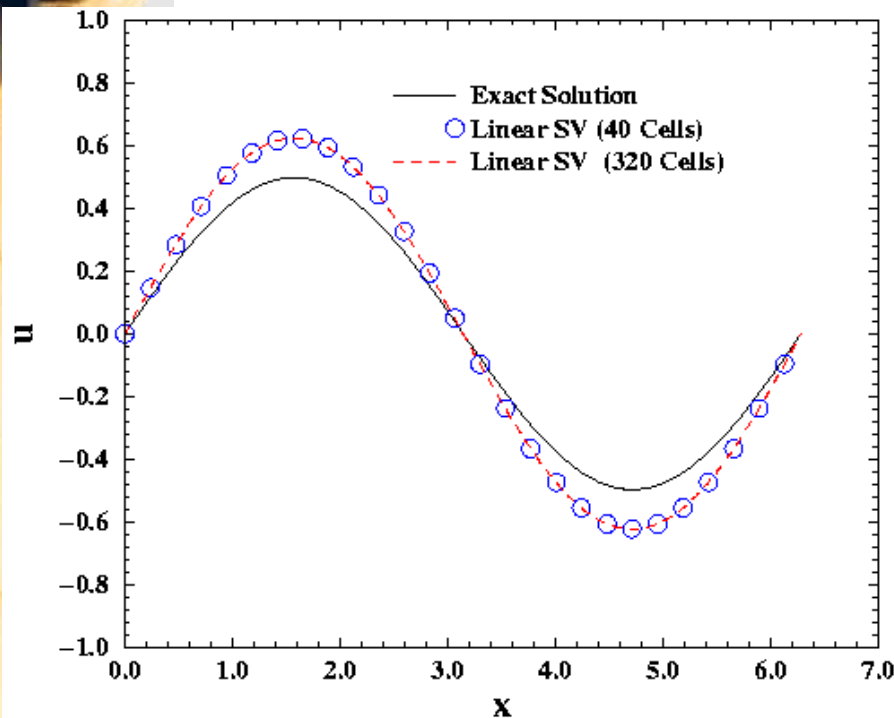
Formulation 1-Naïve SV Formulation

$$\hat{u}_x|_{i,j+1/2} = \frac{1}{2} [(u_x)^+_{i,j+1/2} + (u_x)^-_{i,j+1/2}]$$



Behaviors of the Naïve SV Formulation

$t = 0.7$



This formulation converges to the wrong solution !
Similar result by Cockburn and Shu



Formulation 1 - Local DG Formulation

Introducing an auxiliary unknown $q = u_x$

$$\begin{cases} u_t - q_x = 0 \\ q - u_x = 0 \end{cases}$$

Integrating in a CV

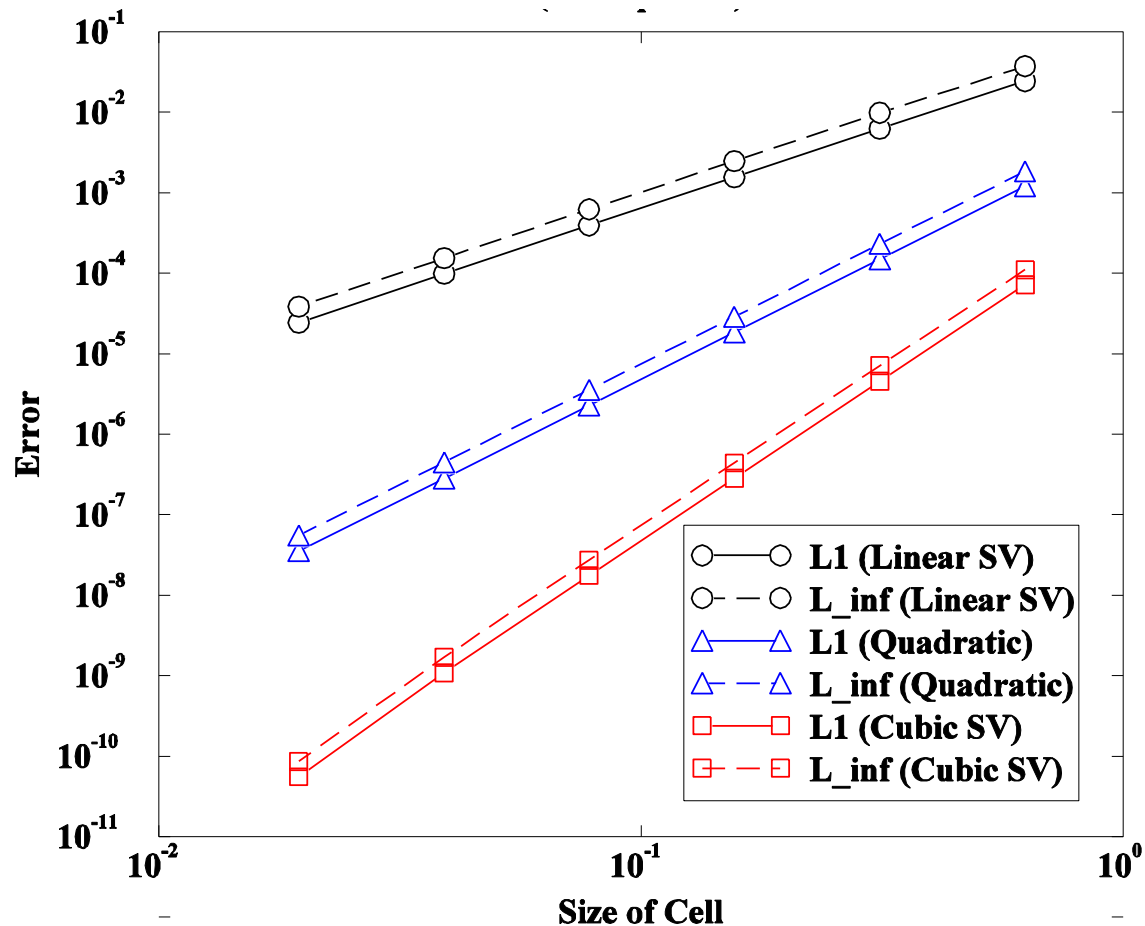
$$\begin{cases} \frac{d\bar{u}_{i,j}}{dt} - \frac{1}{h_{i,j}} (\hat{q}|_{i,j+1/2} - \hat{q}|_{i,j-1/2}) = 0 \\ \bar{q}_{i,j} - \frac{1}{h_{i,j}} (\hat{u}|_{i,j+1/2} - \hat{u}|_{i,j-1/2}) = 0. \end{cases}$$

Selecting “numerical flux” following LDG

$$\hat{u}|_{i,j+1/2} = u|_{i,j+1/2}^+ \quad \hat{q}|_{i,j+1/2} = q|_{i,j+1/2}^-$$



Computational Results of LDG



$(k+1)$ -th order achieved for a degree k polynomial reconstruction



Formulation 2 – Penalty Formulation

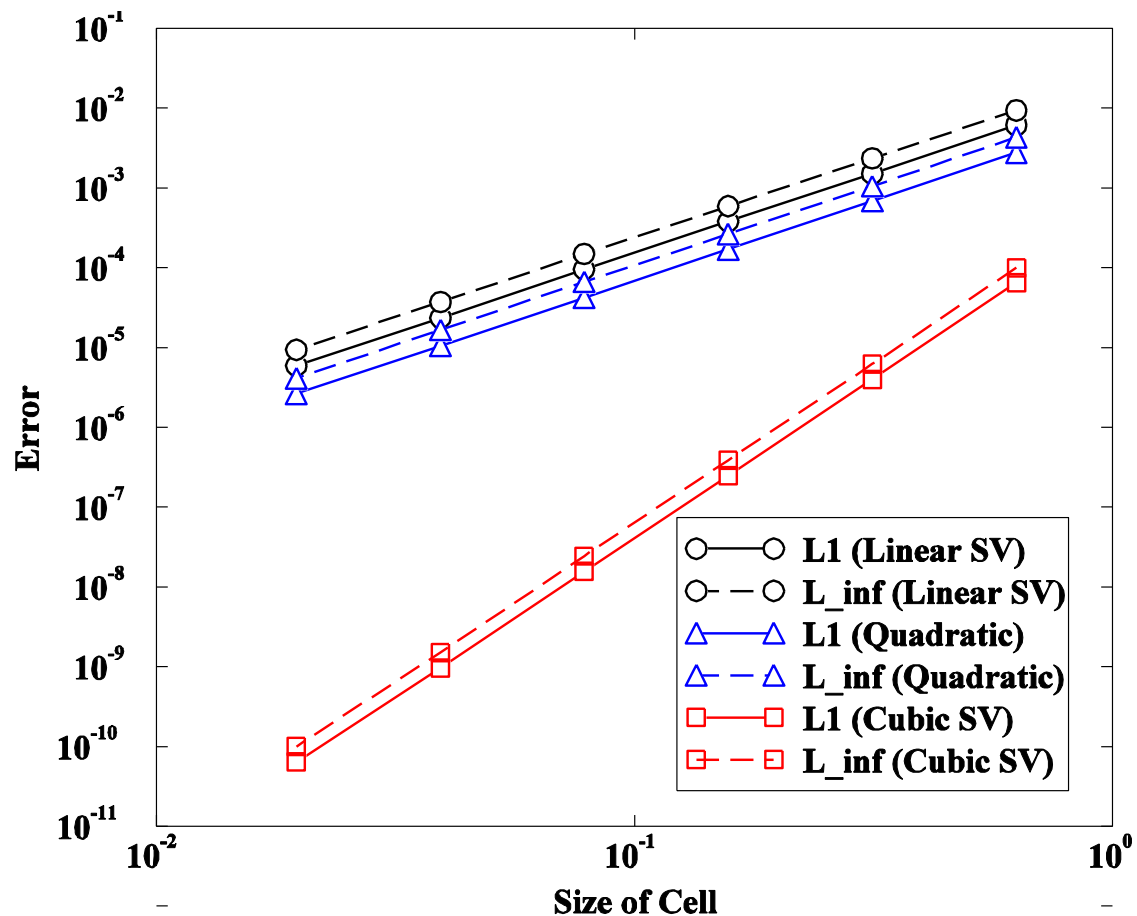
Numerical flux given by

$$\hat{u}_x|_{i,j+1/2} = \frac{1}{2} \left[(u_x)^+_{i,j+1/2} + (u_x)^-_{i,j+1/2} \right] + \frac{\varepsilon}{h_{i,j}} (u|_{i,j+1/2}^+ - u|_{i,j+1/2}^-)$$

where ε is a constant. A Fourier analysis performed to choose the value ε . It was found $\varepsilon = 1$ gives the highest order of accuracy for linear reconstruction.



Results of the Penalty Formulation



$(k+1)$ -th order achieved for a degree k polynomial if k odd, otherwise k -th order.



CPR Formulation for Computing Gradients

Introduce another variable

$$R = Q_x$$

Apply weighted residual to the above equation

$$\begin{aligned} \int_{V_i} RW dx &= \int_{V_i} W Q_x dx = \int_{V_i} [(WQ)_x - QW_x] dx \\ &= (WQ_{com}) \Big|_L^R - \int_{V_i} QW_x dx = [W(Q_{com} - Q)] \Big|_L^R + \int_{V_i} WQ_x dx \end{aligned}$$

Let

$$\int_{V_i} \delta W dx = [W(Q_{com} - Q)] \Big|_L^R$$

Then

$$R_{i,j} = (Q_i)_{x,j} + \alpha_{L,j} (Q_{com,L} - Q_L) + \alpha_{R,j} (Q_{com,R} - Q_R)$$



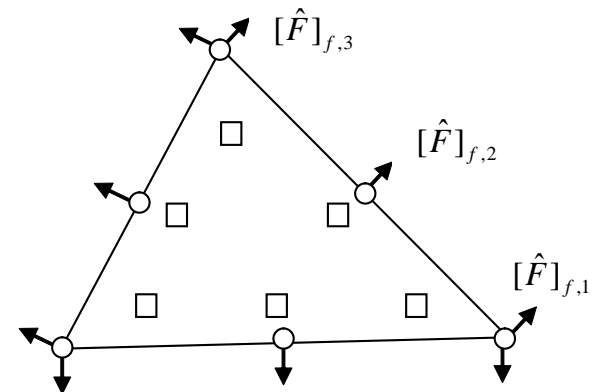
CPR Formulation for Computing Gradients

Need to compute gradient

$$\vec{R} = \nabla Q$$

Applying CPR to the above equation, we obtain

$$R_{i,j} = \left(\nabla Q_i^h \right)_j + \frac{1}{|V_i|} \sum_{f \in \partial V_i} \sum_l \alpha_{j,f,l} [Q_{f,l}^{com} - Q_{i,f,l}]_{f,l} \vec{n}_f S_f$$





LDG on 2D Convection-Diffusion Equations

Consider

$$u_t + \nabla \cdot (\boldsymbol{\beta} u) - \nabla \cdot (\mu \nabla u) = 0$$

Introducing auxiliary variables

$$\mathbf{q} = \nabla u$$

Integrating in a CV to obtain

$$\bar{\mathbf{q}}_{i,j} - \frac{1}{V_{i,j}} \sum_{r=1}^K \int_{A_r} \hat{u} \cdot \mathbf{n} dA = 0$$

$$\frac{d\bar{u}_{i,j}}{dt} + \frac{1}{V_{i,j}} \left\{ \sum_{r=1}^K \int_{A_r} (\boldsymbol{\beta} \tilde{u} \cdot \mathbf{n}) dA - \sum_{r=1}^K \int_{A_r} \mu \hat{\mathbf{q}} \cdot \mathbf{n} dA \right\} = 0$$



Numerical Flux Computation

Upwind for inviscid flux

$$\tilde{u} = \begin{cases} u_L & \boldsymbol{\beta} \cdot \mathbf{n} > 0 \\ u_R & \boldsymbol{\beta} \cdot \mathbf{n} < 0 \end{cases}$$

Alternate directions for viscous and auxiliary “numerical fluxes”

or

$$\hat{u} \approx u_R \quad \hat{q} \approx q_L$$

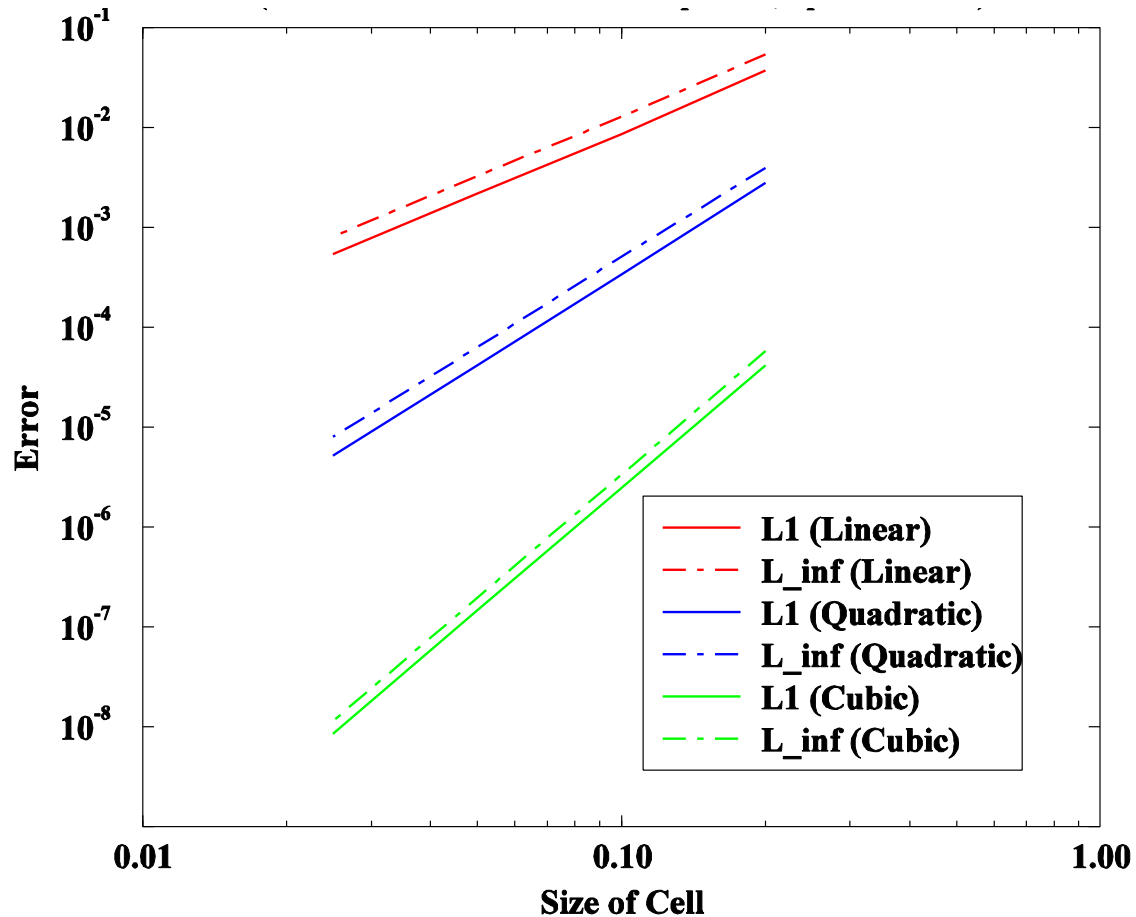
$$\hat{u} \approx u_L \quad \hat{q} \approx q_R$$



Results for 2D Convection-Diffusion Equations

$$u_t + (u_x + u_y) - 0.01(u_{xx} + u_{yy}) = 0, \quad (x, y) \in [-1,1] \times [-1,1]$$

$$u(x, y, 0) = \sin(\pi(x + y))$$





Numerical Experiments on NS Equations

- Couette Flow
- Laminar Flow along a Flat Plate
- Subsonic Flow over a Circular Cylinder
- Laminar Subsonic Flow around NACA0012 Airfoil

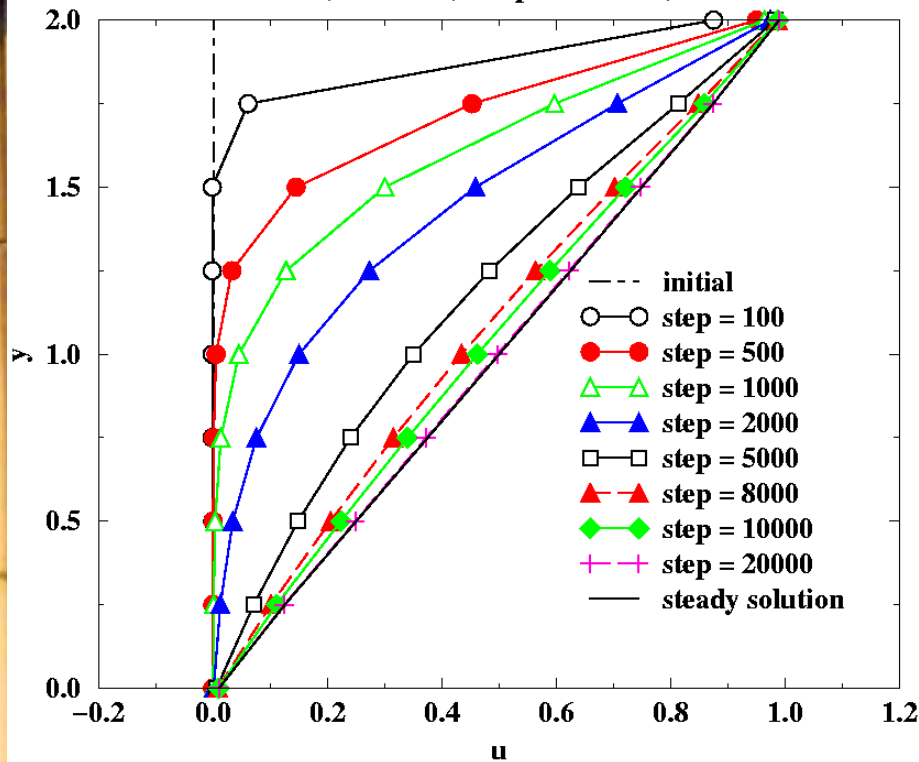




Couette Flow - Convergence

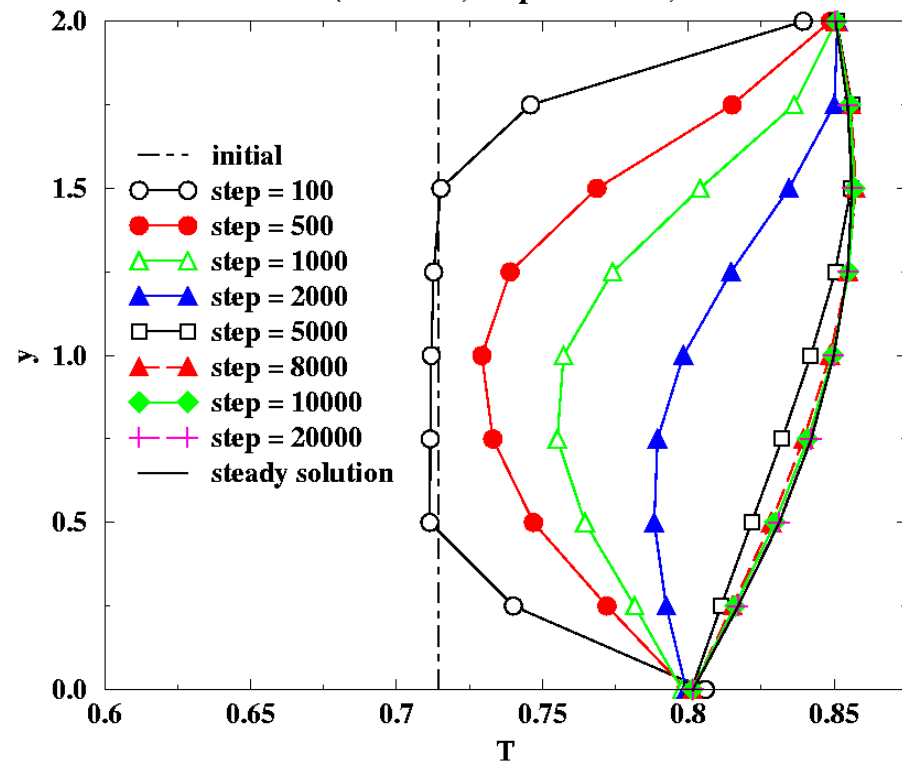
u-velocity Profile

(order = 3, simple8x8.DTF)



Temperature Profile

(order = 3, simple8x8.DTF)



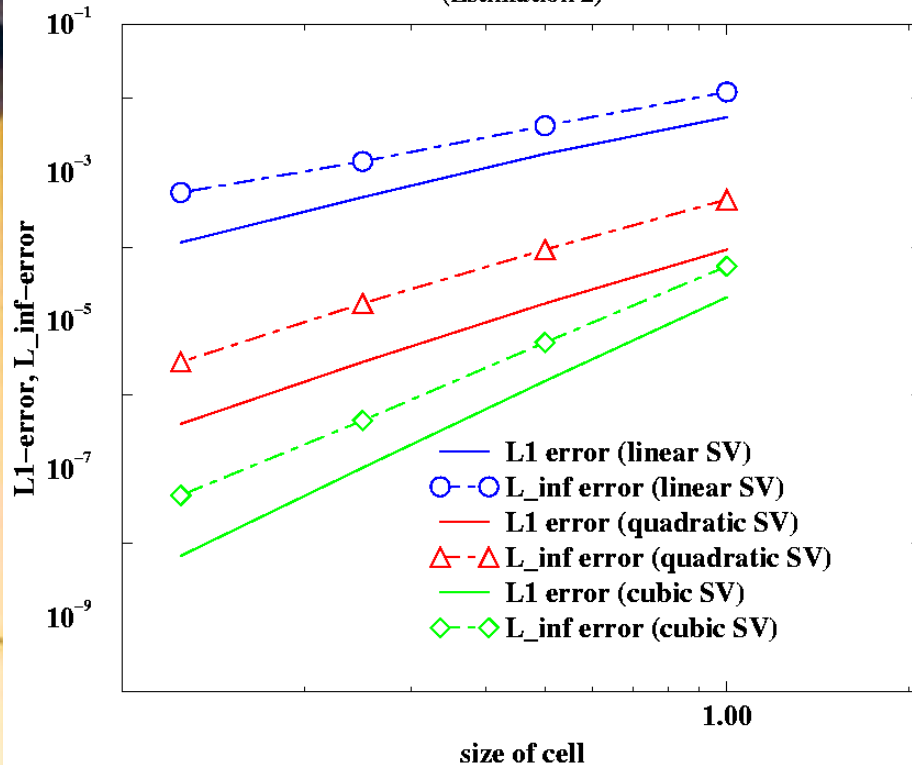
Convergence History



Couette Flow – Numerical Accuracy Order

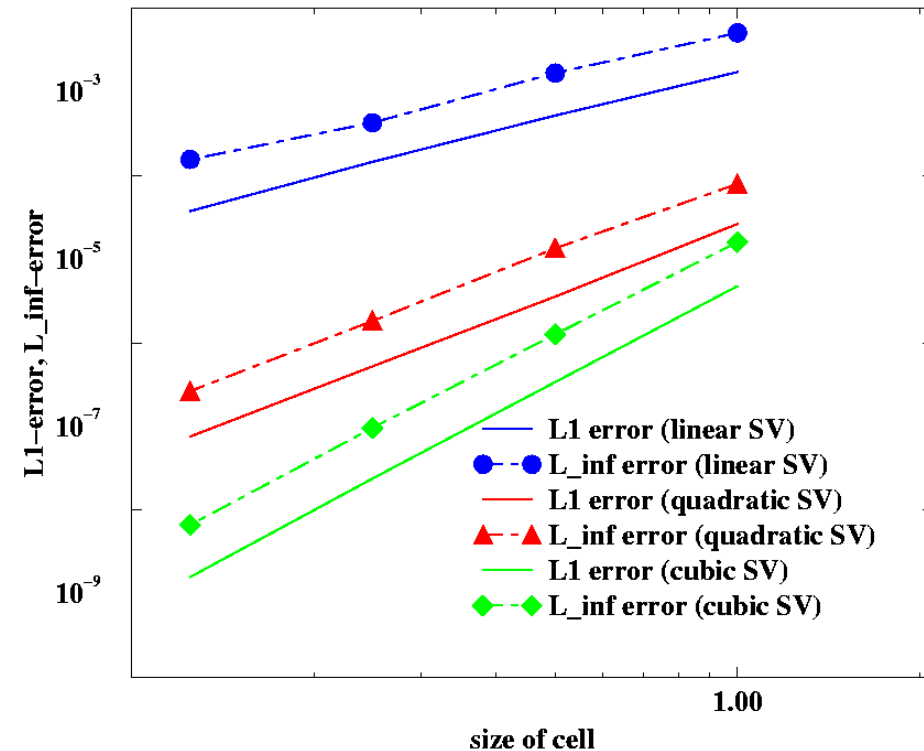
Accuracy Study on Density for Couette Flow

(Estimation 2)



Accuracy Study on Temperature for Couette Flow

(Estimation 2)





Laminar Flow along a Flat Plate

Flow Conditions:

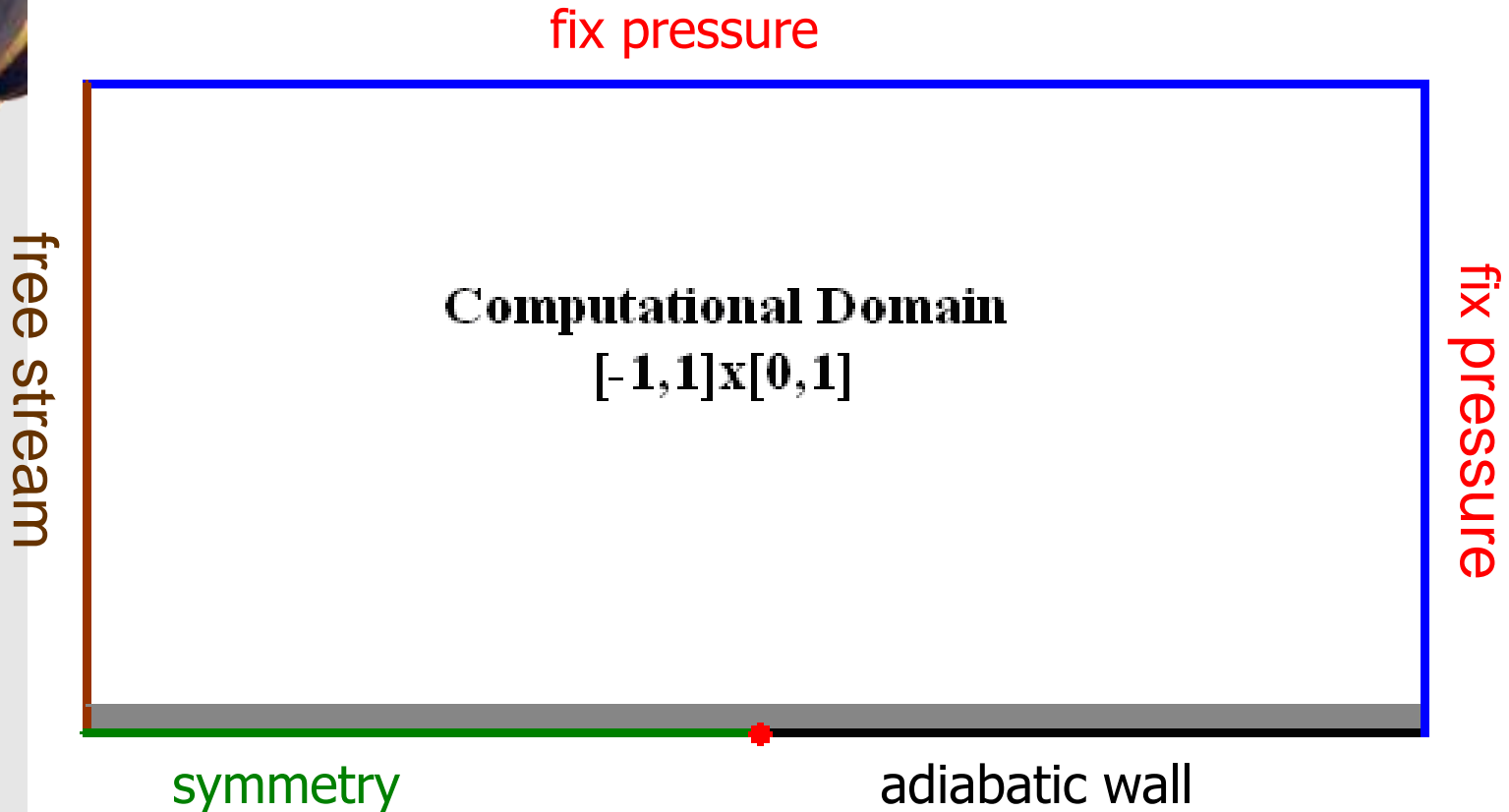
- Free stream $Ma = 0.3$, $Re = 10000$
- Adiabatic plate, length = 1.0

The Thickness of Boundary Layer (at $x=1.0$):

$$\delta|_{x=1.0} = 5 \cdot \sqrt{\frac{\mu \cdot x}{\rho_{\infty} \cdot u_{\infty}}}|_{x=1.0} = 5 \cdot \frac{x}{\sqrt{Re}|_{x=1.0}} = 0.05$$



Schematic Structure



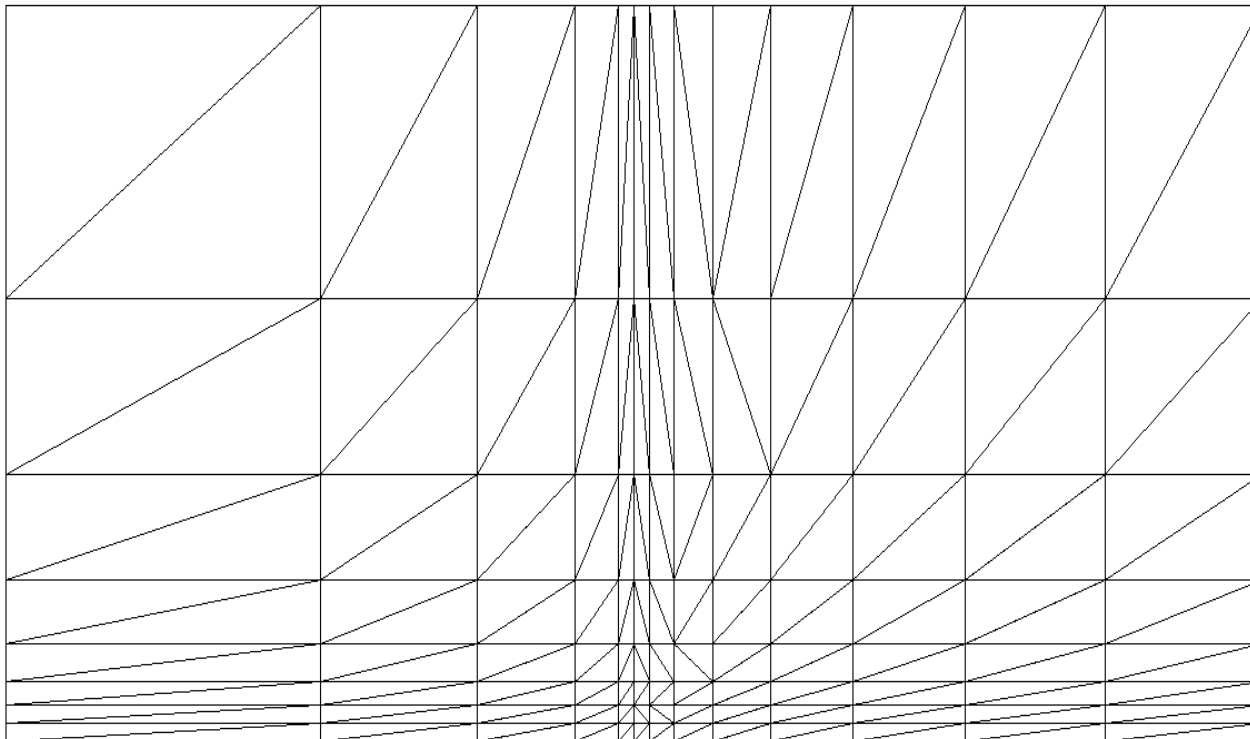


Mesh

Coarse mesh - 208 cells (8 cells along the plate)

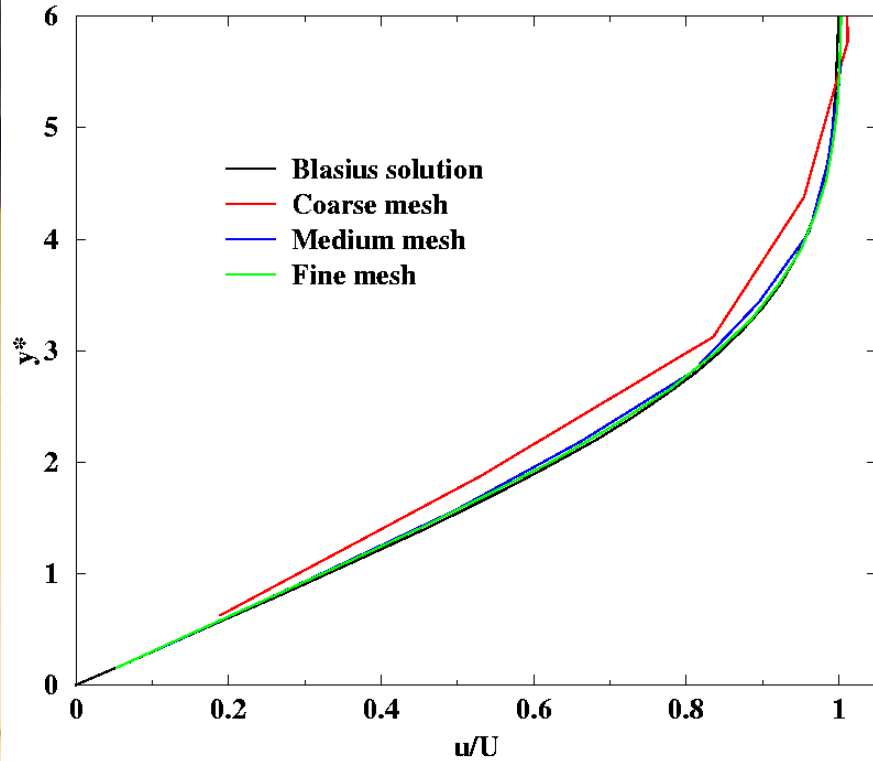
Medium mesh - 832 cells (16 cells along the plate)

Fine mesh - 3328 cells (32 cells along the plate)

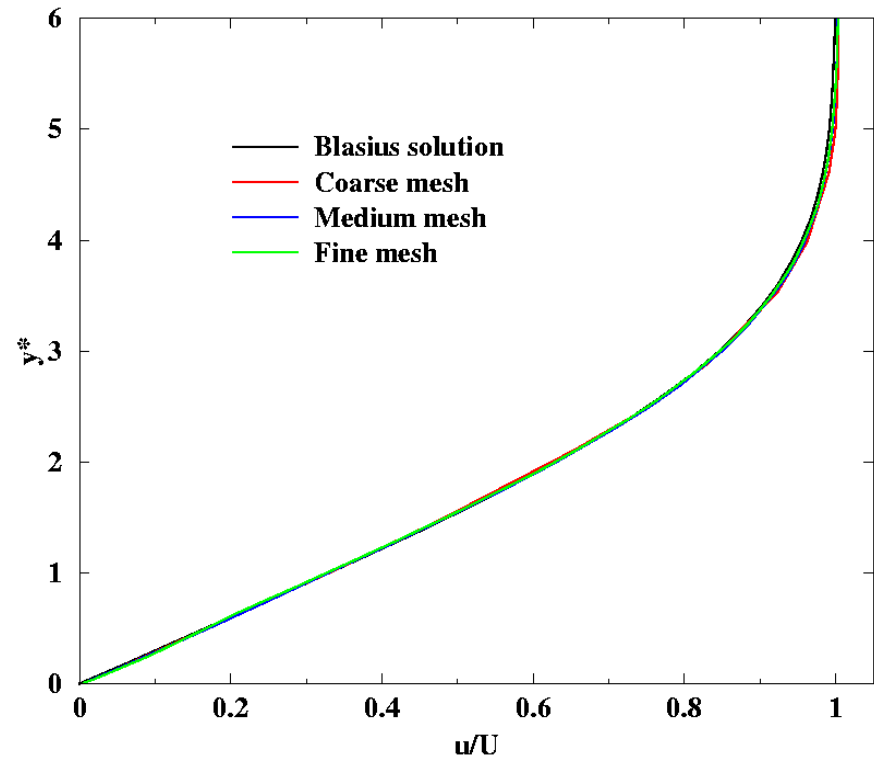




u-velocity Profiles with Different SVs



Linear SV

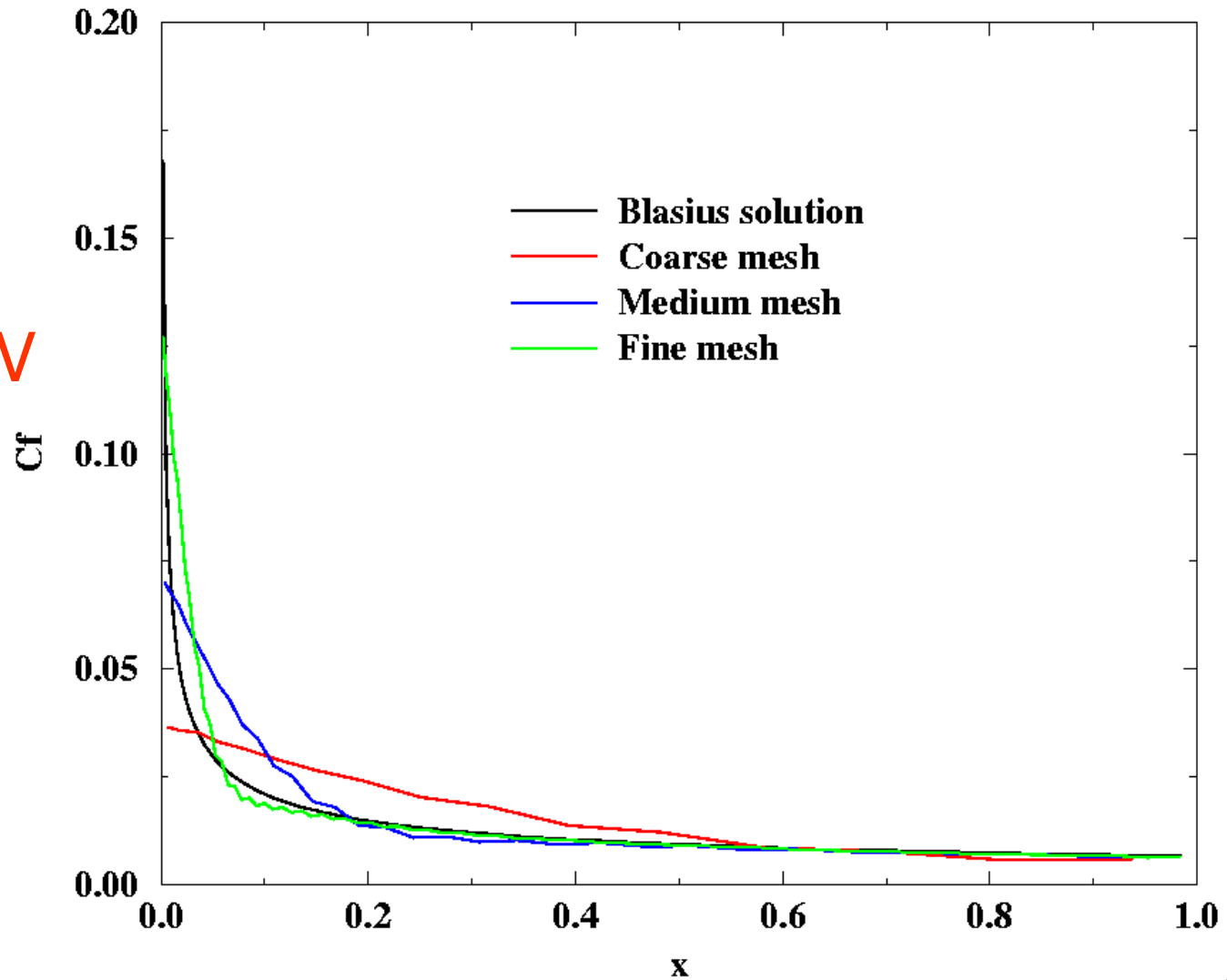


Cubic SV



Skin Fraction Coefficient along the plate

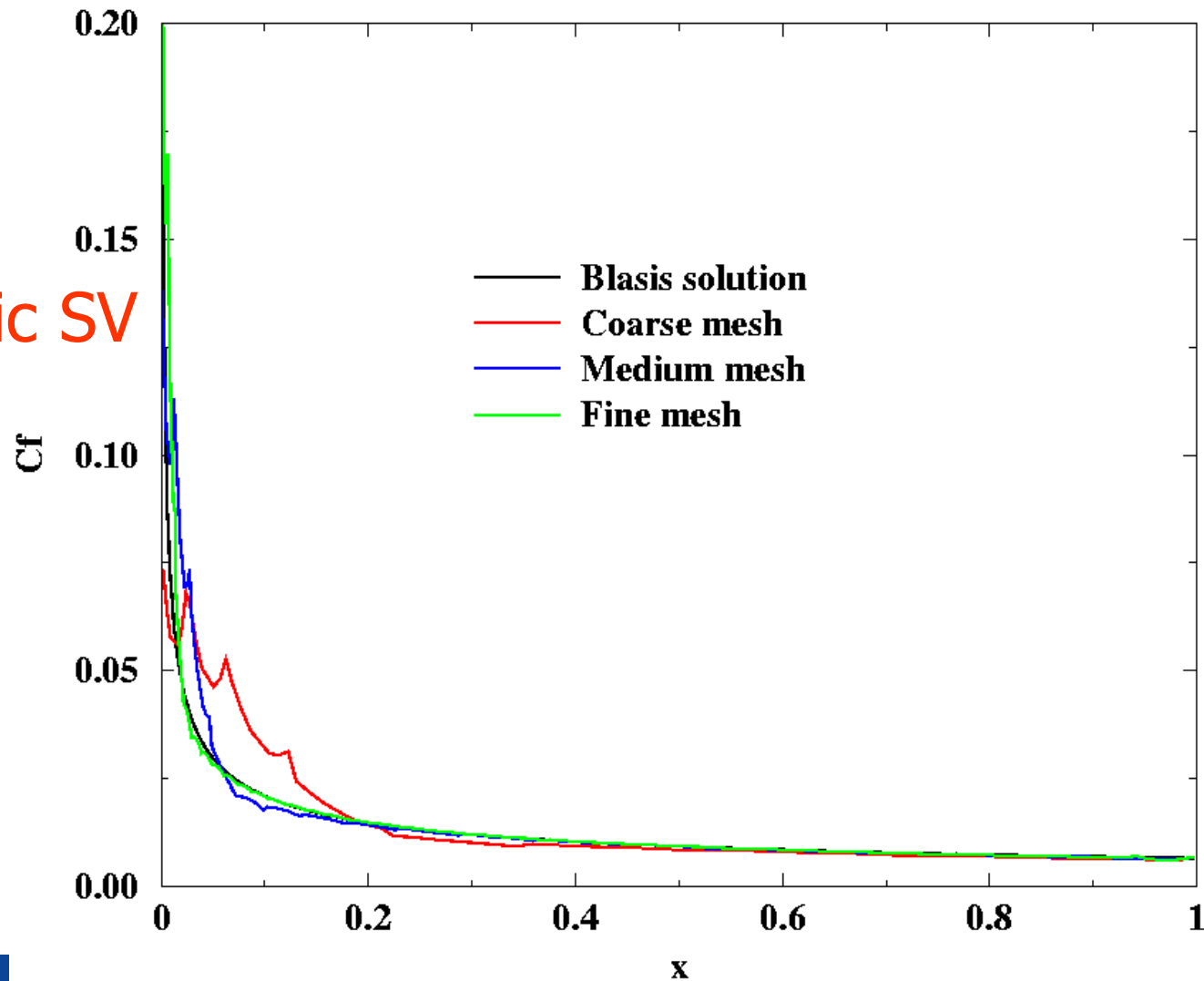
Linear SV





Skin Fraction Coefficient (con'd)

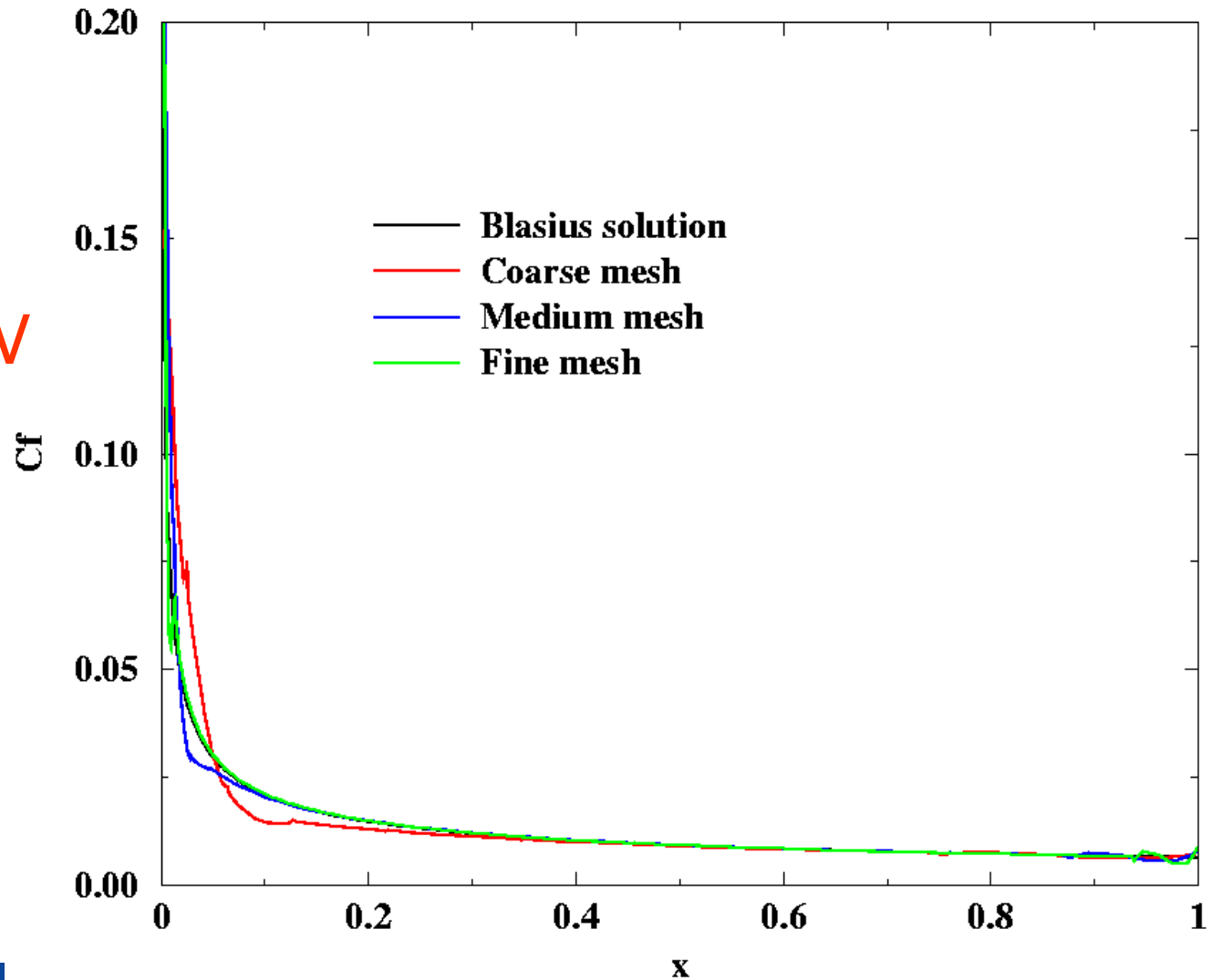
Quadratic SV





Skin Friction Coefficient (con'd)

Cubic SV

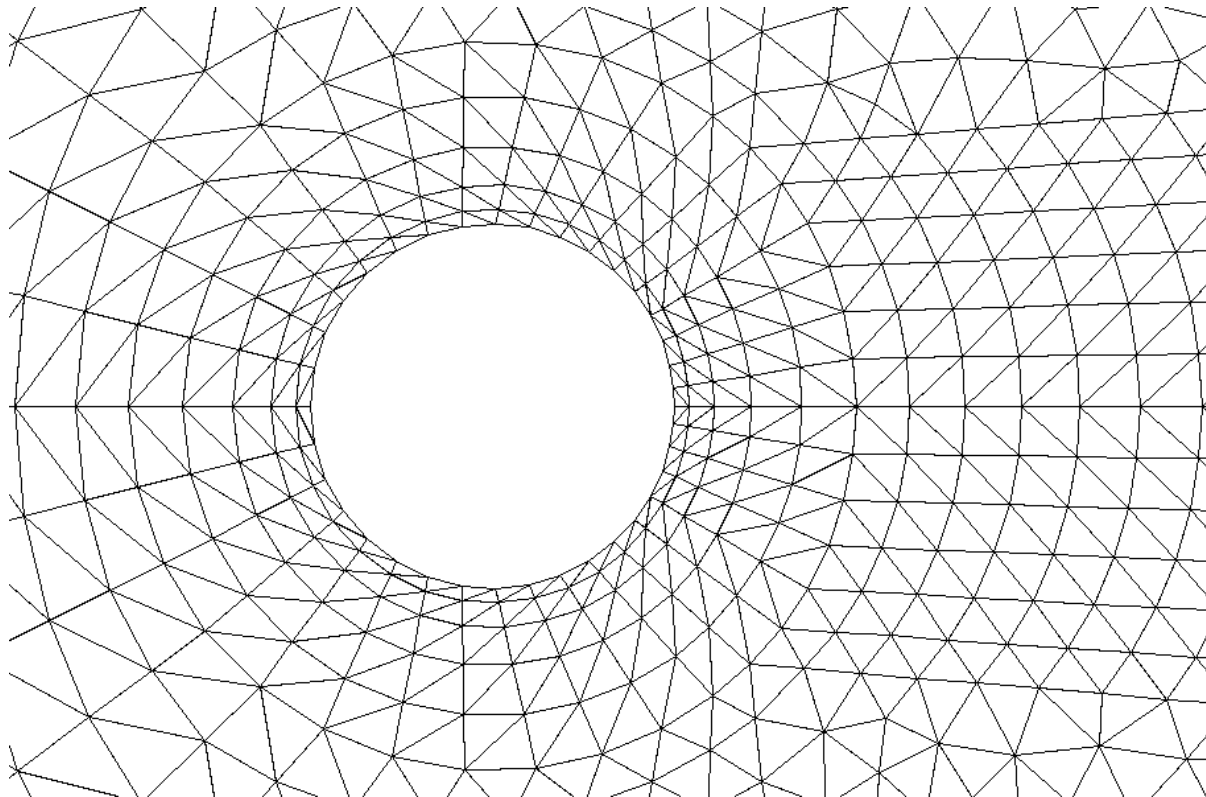




Subsonic Flow over a Circular Cylinder

Flow Conditions: $Ma = 0.2$, $Re = 75$

Mesh Near the Cylinder

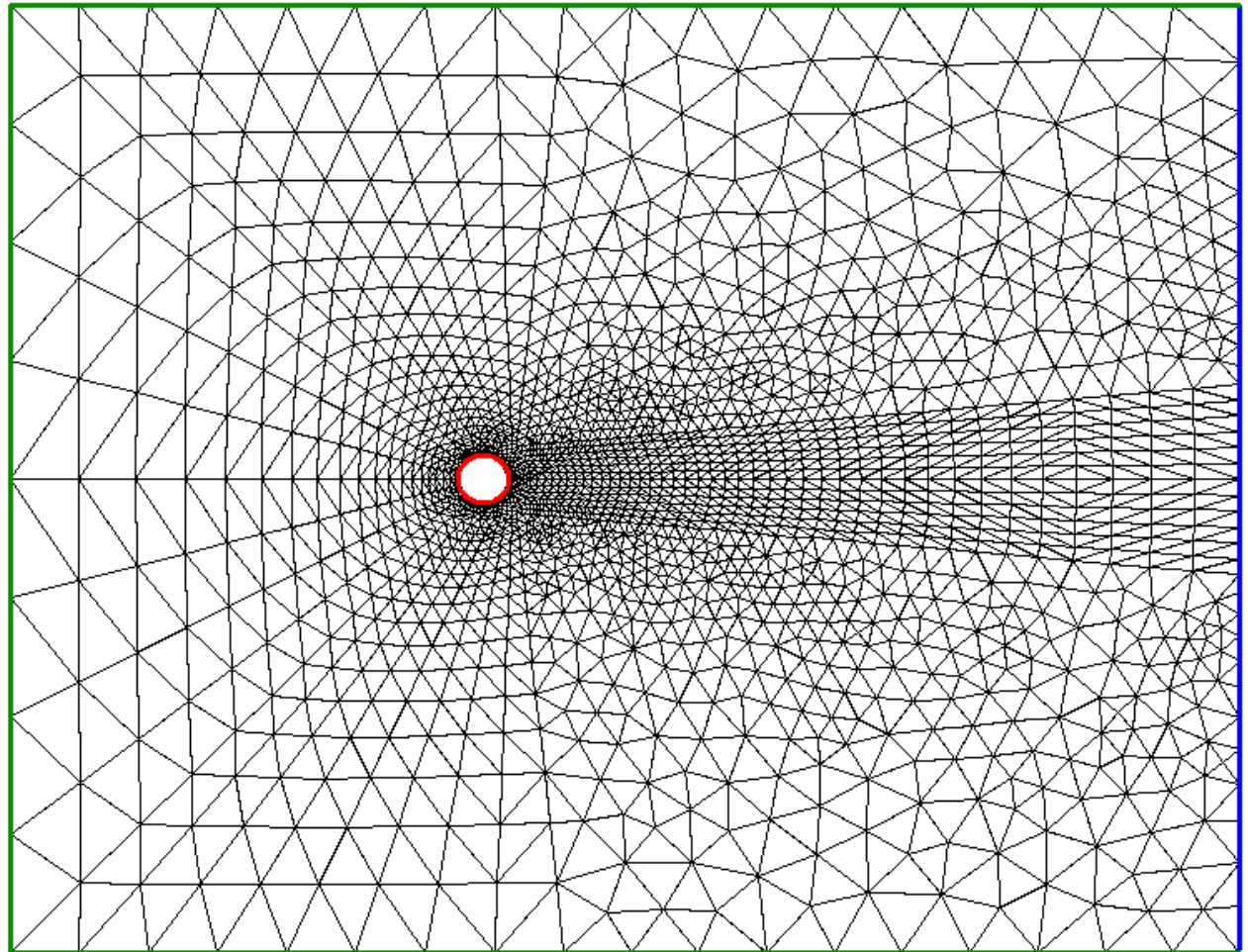




Schematic Structure and Mesh



- Adiabatic wall
- Fix every thing
- Fix pressure



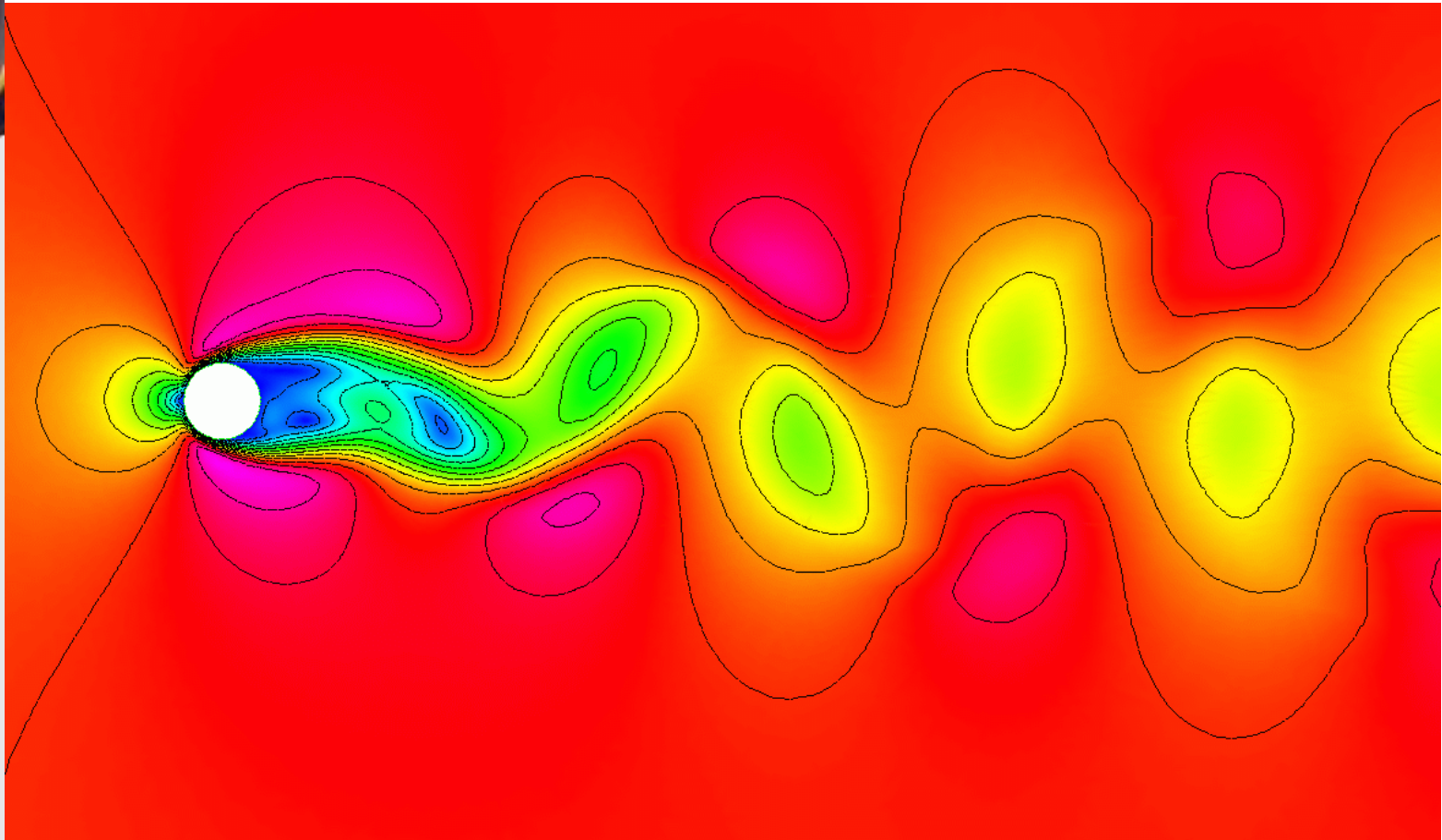


Interested Phenomena

- The Von Karmen Vortex Street (generated by the cylinder)
 - Mach contours
 - Entropy contours
 - Vorticity contours
- The Periodic Nature of the Flow
 - Pressure histories at different locations
 - The period of oscillations corresponds to a Strouhal number of 0.151



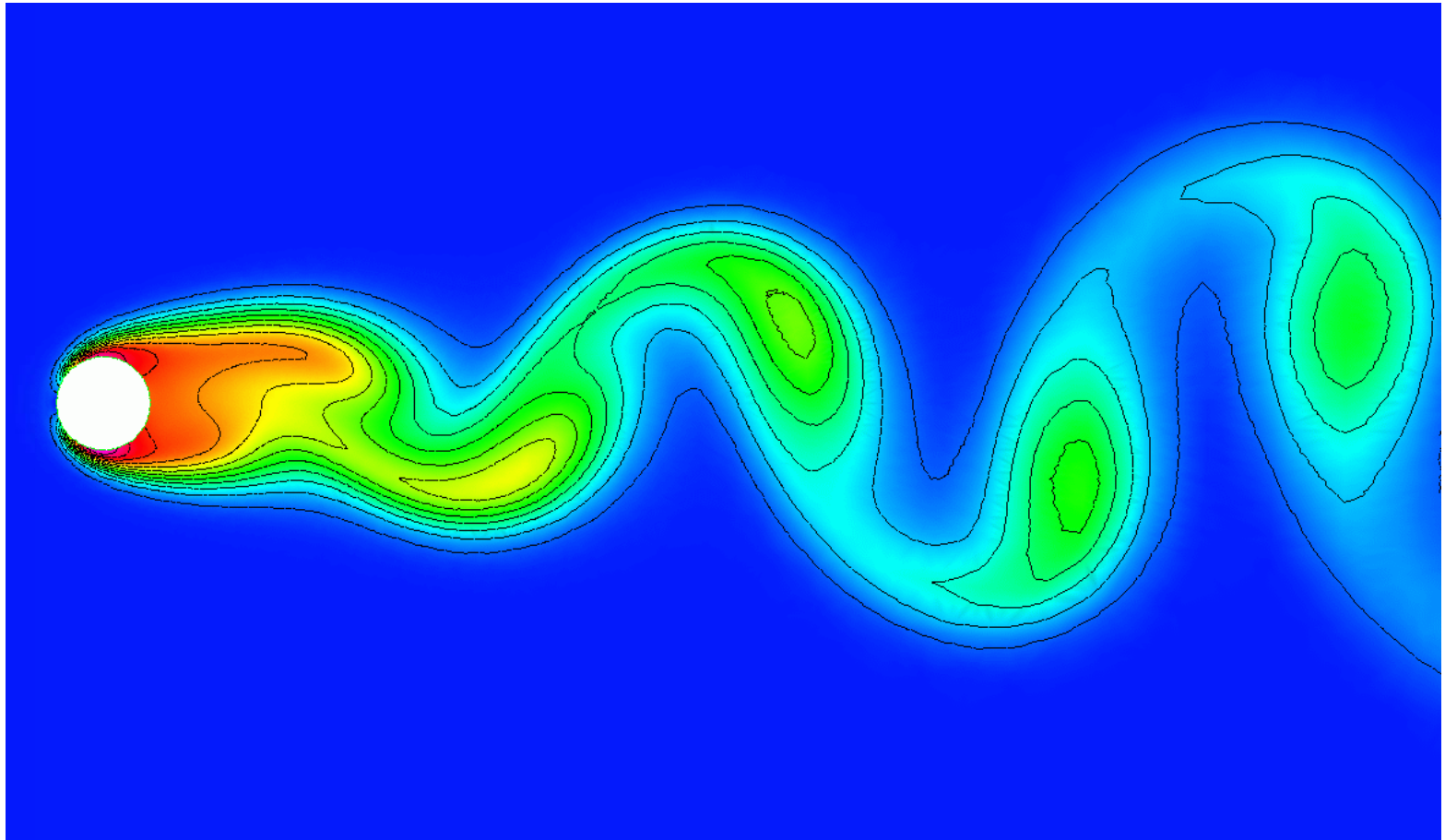
Instantaneous Mach Contours



$M = 0.2$ flow over a circular cylinder at $Re = 75$



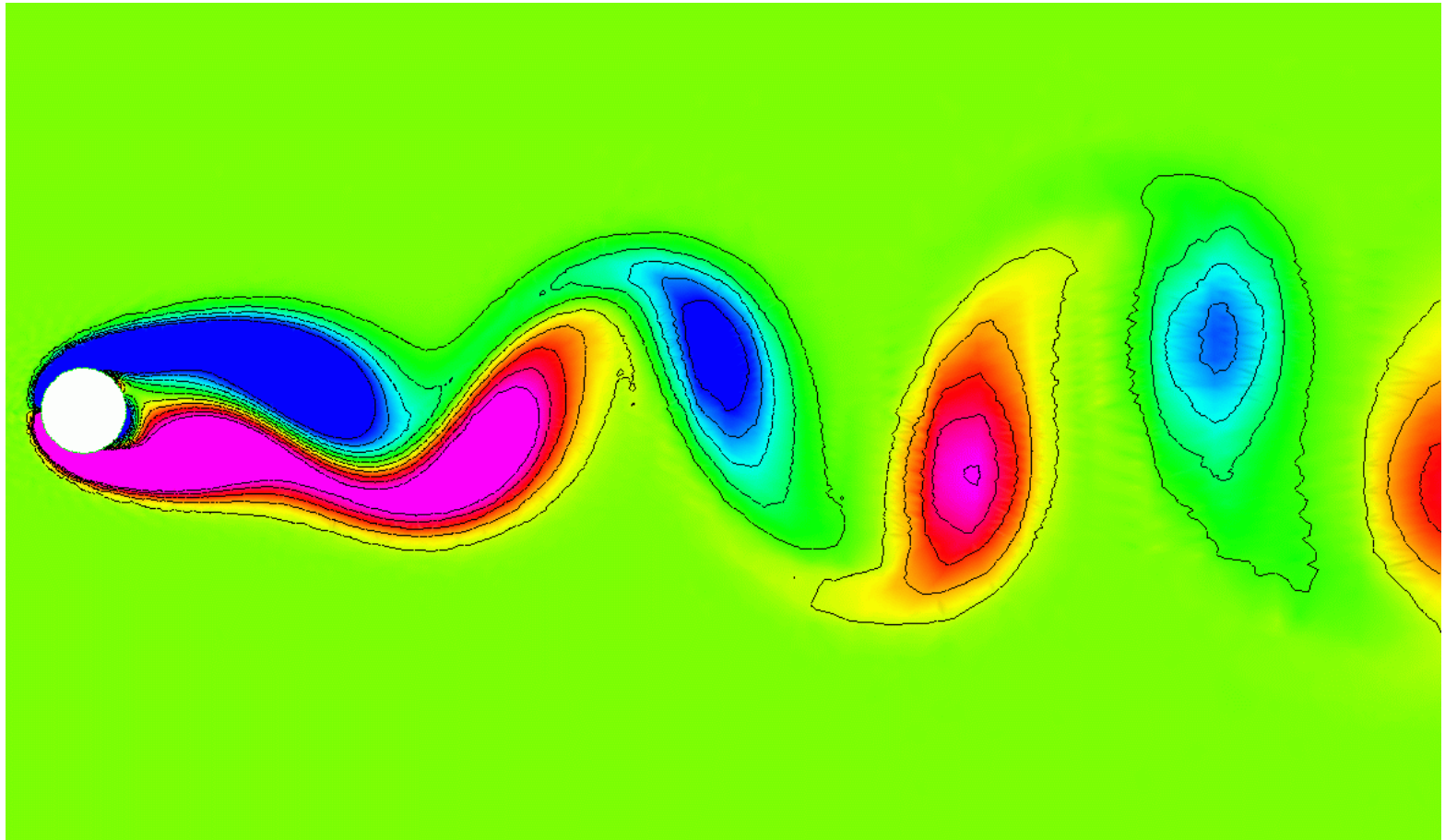
Instantaneous Entropy Contours



$M = 0.2$ flow over a circular cylinder at $Re = 75$



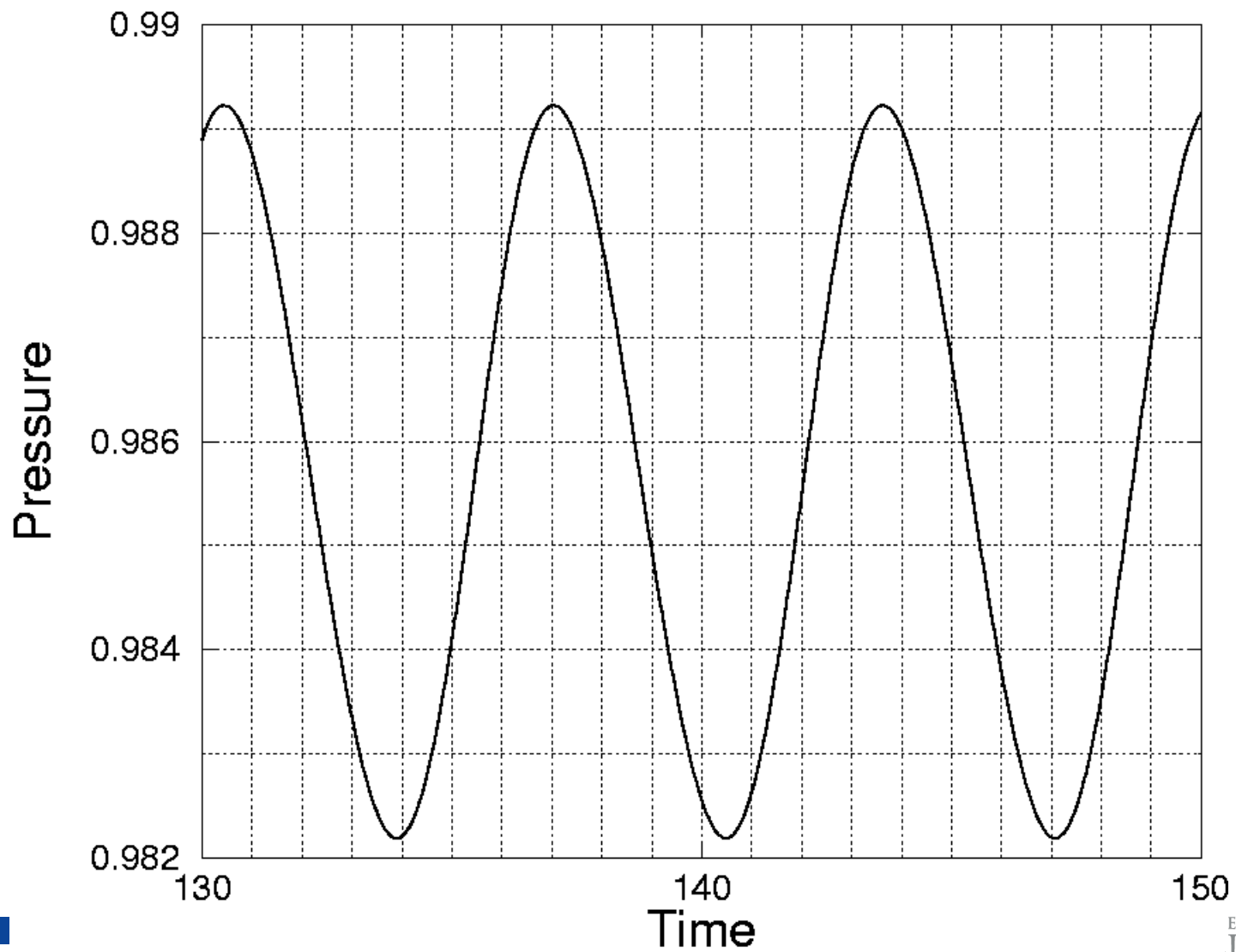
Instantaneous Vorticity Contours



$M = 0.2$ flow over a circular cylinder at $Re = 75$

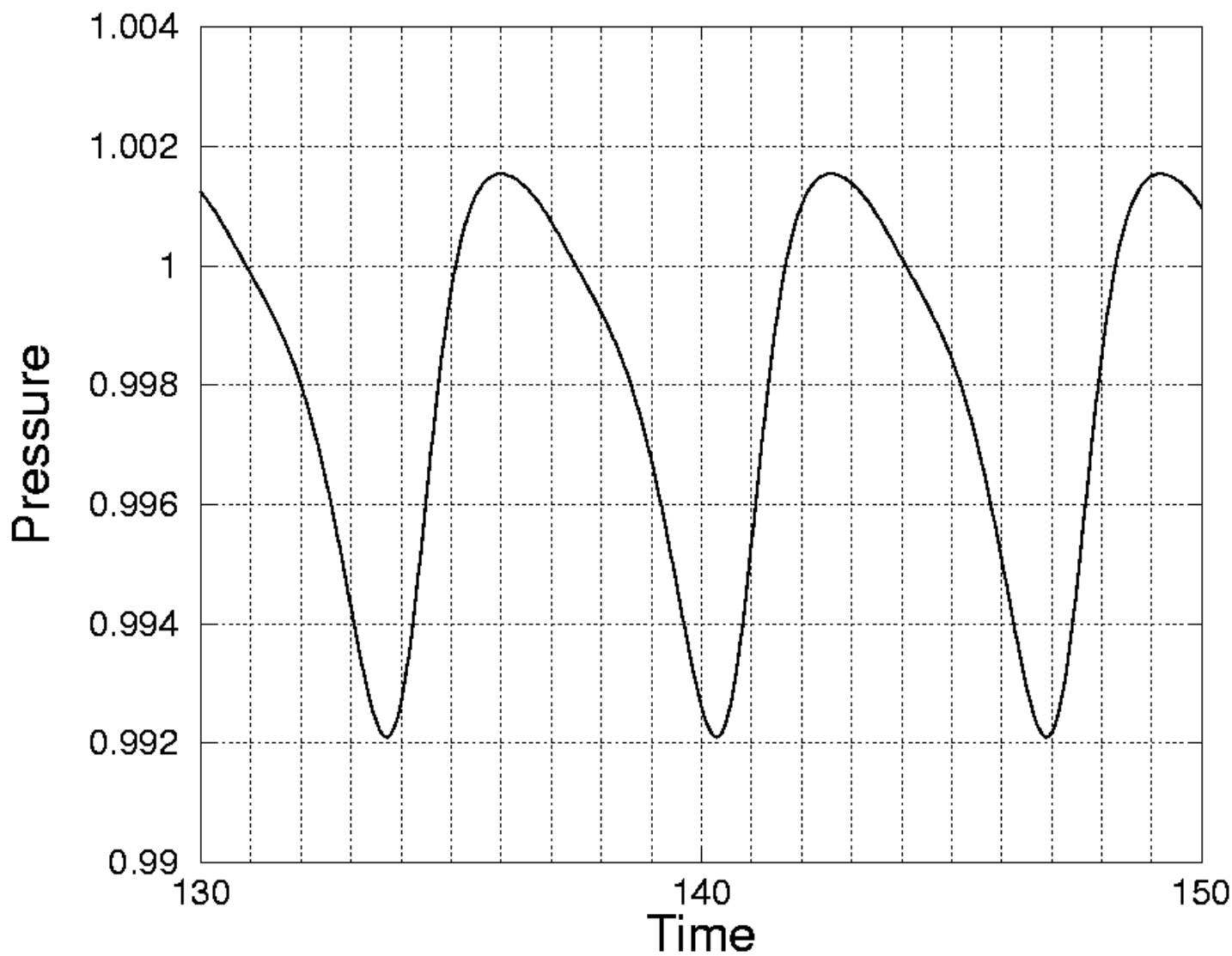


Pressure History at Point (1,1)



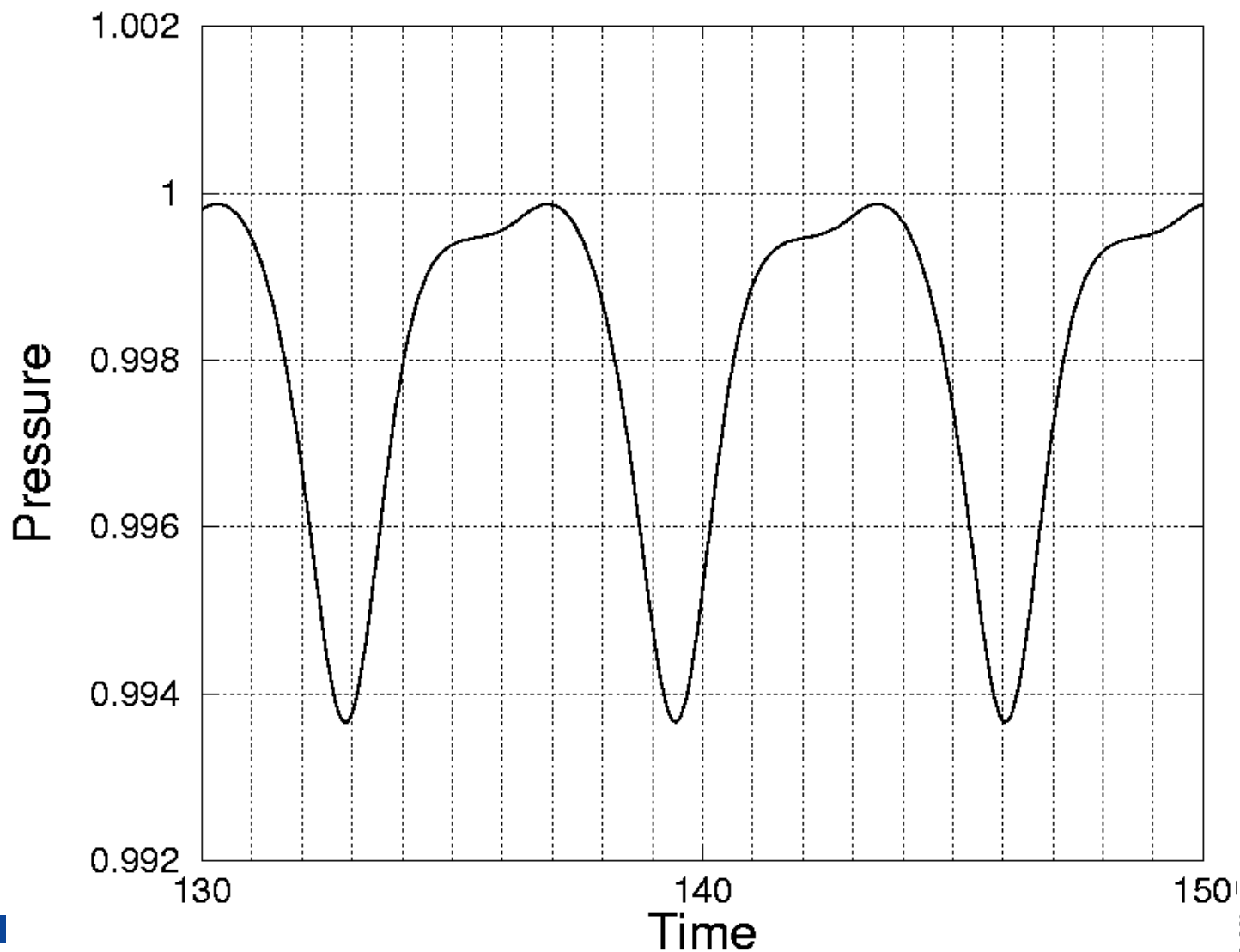


Pressure History at Point (5,1)





Pressure History at point (10,1)





Outline

- Lecture 3:
 - Boundary conditions
 - Discontinuity capturing
 - Limiter
 - Artificial viscosity



Subsonic Inlet BC

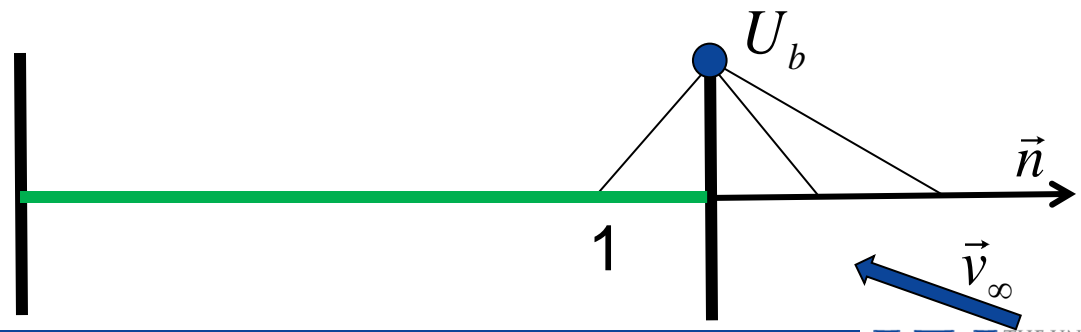
The 1D characteristic theory is applied in the normal direction (approximately)

Since $v_n = \vec{v}_\infty \cdot \vec{n} < 0$, there are two incoming and one outgoing characteristics

The three incoming Riemann invariants are:

$$p / \rho^\gamma, v_t, v_n - 2c / (\gamma - 1)$$

which can be fixed at the free stream value. The outgoing invariant $v_n + 2c / (\gamma - 1)$ is computed at the interior point 1.





Subsonic Inlet BC (cont.)

Since the tangential velocity does not affect the normal flux, the following equations are sufficient to determine the flux

$$p / \rho^\gamma = p_\infty / \rho_\infty^\gamma,$$

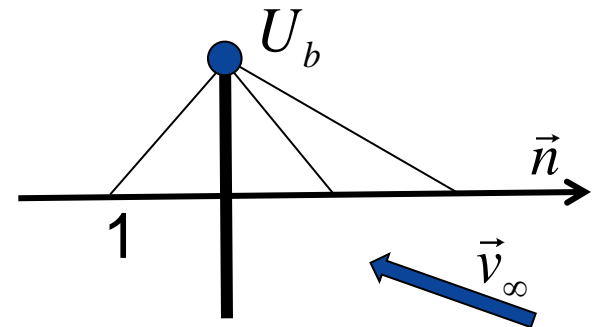
$$v_n - 2c / (\gamma - 1) = v_{\infty,n} - 2c_\infty / (\gamma - 1)$$

$$v_n + 2c / (\gamma - 1) = v_{1,n} + 2c_1 / (\gamma - 1)$$

Alternatively, the incoming acoustic invariant can be replaced by the total enthalpy

$$(E + p) / \rho = (E_\infty + p_\infty) / \rho_\infty$$

Finally the flux is computed using full flux $F^n(U_b)$





Subsonic Outlet BC

There are 3 outgoing and 1 incoming characteristics since $v_n = \vec{v} \cdot \vec{n} > 0$, only one physical condition can be fixed. One can either fix the incoming acoustic invariant or the exit pressure

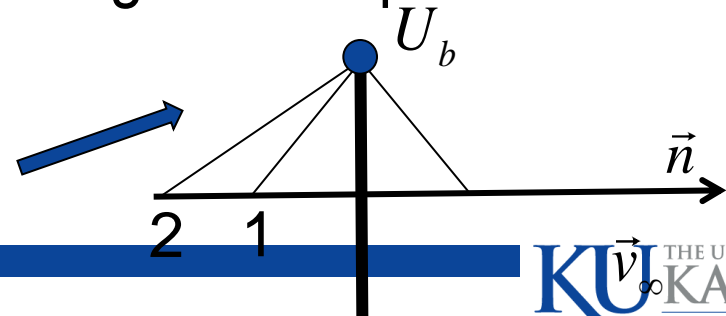
$$p / \rho^\gamma = p_1 / \rho_1^\gamma$$

$$v_n + 2c / (\gamma - 1) = v_{2,n} + 2c_2 / (\gamma - 1)$$

$$v_n - 2c / (\gamma - 1) = v_{exit,n} - 2c_{exit} / (\gamma - 1) \text{ or } p = p_{exit}$$

Then the full flux is computed using the computed solution

$$F^n(U_b)$$





Symmetry BC

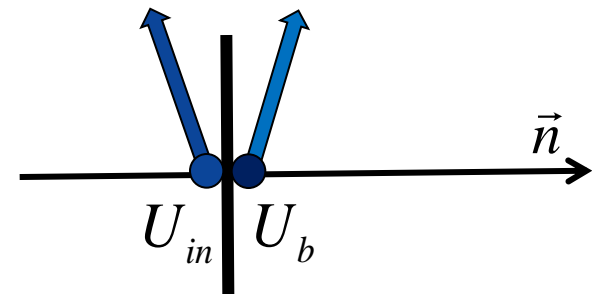
For a symmetry BC, in order to achieve full compatibility with interior cells, split flux is used, i.e., $\tilde{F}(U_{in}, U_b, \vec{n})$

where U_{in} is the reconstructed solution at the boundary face from the interior cell, and U_b is computed based on the symmetry condition, i.e.,

$$p_b = p_{in}$$

$$\rho_b = \rho_{in}$$

$$\vec{v}_b = \vec{v}_{in} - 2(\vec{v}_{in} \cdot \vec{n})\vec{n}$$

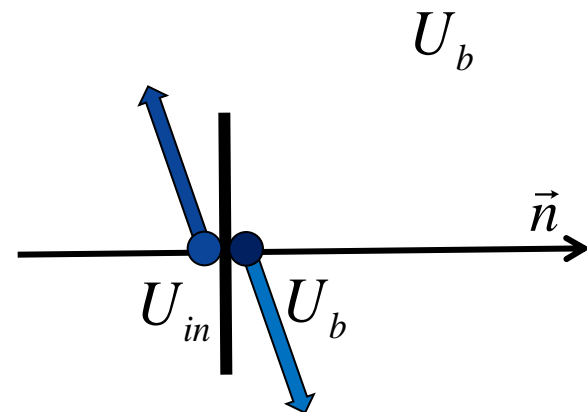




Wall BC

- Either full or split flux can be used for a wall BC.
 - At a wall, since the normal velocity vanishes, only a pressure term remains in the momentum flux. We could set the wall pressure to $p_b = p_{in}$
 - An inviscid wall is identical to the symmetry boundary condition using a split flux.
 - For a viscous wall assuming no-slip BC, the velocity is set at

$$\vec{v}_b = -\vec{v}_{in}$$





Shock Capturing

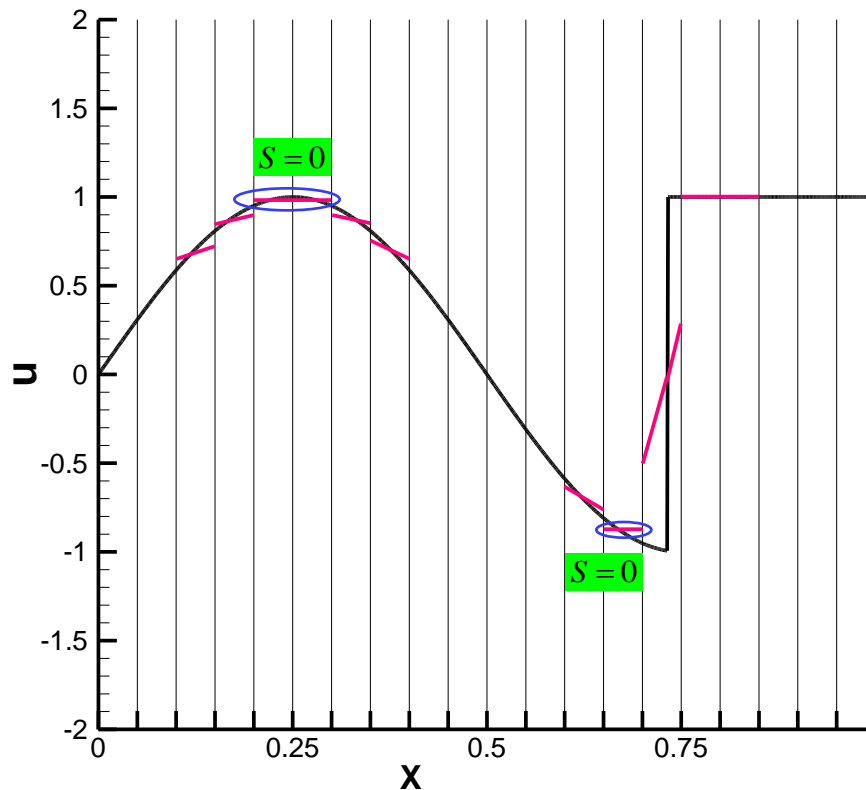
- Solution truly discontinuous
- Smooth features look like discontinuities due to a lack of resolution
- There are two approaches
 - Limiter – reconstruct the troubled cells to remove oscillations
 - Artificial viscosity – by adding a dissipation term near the shock wave





Problem:

- How to capture discontinuity sharply while preserving accuracy at local extrema?



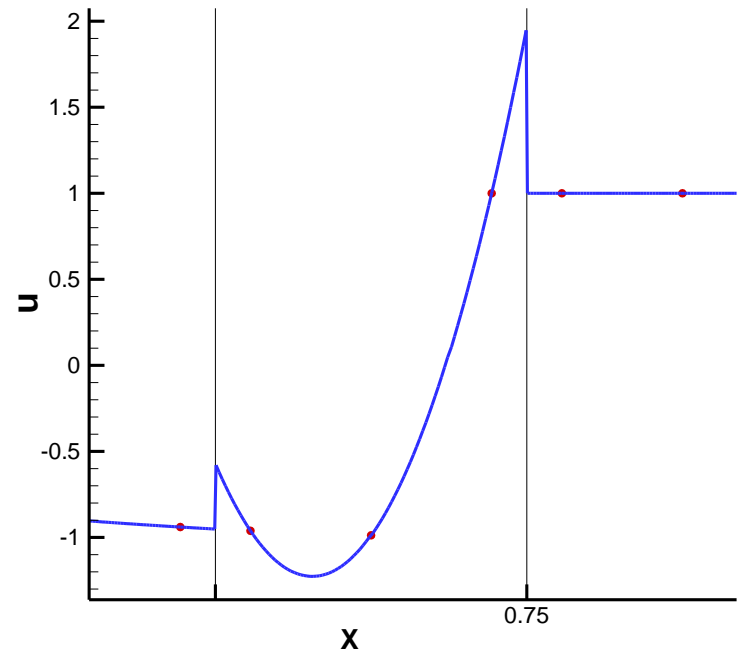
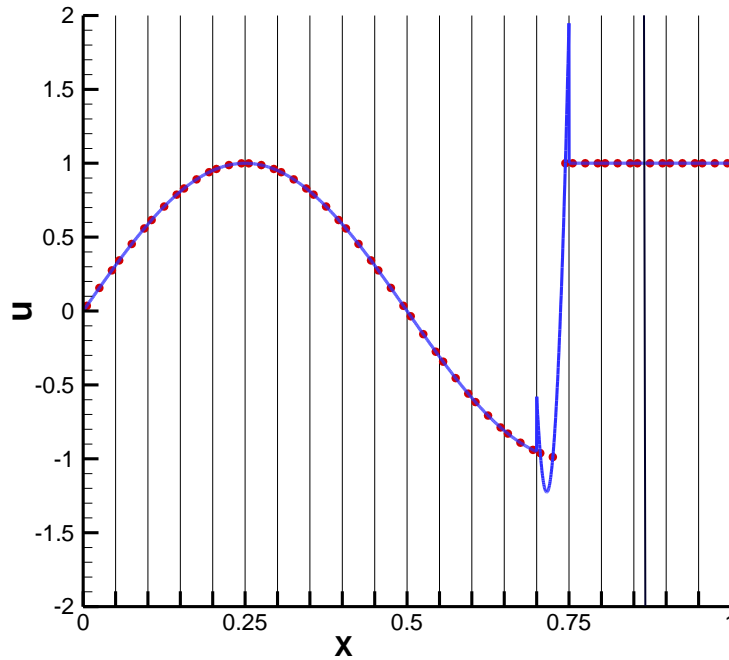
$p = 1$ (2nd order scheme)

$$S_i = \frac{1}{\Delta x} \min \text{mod}(\bar{u}_{i+1} - \bar{u}_i, \bar{u}_i - \bar{u}_{i-1})$$



Gibbs Phenomenon

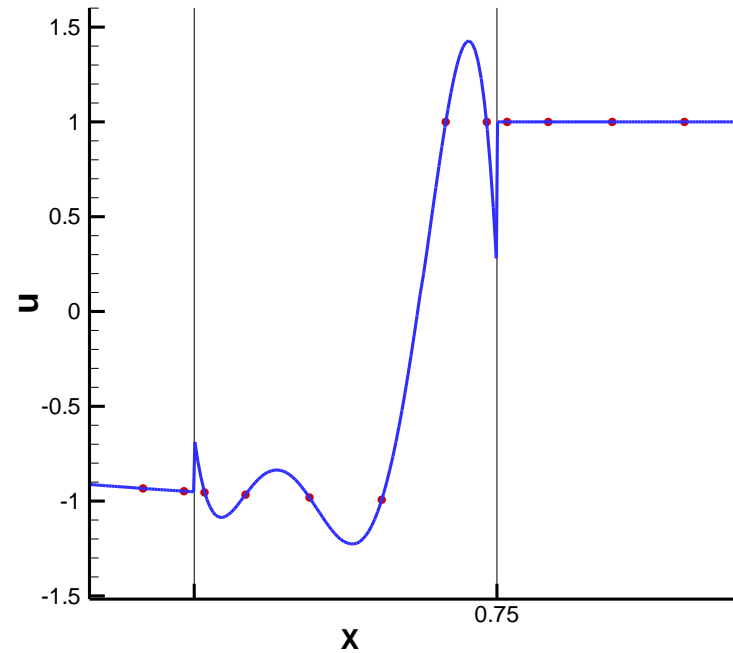
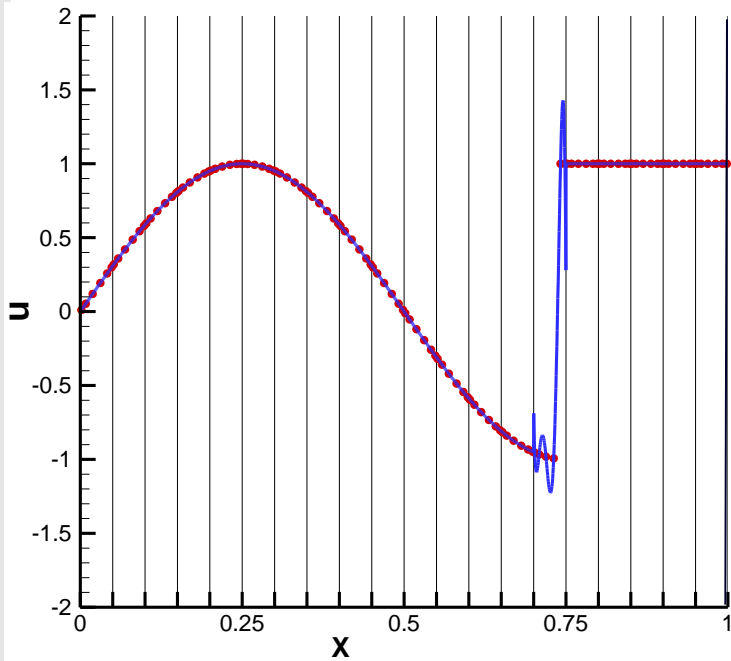
$P = 2$





Gibbs Phenomenon (cont.)

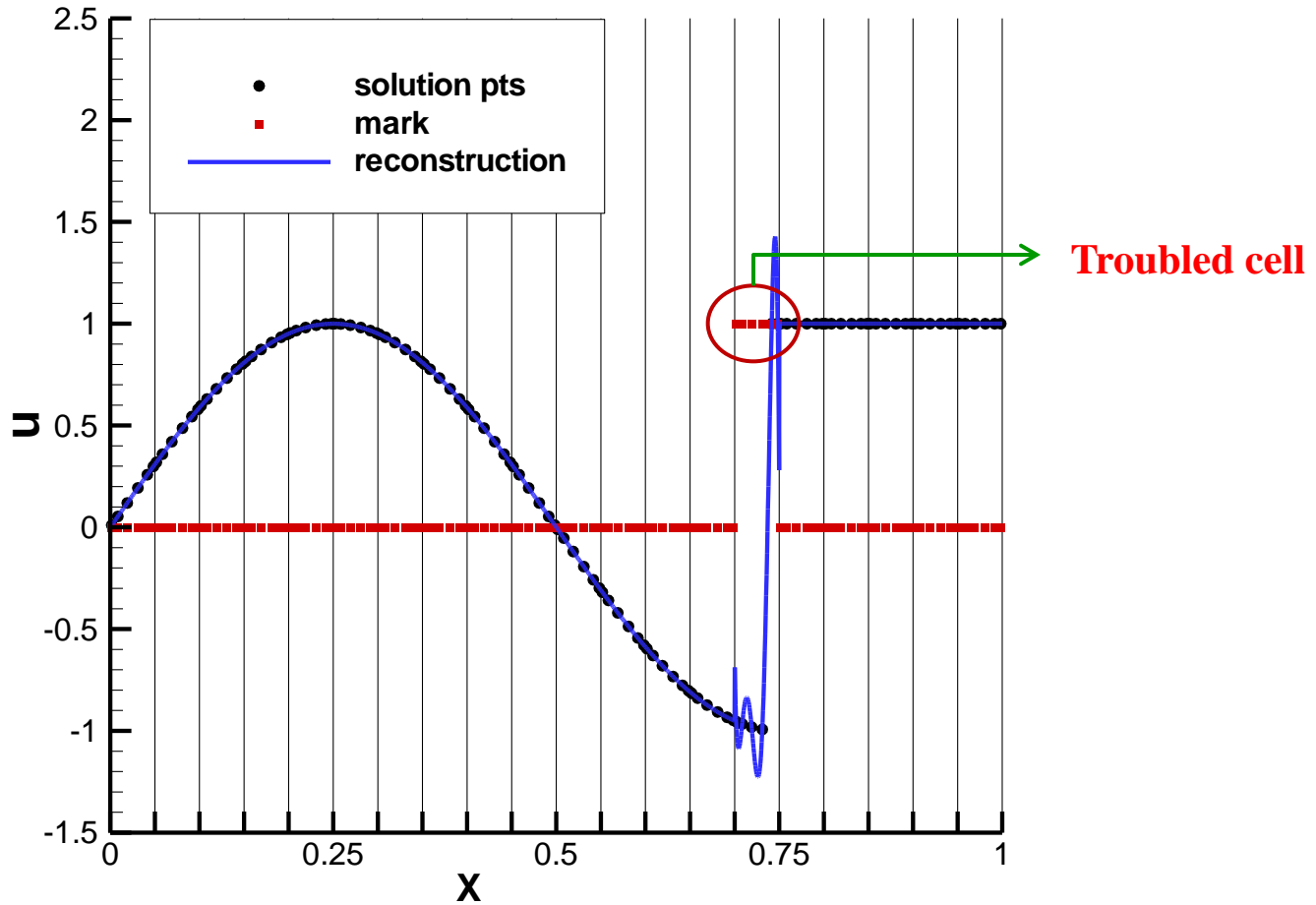
$$P = 5$$





Parameter-Free AP-TVD Marker

➤ Troubled cell method: Marker + Limiter





Parameter-Free Accuracy-Preserving TVD Marker

1) $\bar{u}_{\max,i} = \max(\bar{u}_{i-1}, \bar{u}_i, \bar{u}_{i+1})$ and $\bar{u}_{\min,i} = \min(\bar{u}_{i-1}, \bar{u}_i, \bar{u}_{i+1})$

If $u_{j,i} > 1.001 \cdot \bar{u}_{\max,i}$ or $u_{j,i} < 0.999 \cdot \bar{u}_{\min,i}$, ($j = 1, p + 2$)

then cell i is considered as a **possible** troubled cell.

2) $\tilde{u}_i^{(2)} = \min \text{mod}(\bar{u}_i^{(2)}, \beta \frac{\bar{u}_{i+1}^{(1)} - \bar{u}_i^{(1)}}{x_{i+1} - x_i}, \beta \frac{\bar{u}_i^{(1)} - \bar{u}_{i-1}^{(1)}}{x_i - x_{i-1}})$. (for $p > 1$)

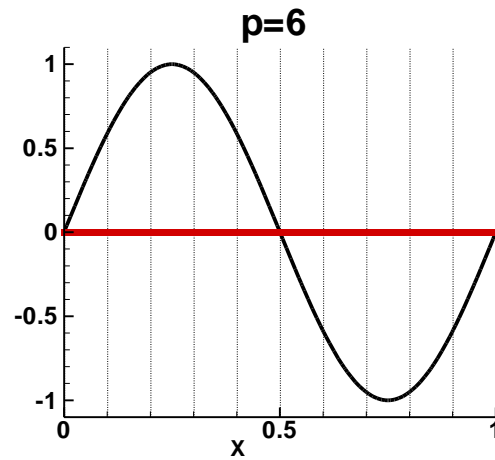
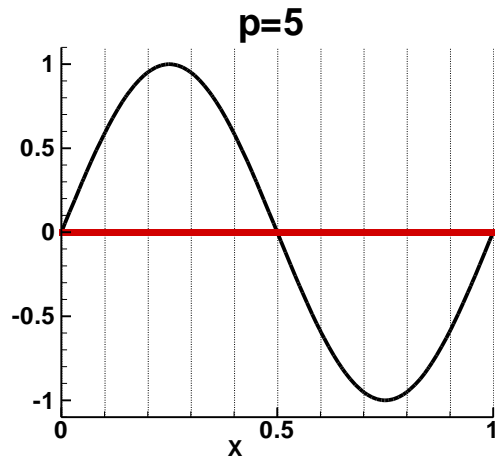
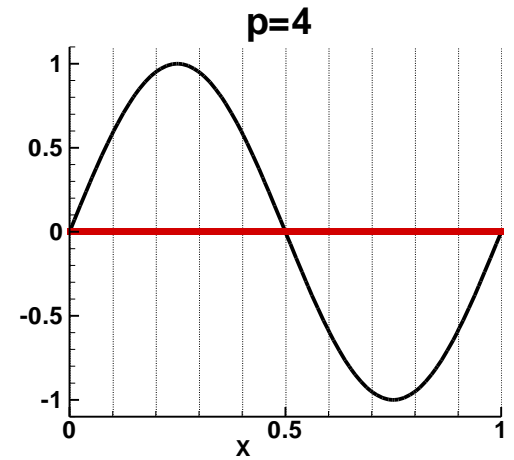
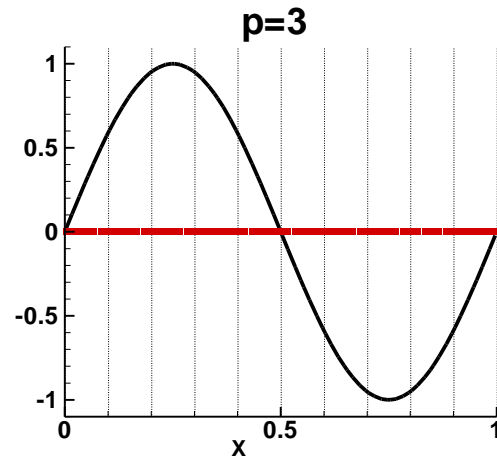
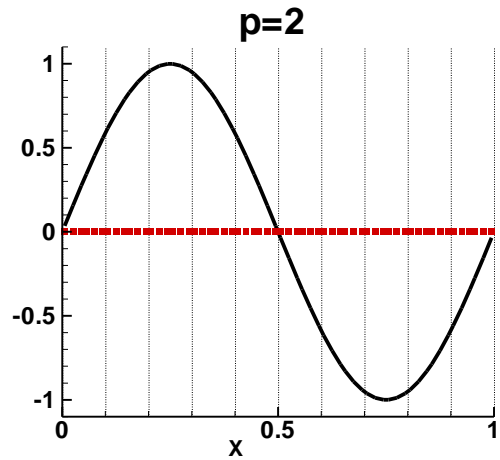
If $\tilde{u}_i^{(2)} = \bar{u}_i^{(2)}$, then cell i is **unmarked** as a troubled cell;

Otherwise cell i is **confirmed** as a troubled cell.

$(\beta = 1.5)$

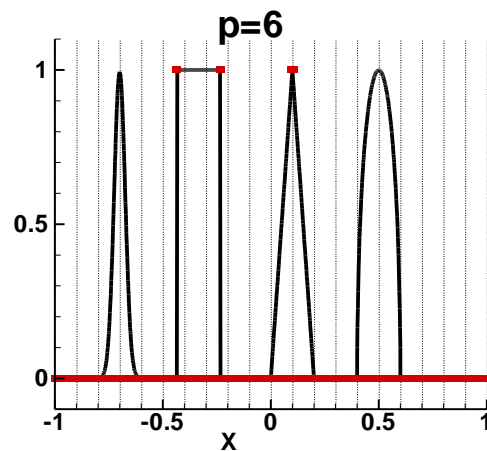
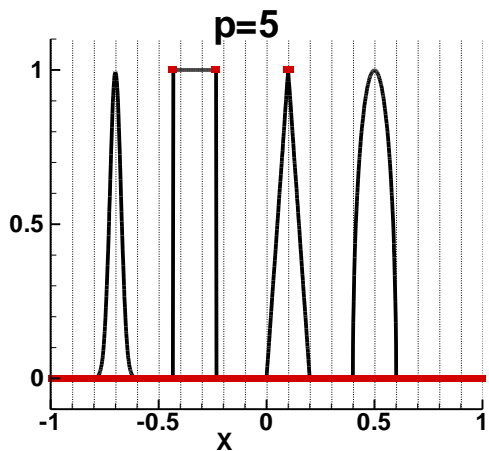
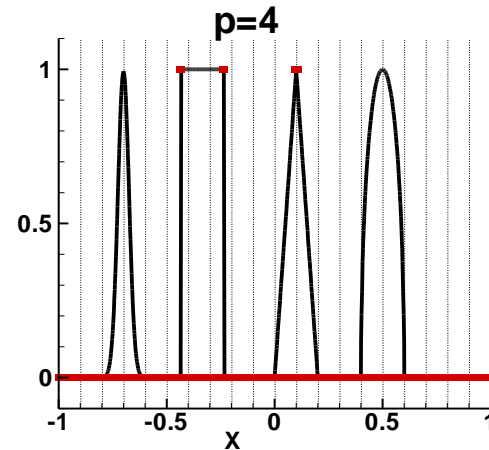
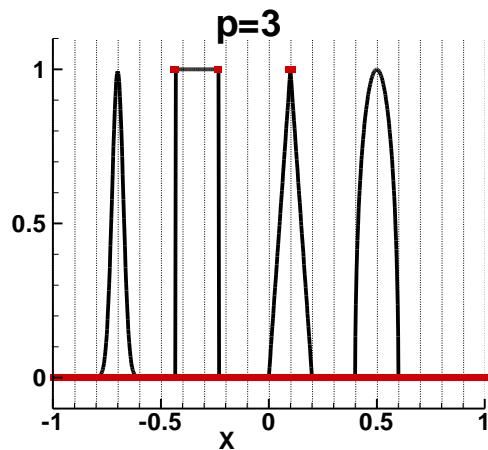
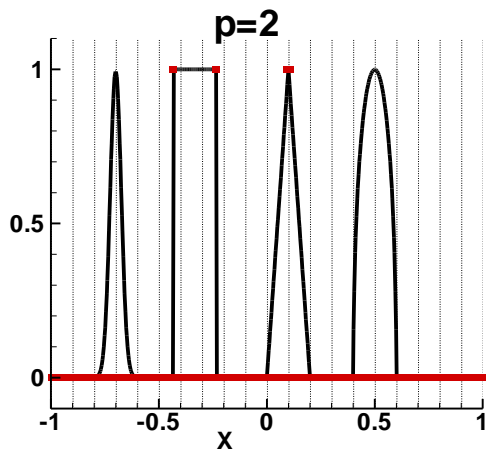


Parameter-Free AP TVD Marker



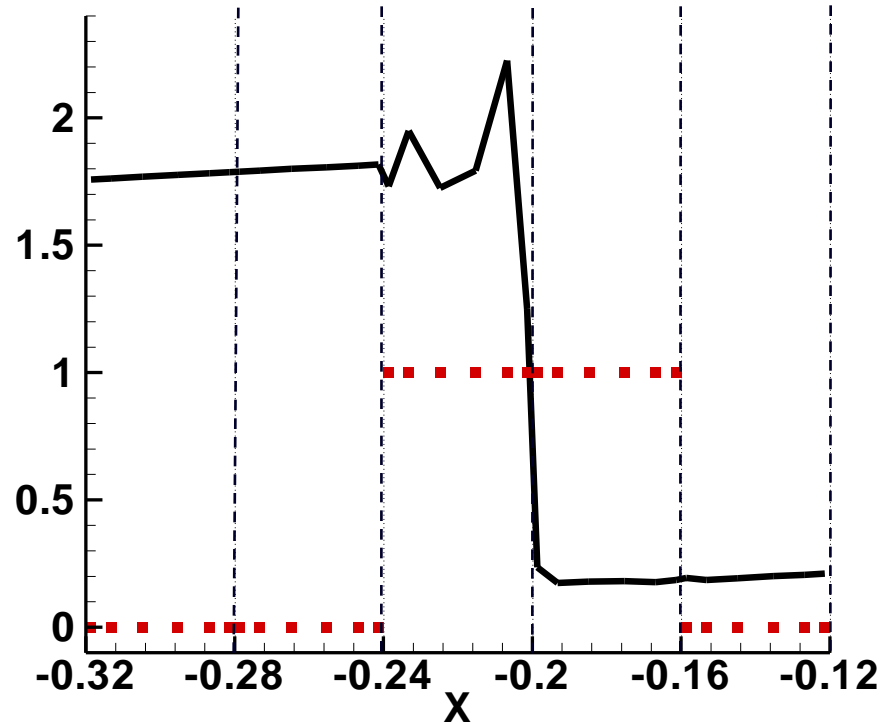


Parameter-Free AP TVD Marker





Parameter-Free AP TVD Marker





Generalized Moment Limiter: 1D

If cell i has been marked as a troubled cell, then

(1) Reconstruction

$$\begin{aligned}u_i(x) = & \bar{u}_i + \bar{u}_i'(x - x_i) \\ & + \frac{1}{2} \bar{u}_i^{(2)} [(x - x_i)^2 - \frac{1}{12} h_i^2] \\ & + \frac{1}{6} \bar{u}_i^{(3)} [(x - x_i)^3 - \frac{1}{4} h_i^2 (x - x_i)] \\ & + \frac{1}{24} \bar{u}_i^{(4)} [(x - x_i)^4 - \frac{1}{2} h_i^2 (x - x_i)^2 + \frac{7}{240} h_i^4] \\ & + \dots\end{aligned}$$

Functional Equivalent to the original solution polynomial



Generalized Moment Limiter: 1D

(2) Hierarchically Limiting

$$\bar{Y}_i^{(p)} = \min \text{mod} \left(\bar{u}_i^{(p)}, \beta \frac{\bar{u}_{i+1}^{(p-1)} - \bar{u}_i^{(p-1)}}{x_{i+1} - x_i}, \beta \frac{\bar{u}_i^{(p-1)} - \bar{u}_{i-1}^{(p-1)}}{x_i - x_{i-1}} \right).$$

If $\bar{Y}_i^{(p)} = \bar{u}_i^{(p)}$, then **NO** limiting for (1).

Otherwise,

$$\bar{Y}_i^{(k)} = \min \text{mod} \left(\bar{u}_i^{(k)}, \beta \frac{\bar{u}_{i+1}^{(k-1)} - \bar{u}_i^{(k-1)}}{x_{i+1} - x_i}, \beta \frac{\bar{u}_i^{(k-1)} - \bar{u}_{i-1}^{(k-1)}}{x_i - x_{i-1}} \right), \quad (k = p - 1)$$

$$\bar{Y}_i^{(k)} \stackrel{?}{=} \bar{u}_i^{(k)} \quad (k = p - 1).$$

Yes. \rightarrow **NO** further limiting

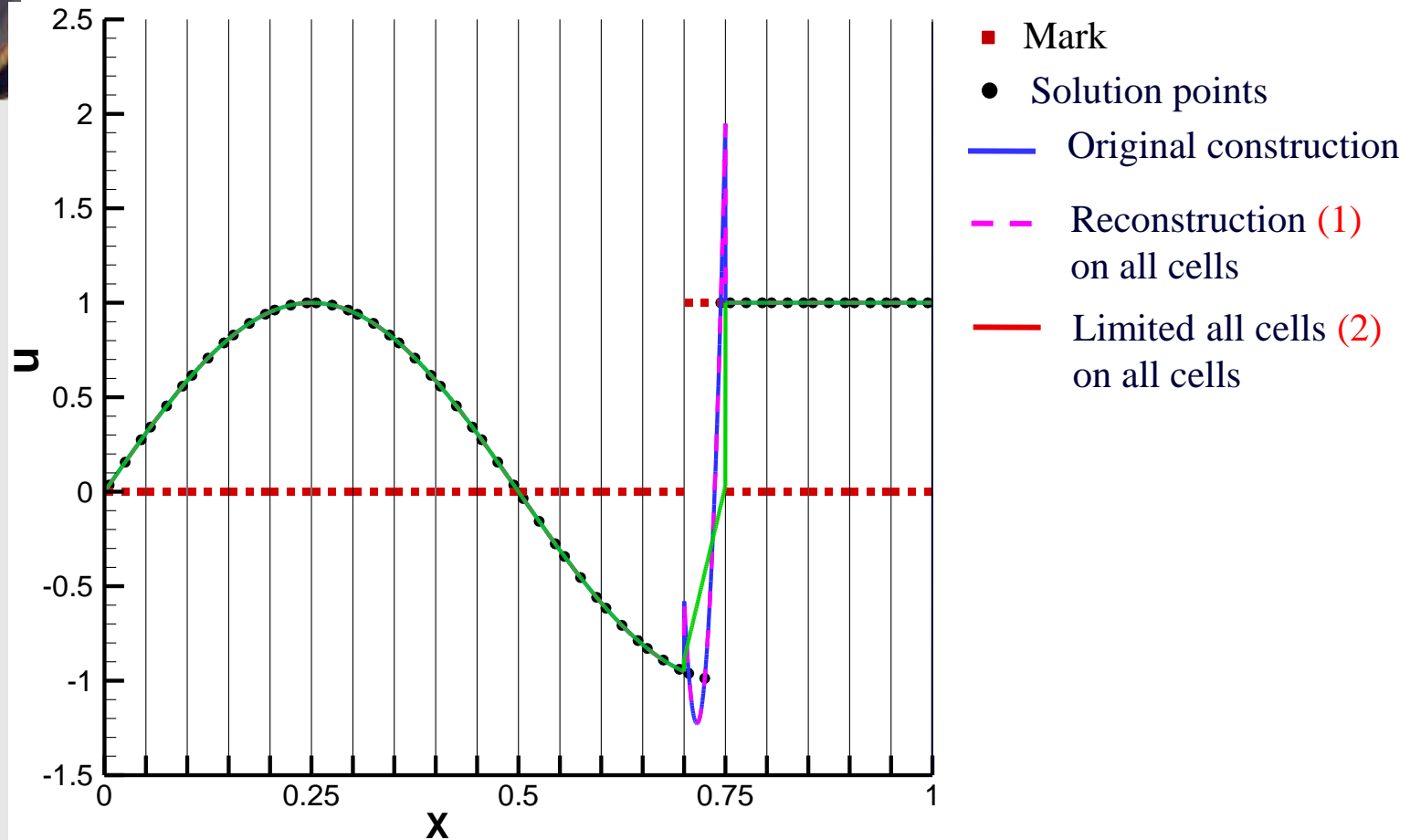
NO. \rightarrow **Do limiting and check for** $k = p - 2$

.....



Generalized Moment Limiter

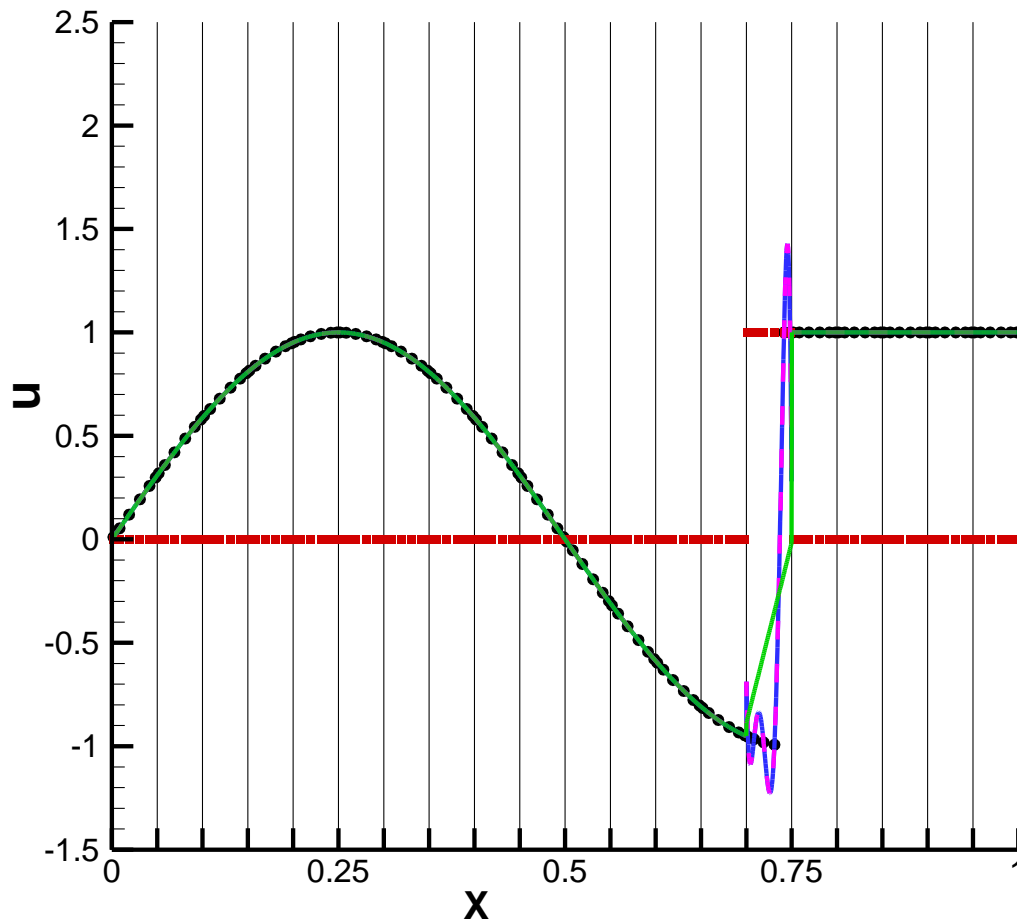
➤ $P = 2$





Generalized Moment Limiter

Example: $p = 5$

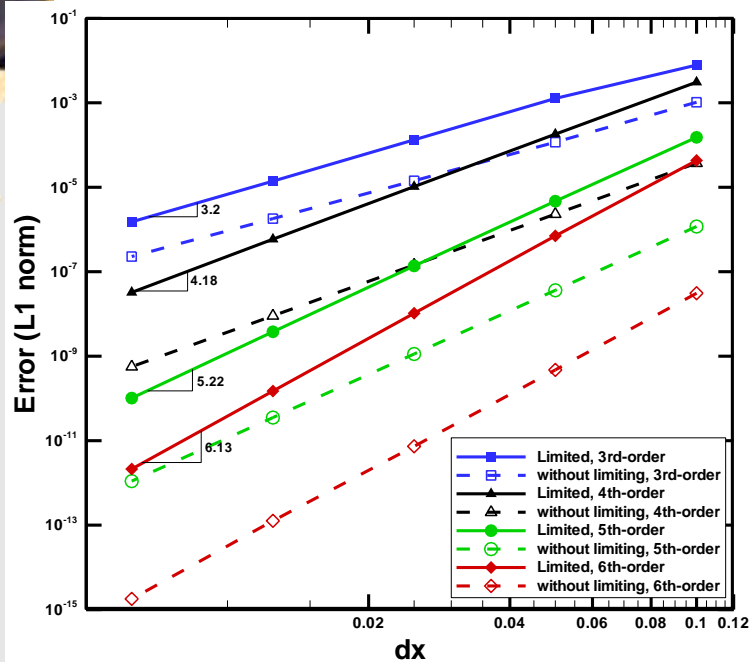


- Mark
- Solution points
- Original construction
- - - Reconstruction (1) on all cells
- - - Limiting (2) on all cells



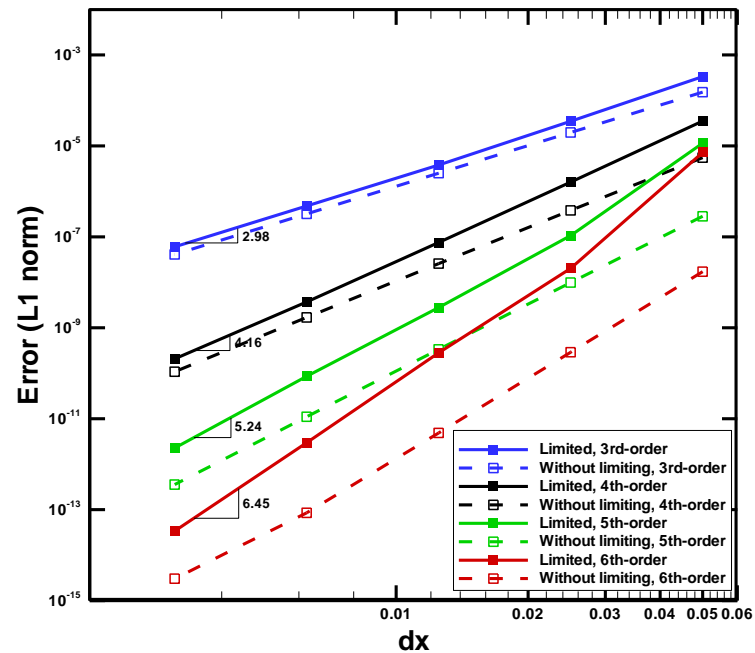
Numerical Tests

1. Accuracy study



Linear Advection Equation

$$u_t + u_x = 0$$



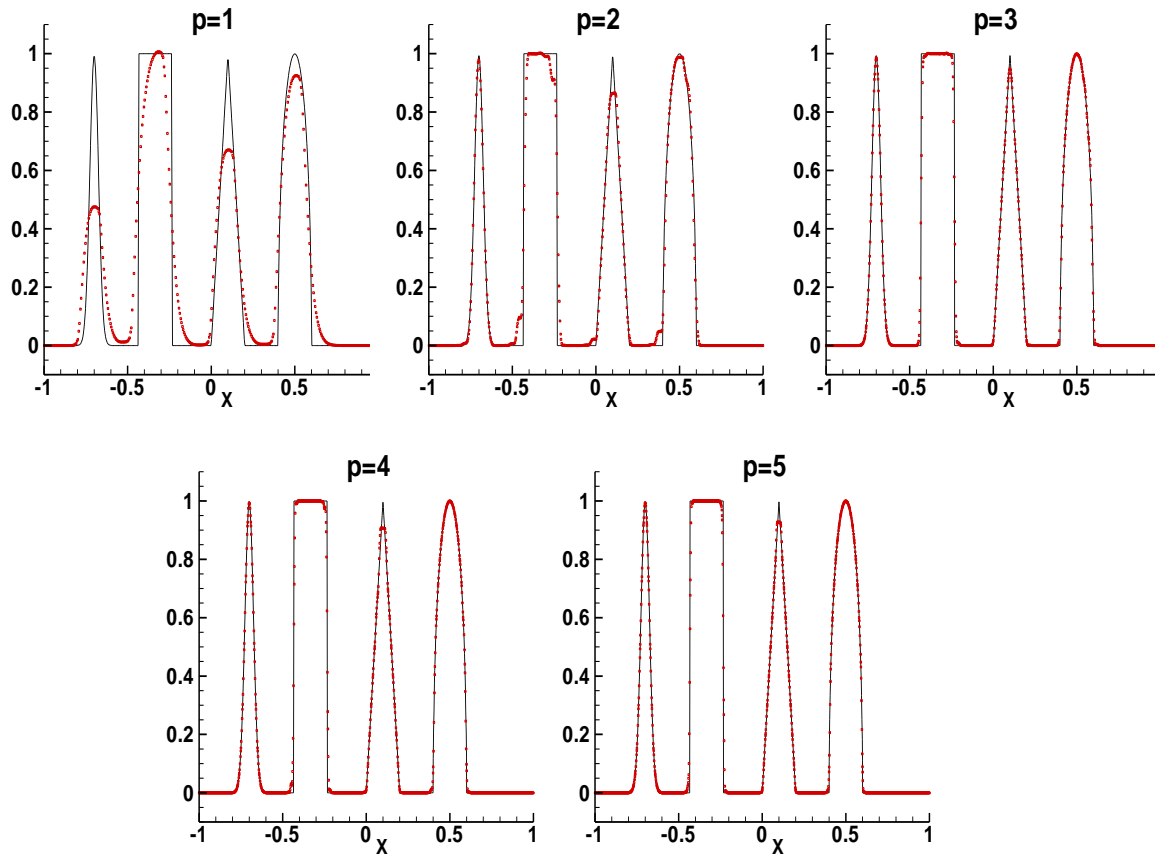
Non-Linear Burgers Equation

$$u_t + (u^2 / 2)_x = 0$$



Numerical Tests

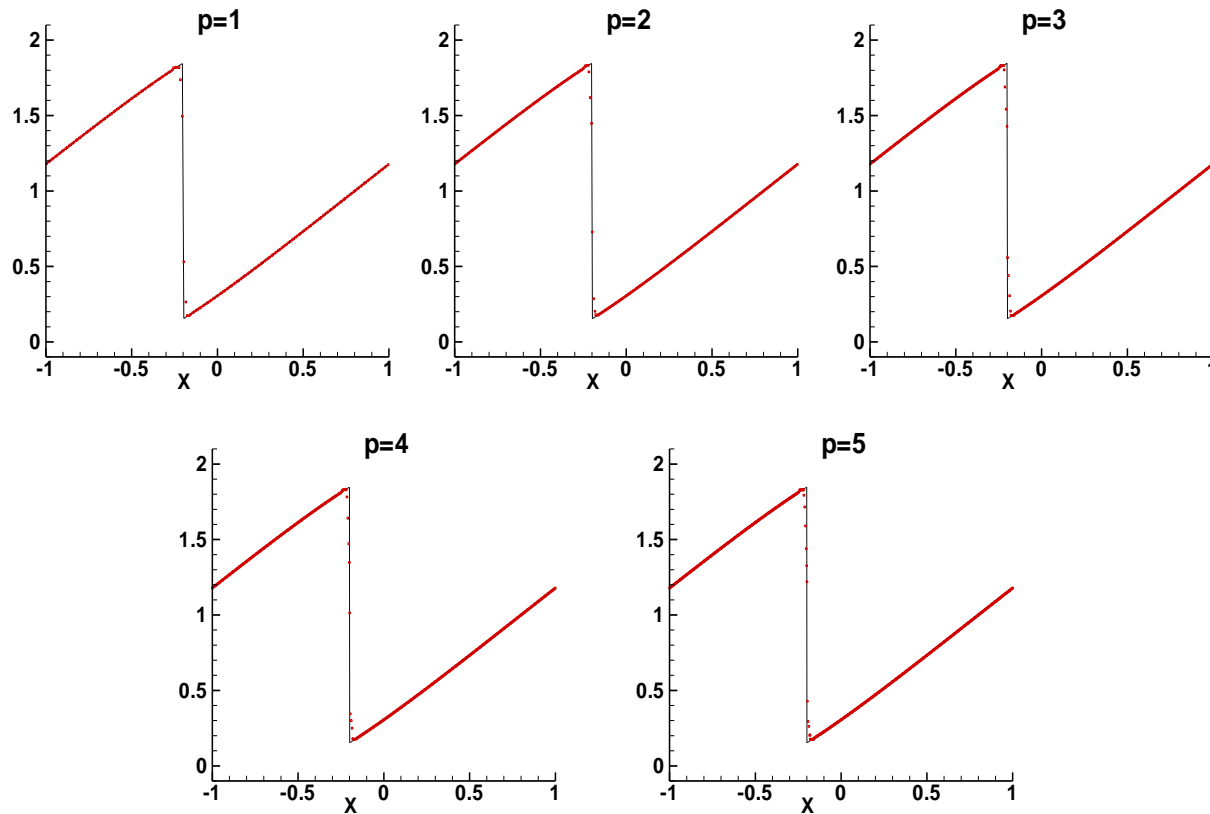
2. 1D Discontinuity with $u_t + u_x = 0$





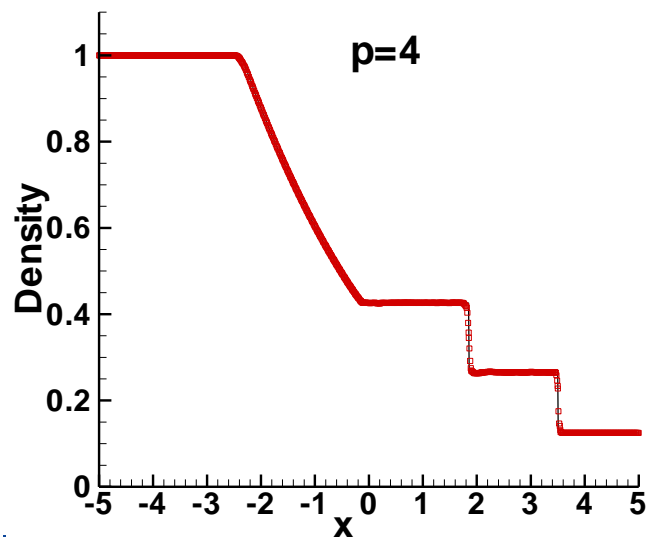
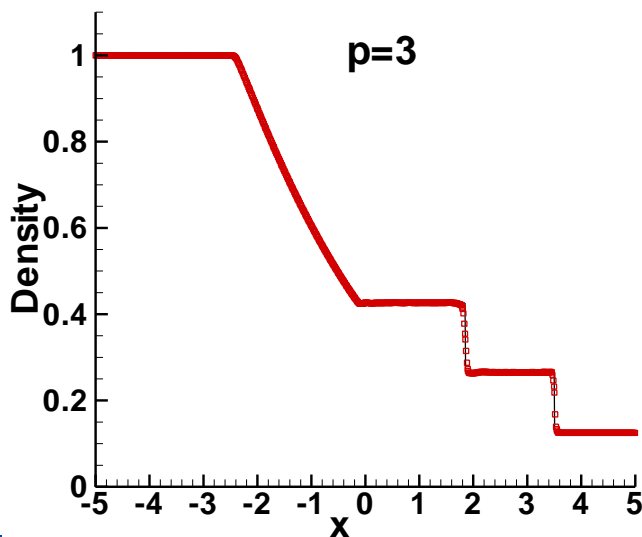
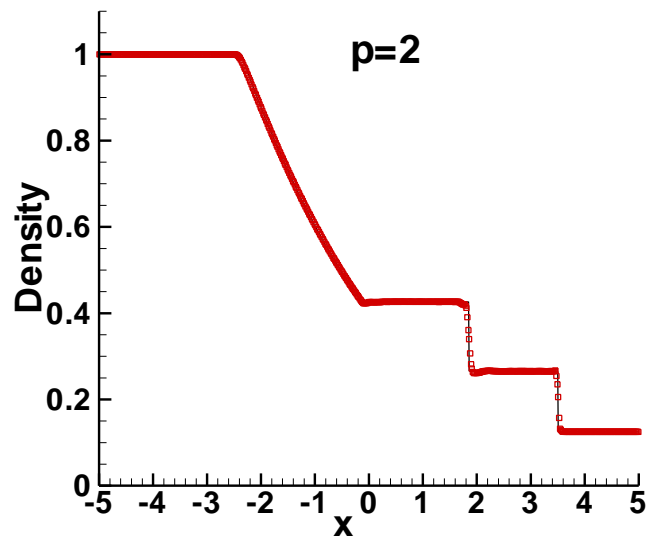
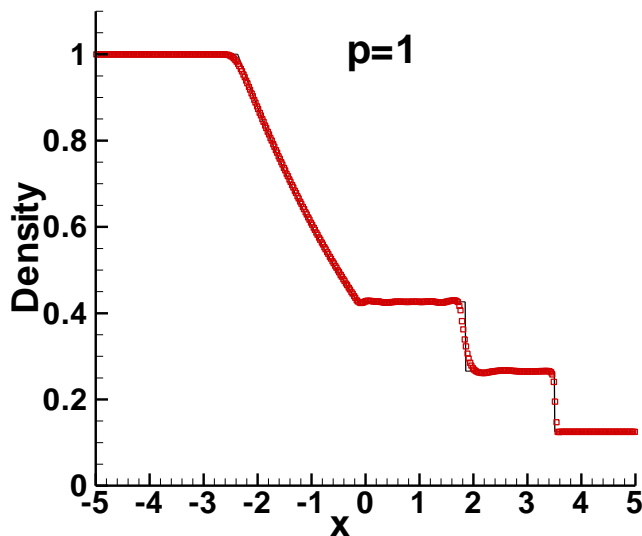
Numerical Tests

3. 1D Burgers Equation $u_t + (u^2 / 2)_x = 0$



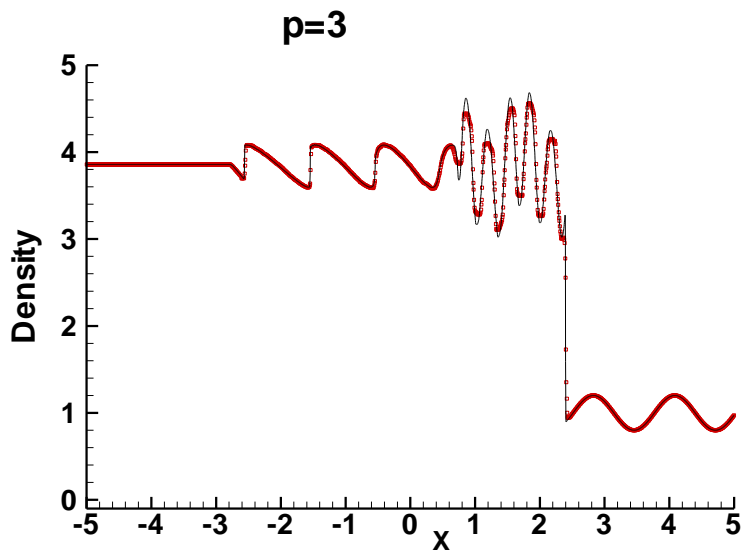
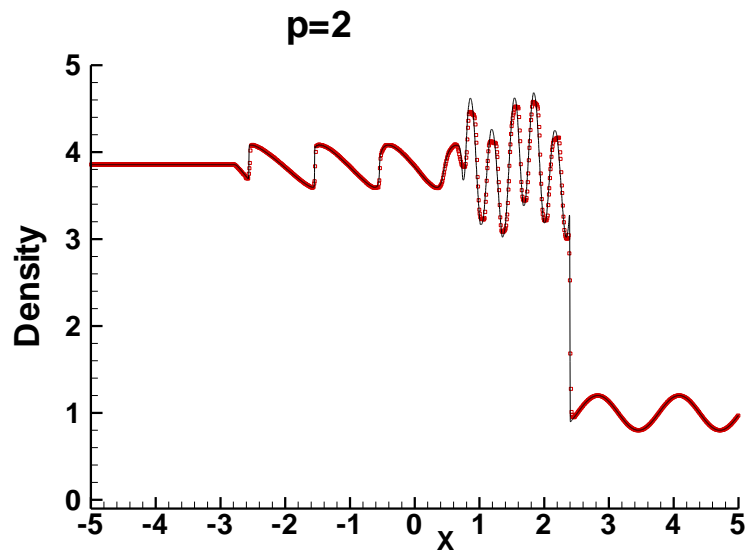
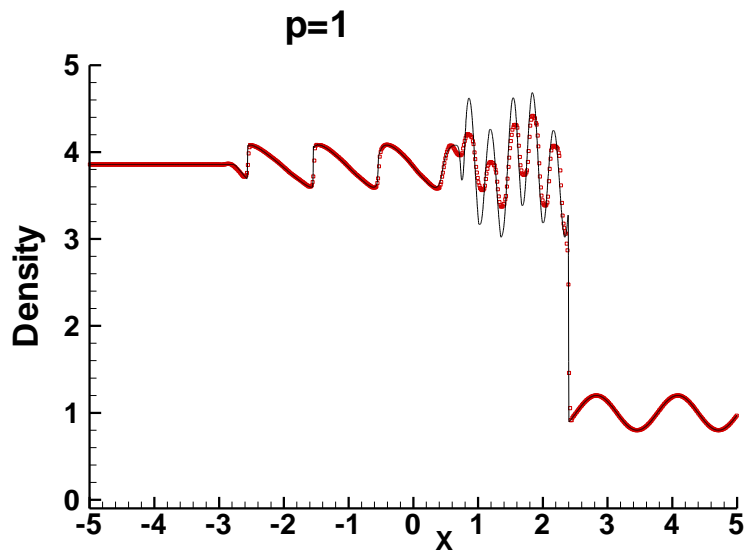


Sod Shock Tube Problem





Shock Acoustic-Wave Interaction

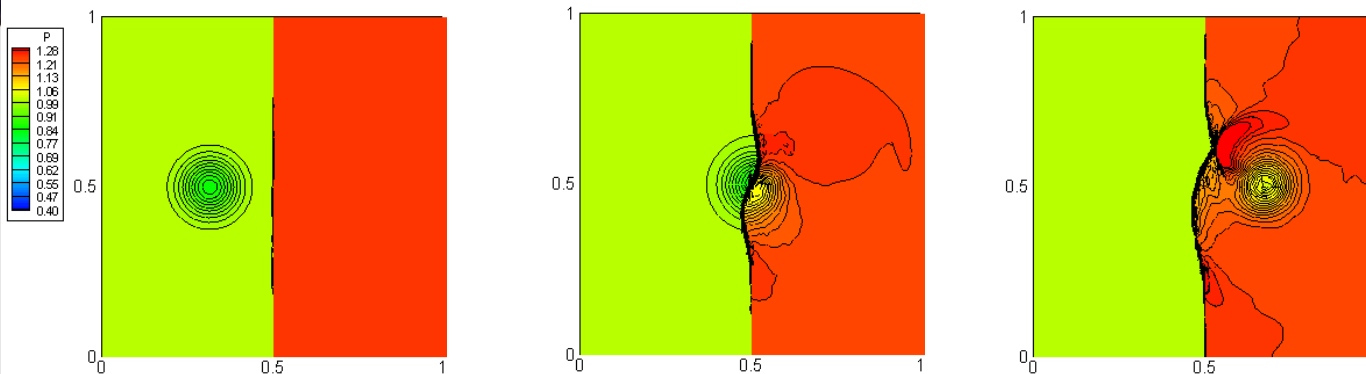




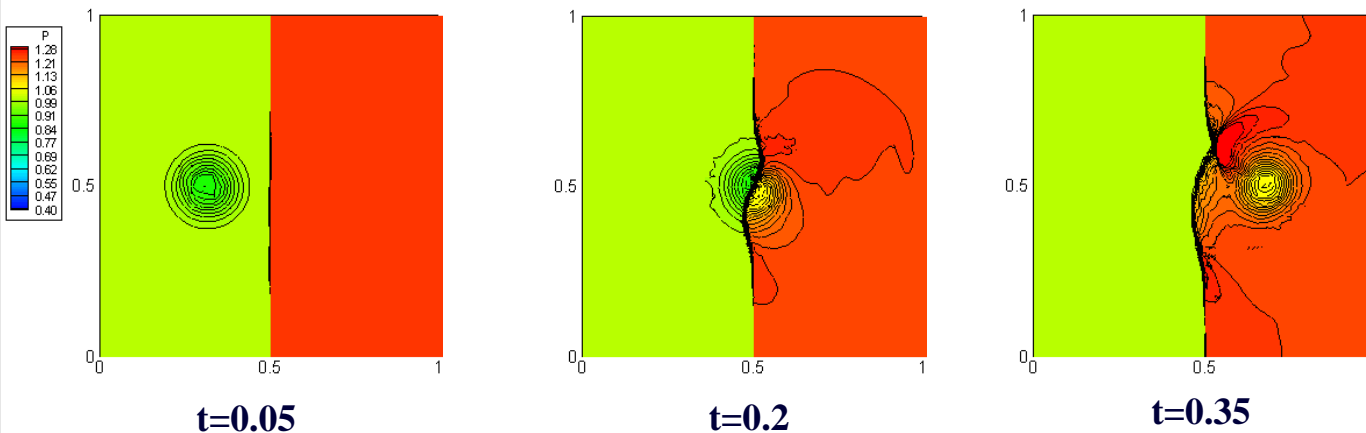
Numerical Tests

6. 2D shock vortex interaction

3rd-order PFGM Limiter



Linear Limiter



t=0.05

t=0.2

t=0.35



Localized Laplacian Artificial Viscosity

$$\frac{\partial Q}{\partial t} + \nabla \cdot \mathbf{F}^{inv}(Q) = \nabla \cdot \mathbf{F}^{av}(Q, \nabla Q)$$

Laplacian: $\mathbf{F}^{av}(Q, \nabla Q) = \varepsilon \nabla Q$

For each element e :

$$\varepsilon_e = \begin{cases} 0 & \text{if } S_e < S_0 - \kappa \\ \frac{\varepsilon_0}{2} \left(1 + \sin \frac{\pi(S_e - S_0)}{2\kappa} \right) & \text{if } S_0 - \kappa \leq S_e \leq S_0 + \kappa \\ \varepsilon_0 & \text{if } S_e > S_0 + \kappa. \end{cases}$$

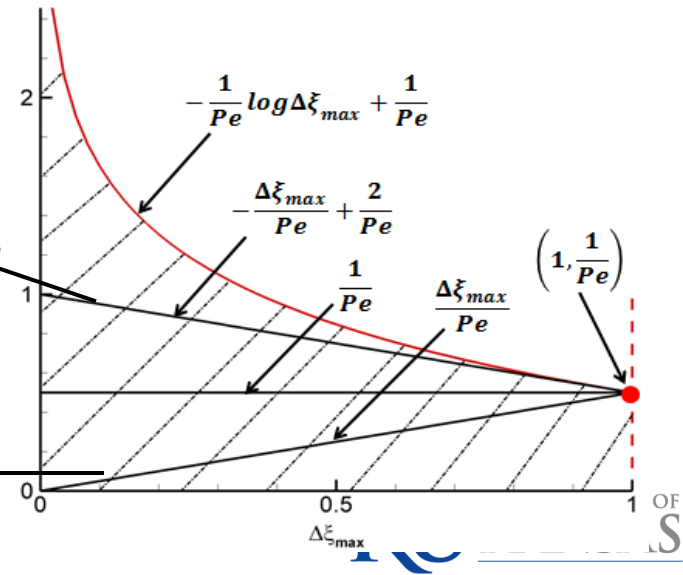
Parameters in ε_e :

$$\varepsilon_0 = f(\Delta \xi_{max}) \cdot h \cdot |\lambda|_{max}$$

$$S_e = \log_{10} \frac{\langle U - U^p, U - U^p \rangle_e}{\langle U, U \rangle_e}$$

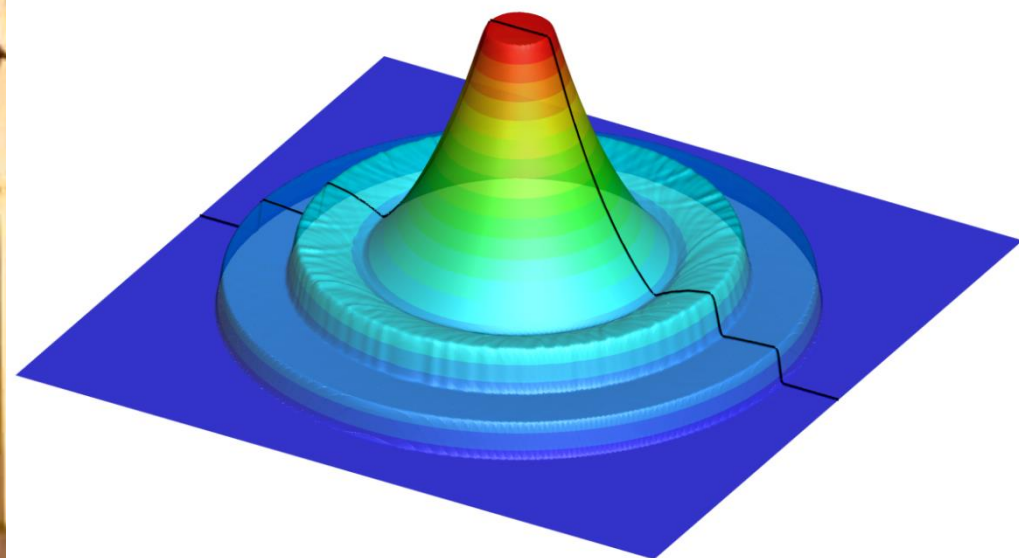
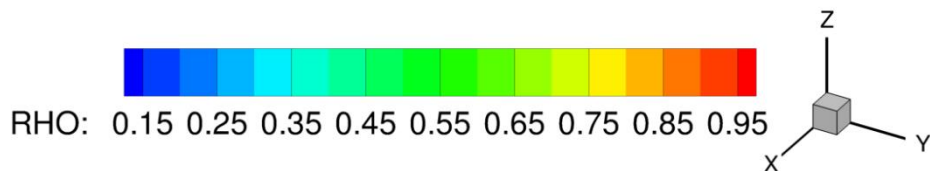
Adopted in current study

P.-O. Persson & J. Peraire

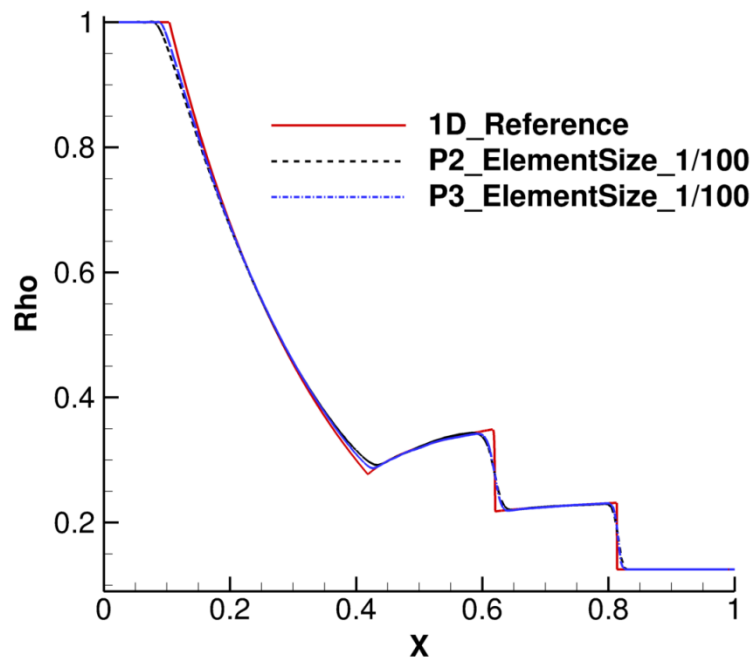




2D Explosion



Density at $t=0.25s$



Comparison of density distribution

P^3 reconstruction (4th order), $t \in [0, 0.25s]$

Computational domain $[-1,1] \times [-1,1]$, 100×100 elements

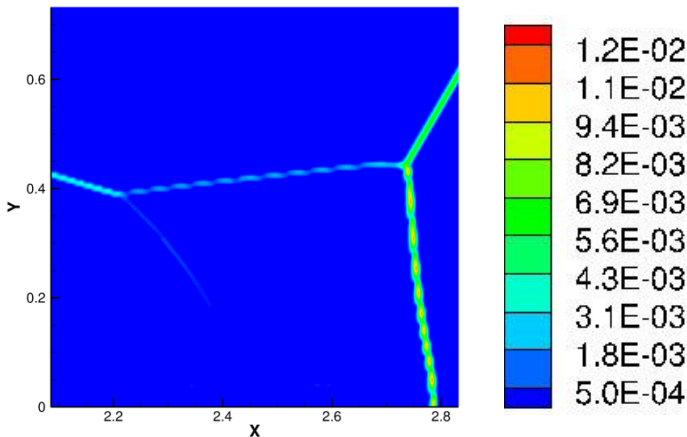


Double Mach Reflection

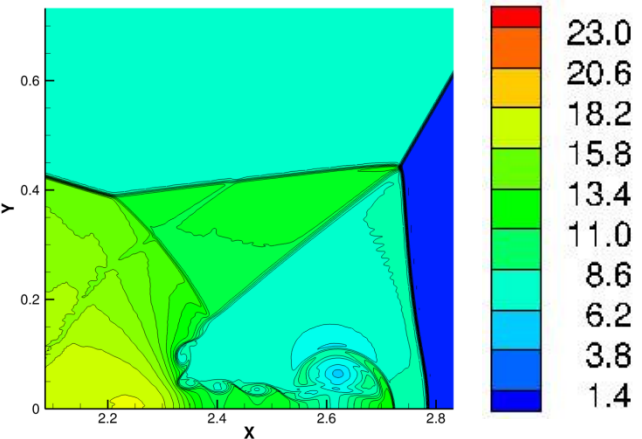
Density



Artificial viscosity at $t=0.2s$



Density at $t=0.2s$

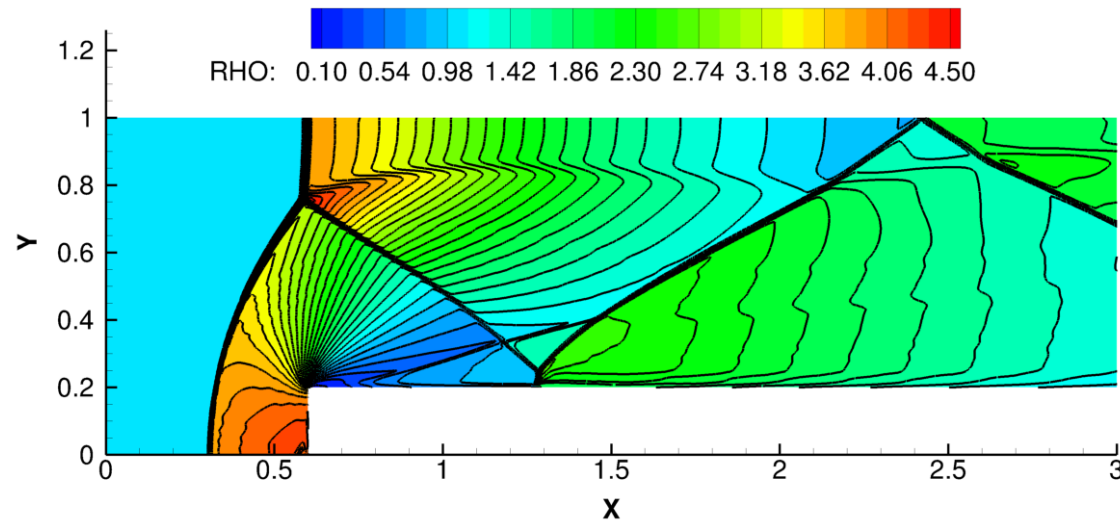


$Ma = 10$, P^3 reconstruction (4th order), $t \in [0, 0.2s]$

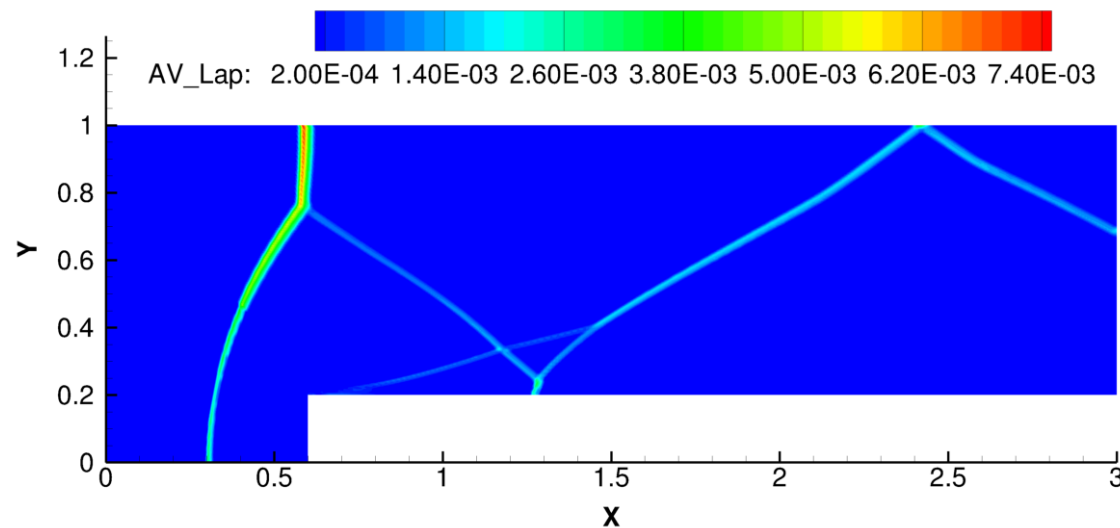
Computational domain $[0,4] \times [0,1]$, 816×204 elements



Ma 3 Wind Tunnel with a Foreword Step



Density at t=4s

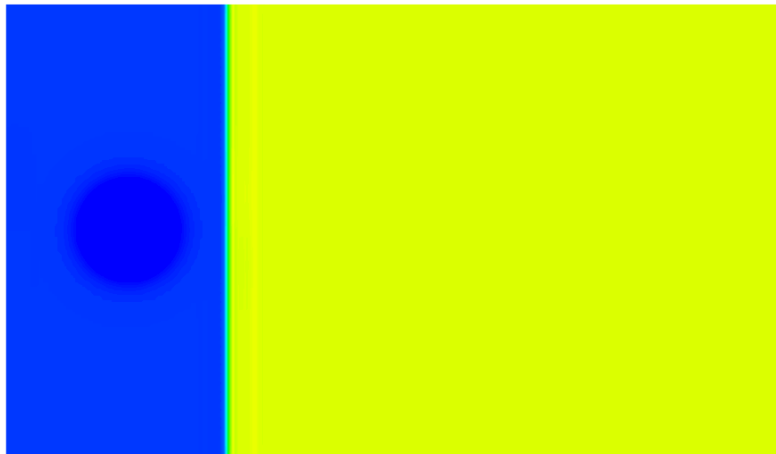
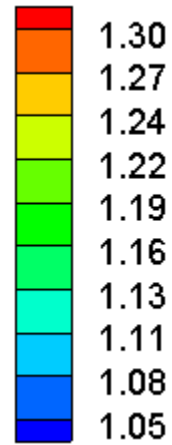


Artificial viscosity at t=4s

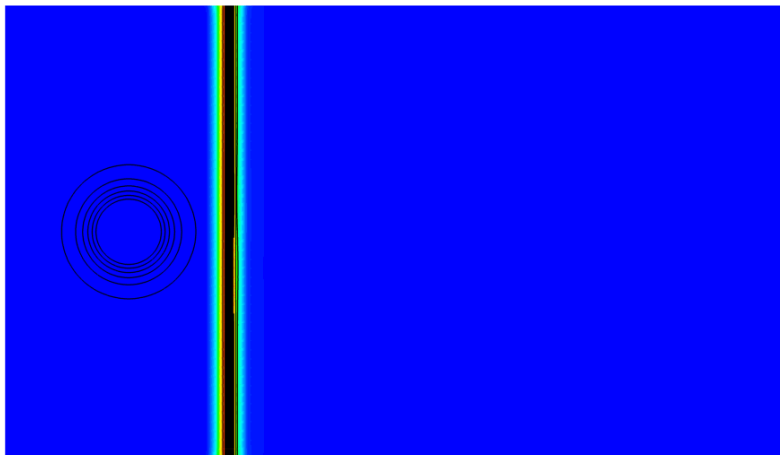
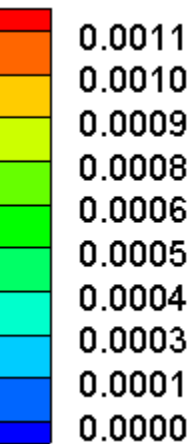
Free stream $Ma = 3$,
 P^2 reconstruction (3rd
order),
Grid size: 1/80, with
clustered elements of
size 1/320 near the
sharp corner.



Shock-Vortex Interaction



Pressure



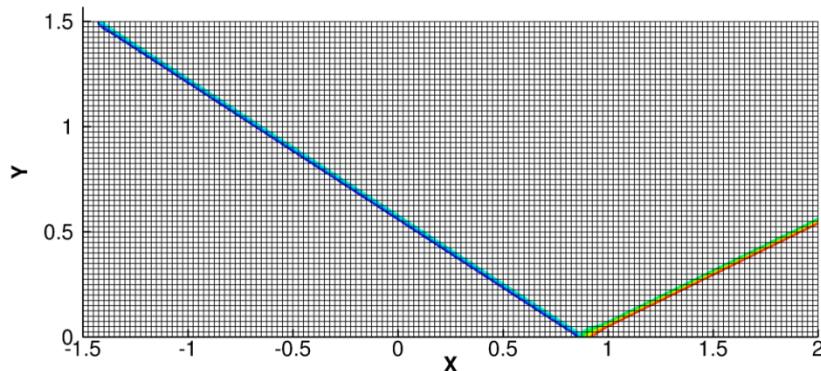
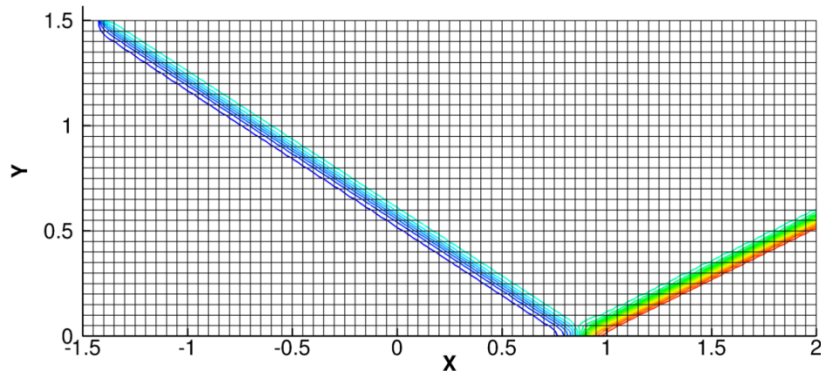
Artificial viscosity

Free stream $Ma = 1.1$,
 P^3 reconstruction (4th order),
Computational domain:
 $[0,2] \times [0,1]$,
 100×50 elements.

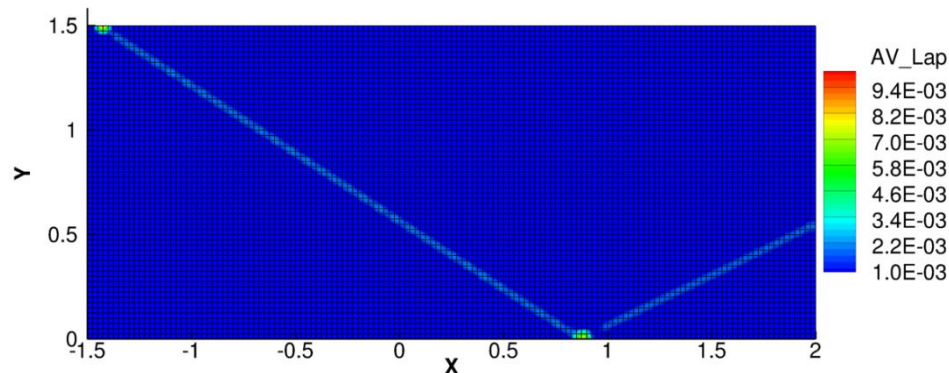
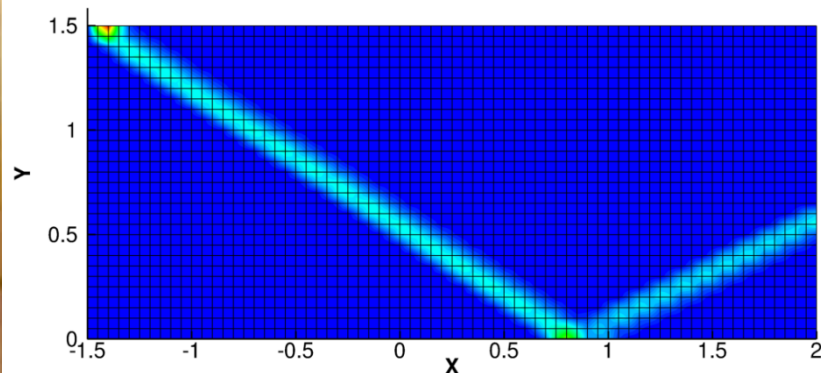
Small isentropic vortex is
superposed to the supersonic
flow.



Ma 3 Oblique Shock



Pressure



Artificial viscosity

Ma =3, P^2 reconstruction
(3rd order), Grid size 1/20

Ma =3, P^4 reconstruction
(5th order), Grid size 1/40



Outline

- Lecture 4:
 - Verification and Validation
 - Solution based hp-adaptations
 - Sample demonstration problems
 - Summary



Introduction

- ❖ Verification: The process of determining that a model implementation accurately represents the developer's conceptual description of the model and the solution to the model
- ❖ Validation: The process of determining the degree to which a model is an accurate representation of the real world from the perspective of the intended uses of the model. (AIAA G-077-1998) – comparison with experimental data



How to Verify Your Code

- ❖ Closure condition of your control volume

$$\oiint_{\partial V_i} \vec{n} dS = 0$$

- ❖ Free-stream preservation (extrapolation boundary condition everywhere)

$$R(Q) = 0$$

- ❖ Exactly preserve a polynomial of a certain degree
- ❖ Accuracy study with grid refinement

$$p = \frac{\ln(\text{Error}_{\Delta x} / \text{Error}_{\Delta x/2})}{\ln(2)}$$



Problems with Analytical Solutions

- Many cases are included in the 1st International Workshop on High-Order CFD Methods (<http://zjwang.com/hiocfd.html>)
 - Vortex propagation
 - Ringleb flow
 - Subsonic inviscid flow: entropy is constant
- Manufactured solutions



Selected Results – hp-Adaptations

- Discretization error reduction
 - P-enrichment: smooth flow regions (Weierstrass theorem)
 - H-refinement: geometry or flow singularities
 - Anisotropic adaptation: shear layers, shocks,...
- Adaptation criteria/error indicators
 - Feature-based: simple, ad hoc, less rigorous
 - Residual-based: may lead to false refinements
 - Adjoint-based: adapt the mesh in regions affecting the output, and estimate the error in the output



Review of Adjoint-Based Adaptive Methods

Adjoint-based adaptive methods

Dynamically distribute computer resources to regions which are important for predicting engineering outputs

Current status of the output-based adaptation methods

- 2D/3D complex geometry
- Steady/unsteady
- Euler/NS/RANS
- Anisotropic hp-adaptations

[Giles and Pierce,1997; Becker and Rannacher,2001; Venditti and Darmofal, 2002; Hartmann and ouston,2002; Nielsen et al, 2004; Fidkowski and Darmofal,2007; Hartmann,2007; Mani and Mavriplis, 2007; Nemeć et al, 2008; Park, 2008; Wang and Mavriplis,2009; Oliver and Darmofal, 2008; Fdikowski and Roe, 2009; Ceze and Fdikowski,2012;...]



Fully Discrete Adjoint

Let $R_h(Q_h)$ be the residual, $J_h(Q_h)$ be the output. Let Q be the exact solution. The solution error is $\delta Q = Q - Q_h$. Since $R(Q) = R(Q_h + \delta Q) = 0$,

We have

$$R(Q_h) + \frac{\partial R_h}{\partial Q_h} \delta Q \approx 0. \quad \delta Q \approx - \left(\frac{\partial R_h}{\partial Q_h} \right)^{-1} R(Q_h)$$

The output error is

$$\delta J_h = J_h(Q) - J_h(Q_h) = \frac{\partial J_h}{\partial Q_h} \delta Q = - \frac{\partial J_h}{\partial Q_h} \left(\frac{\partial R_h}{\partial Q_h} \right)^{-1} R(Q_h)$$

Denote the adjoint $\tilde{\psi}_h^T = - \frac{\partial J_h}{\partial Q_h} \left(\frac{\partial R_h}{\partial Q_h} \right)^{-1}$. Then $\delta J_h = \tilde{\psi}_h^T R(Q_h)$

$$- \frac{\partial J_h}{\partial Q_h} = \tilde{\psi}_h^T \frac{\partial R_h}{\partial Q_h} \qquad - \frac{\partial R_h}{\partial Q_h}^T \tilde{\psi}_h = \frac{\partial J_h}{\partial Q_h}^T$$

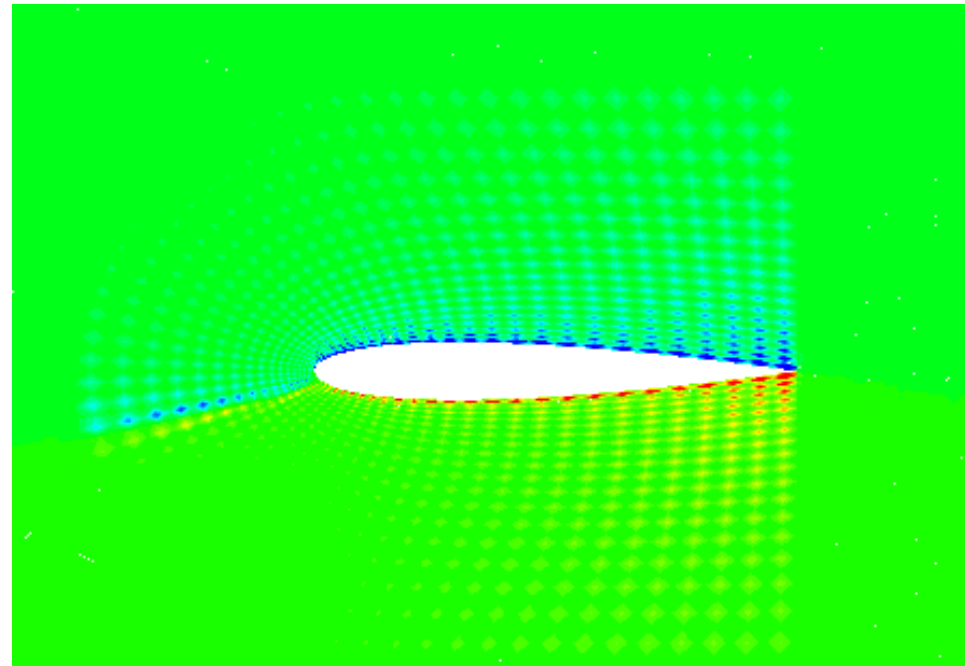
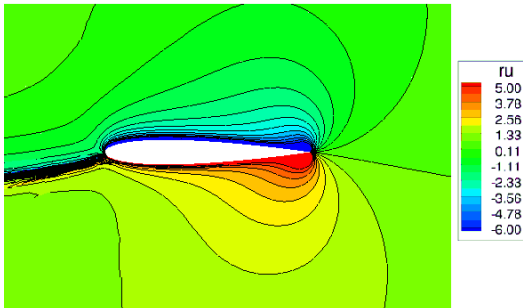


The Fully Discrete Adjoint for the CPR Method

NACA 0012 at $M_\infty = 0.4$, $\alpha = 5^\circ$

- The x-mom of the lift adjoint
- Fully discrete adjoint
- Highly-oscillating adjoint solution

$$-\frac{\partial R_h^T}{\partial Q_h} \tilde{\psi}_h = \frac{\partial J_h^T}{\partial Q_h}$$





Dual Consistency

A residual from a differential schemes at SP j of cell i

$$R(Q)_{i,j} = \nabla \cdot \vec{f}(Q_i)_j + \frac{1}{|V_i|} \sum_{f \in \partial V_i} \sum_l \alpha_{j,f,l} [F^n]_{f,l} S_f$$

With fully discrete approach

$$-\sum_i \sum_j \frac{\partial R_{i,j}}{\partial Q_k} \tilde{\psi}_{i,j} = \frac{\partial J}{\partial Q_k}, \quad k = 1, \dots, N_{DOF}$$

To be dual consistent,

$$-\int_{\Omega} \frac{\partial N(Q)^T}{\partial Q} \psi dV = \frac{\partial J^T}{\partial Q}$$



Discrete Adjoint for the CPR in the Integral Form

$$-\int_{\Omega} \frac{\partial N(Q)^T}{\partial Q} \psi dV = \frac{\partial J^T}{\partial Q}$$

- Approximate ψ_i using the basis L_j from the primal solution space

$$\psi_i = \sum_j L_j \hat{\psi}_{i,j}$$

- Directly discretizing the continuous adjoint eqn

$$-\sum_i \sum_j \frac{\partial R_{i,j}}{\partial Q_k} \omega_j |J_{i,j}| \hat{\psi}_{i,j} = \frac{\partial J}{\partial Q_k}$$

- The difference between $\hat{\psi}_{i,j}$ and $\tilde{\psi}_{i,j}$

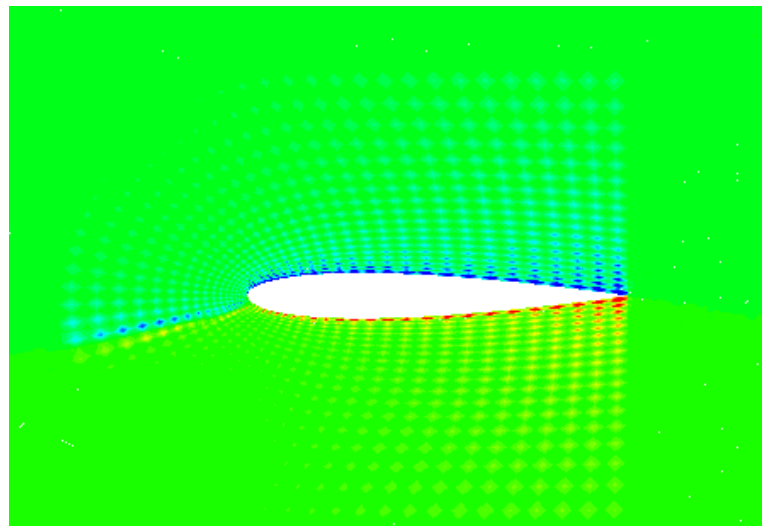
$$\tilde{\psi}_{i,j} = \omega_j |J_{i,j}| \hat{\psi}_{i,j}$$



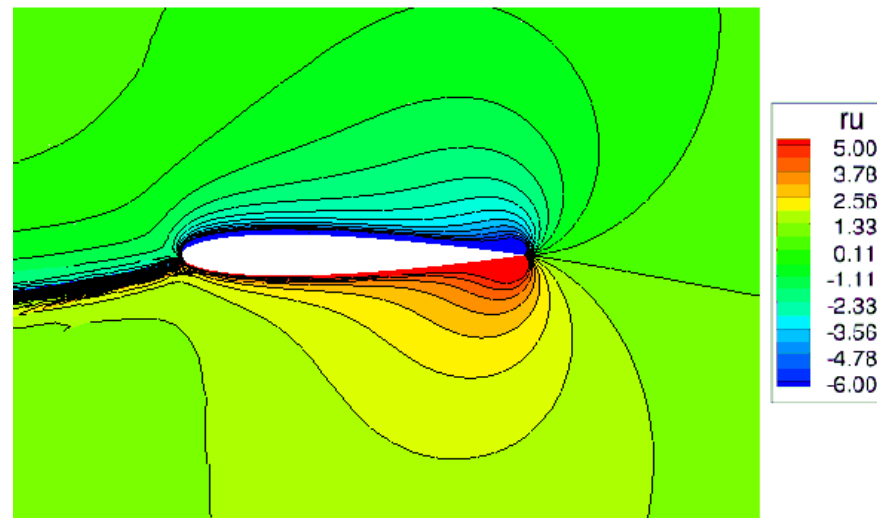
Comparison of the Adjoint with the CPR Method

NACA 0012 at $M_\infty = 0.4$, $\alpha = 5^\circ$

- The x-mom of the lift adjoint
- Fully discrete adjoint
- Discrete adjoint in the integral form



The inconsistent adjoint



Dual consistent adjoint



The Adjoint-based Error Estimation

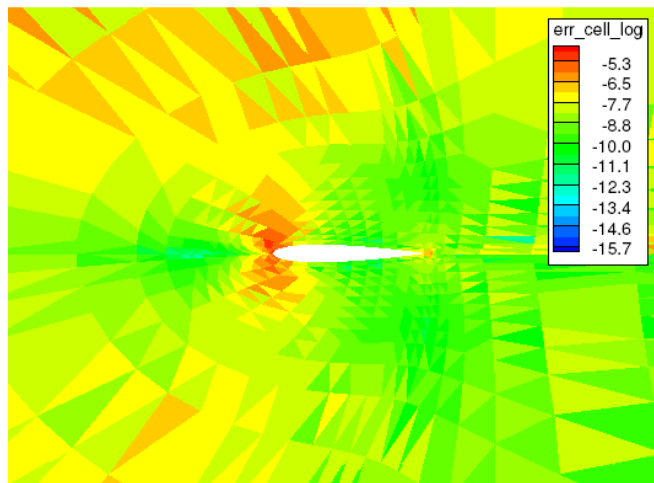
- Output error est.: adjoint solution weighted primal residual

$$\delta J_h(Q_h) = J_h(Q_h) - J_h(Q_H) \approx (\hat{\psi}_h)^T R_h(Q_h^H)$$

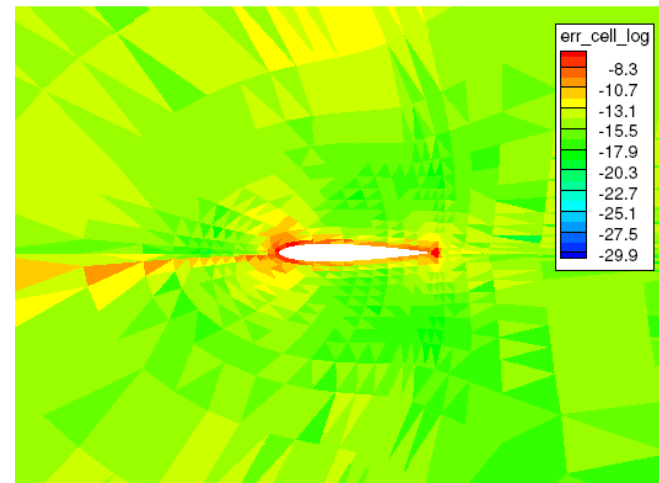
- Adjoint-based local error indicator

$$\eta = \left| (\hat{\psi}_h)^T R_h(Q_h^H) \right|$$

- Multi-p residual-based error indicator $\eta = \left| R_h(Q_h^H) \right|$

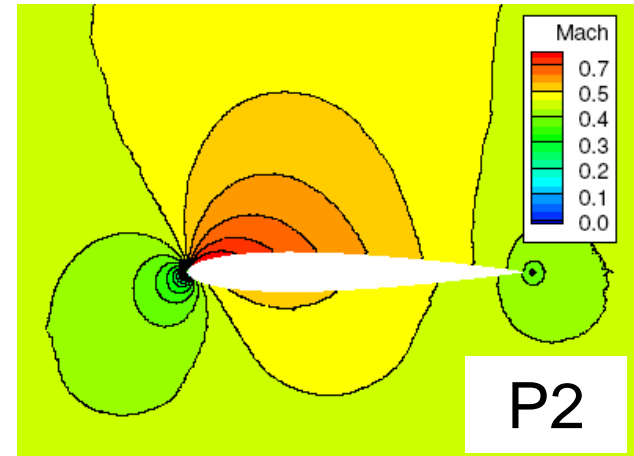
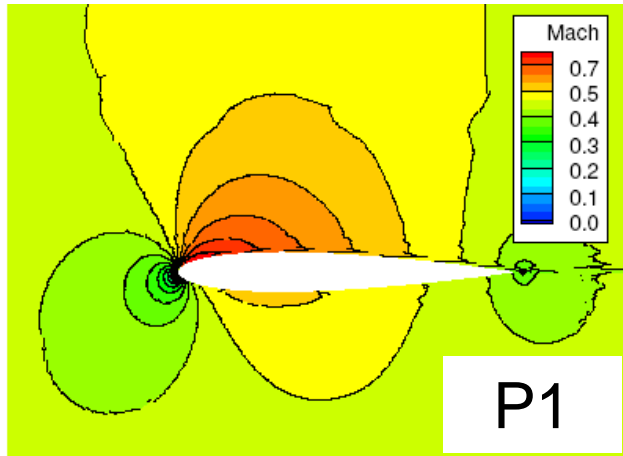


Local residual distribution



Adjoint-based error indicator

Accuracy Test of the Adjoint-based Error Est.



NACA 0012 at $M_\infty = 0.5$, $\alpha = 2^\circ$

- The lift as the output J
- The effectivity of the error est.

$$\eta_H^e = \frac{-(\psi_h)^T R_h(Q_h^H)}{J_H(Q_H) - J_h(Q_h)}$$

Cells	$J_H(Q_H) - J_h(Q_h)$	$-(\psi_h)^T R_h(Q_h^H)$	η_H^e
280	-5.859e-3	-1.103e-3	1.88
1120	-2.638e-3	-4.002e-3	1.52
4480	-8.736e-4	-9.995e-4	1.14
17920	-1.933e-4	-1.988e-4	1.03

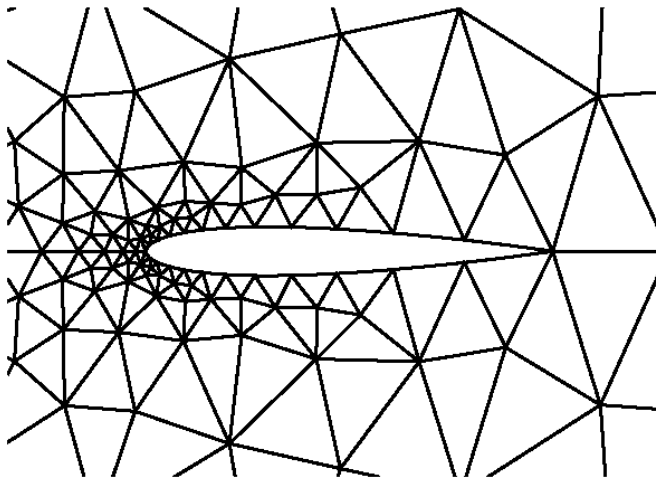


Subsonic Flow Over a NACA 0012 Airfoil

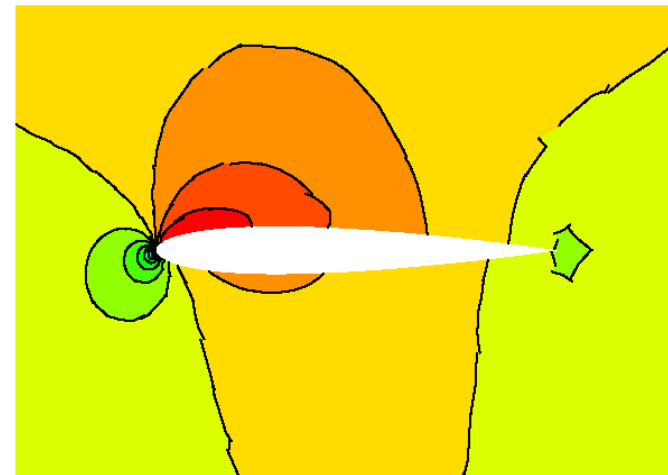
- Iso/aniso H-adaptation
- Fixed fraction $f = 0.1$
- Inviscid, $M_\infty = 0.5$, $\alpha = 2^\circ$
- 3rd order scheme

Adaptation strategies

- Hanging nodes
- No-hanging nodes
- Error indicators
 - lift adjoint
 - drag adjoint



Initial mesh



Initial solution

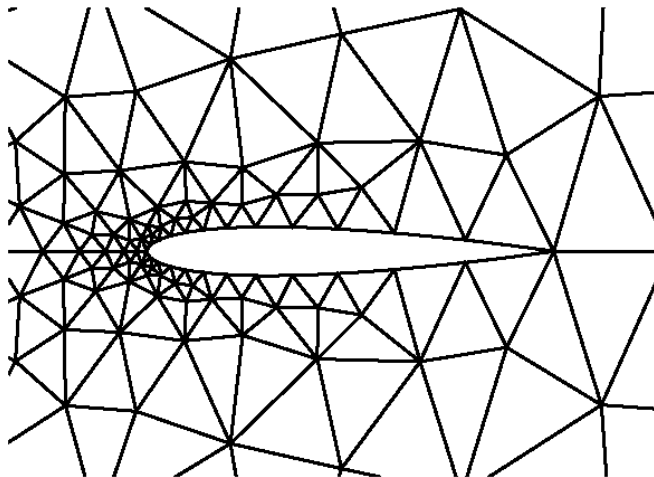


Subsonic Flow Over a NACA 0012 Airfoil

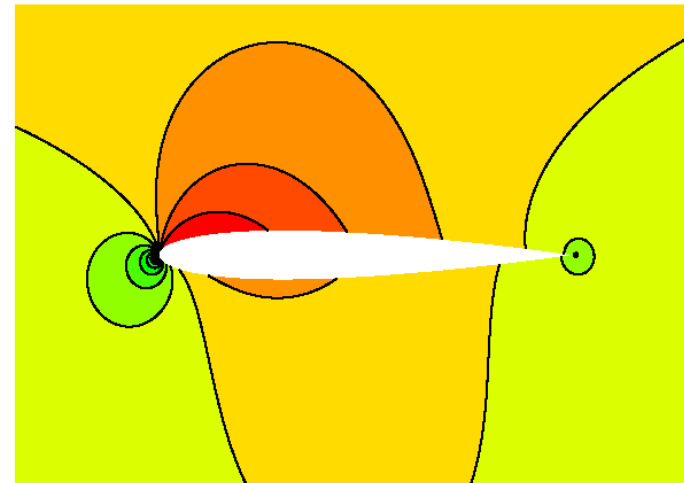
- Iso/aniso H-adaptation
- Fixed fraction $f = 0.1$
- Inviscid, $M_\infty = 0.5$, $\alpha = 2^\circ$
- 3rd order scheme

Adaptation strategies

- Hanging nodes
- No-hanging nodes
- Error indicators
 - lift adjoint
 - drag adjoint



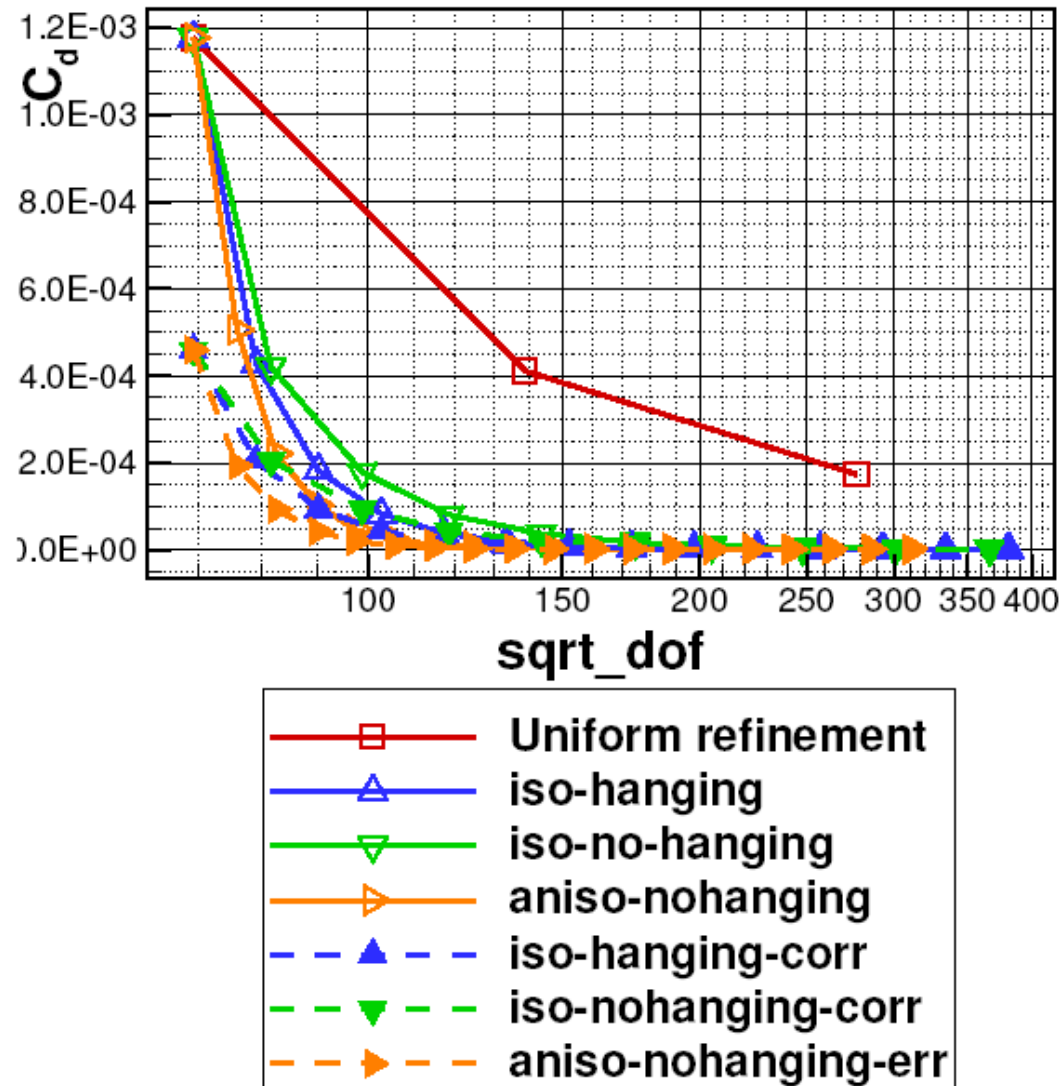
Initial mesh



The adapted solution

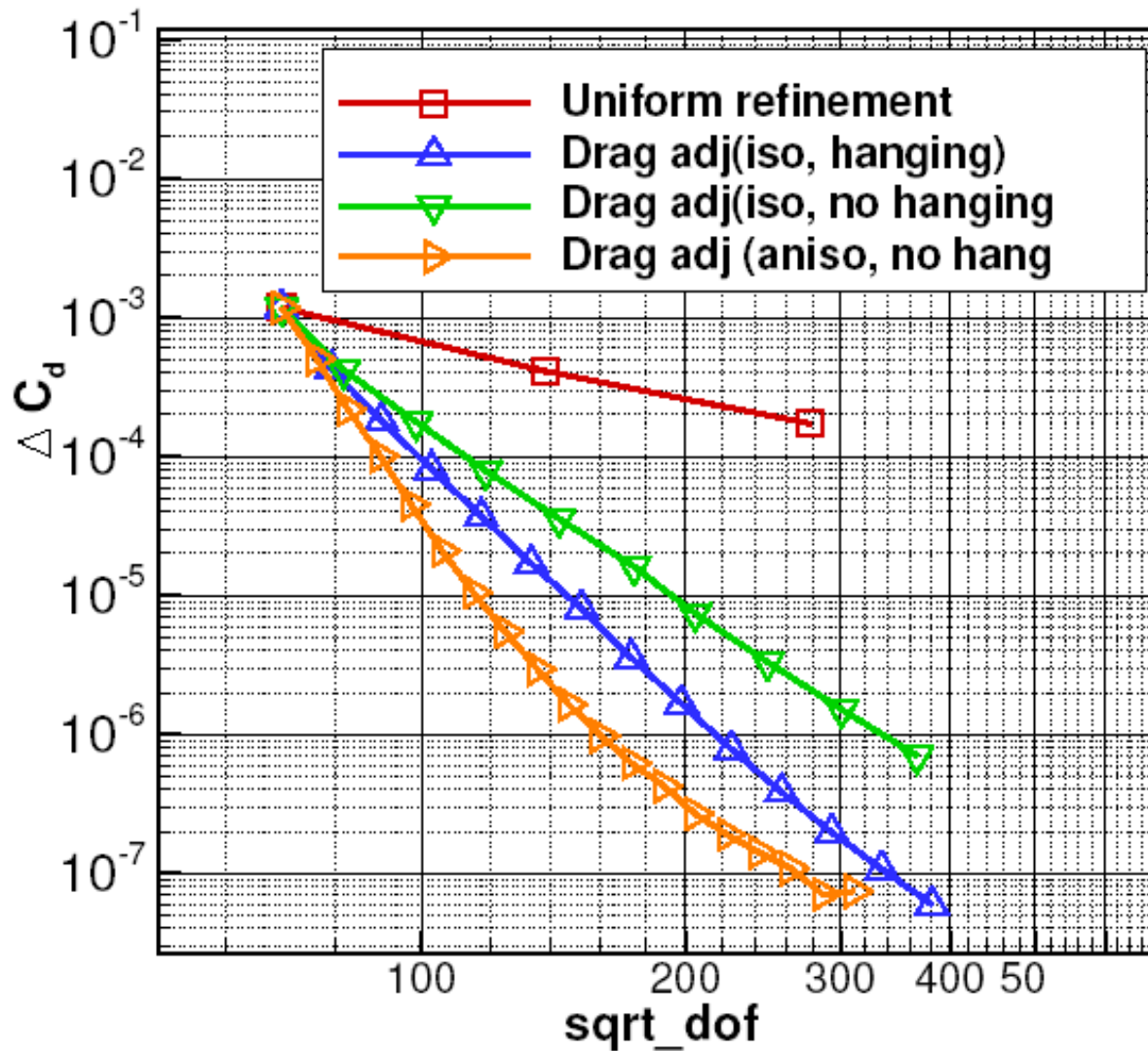


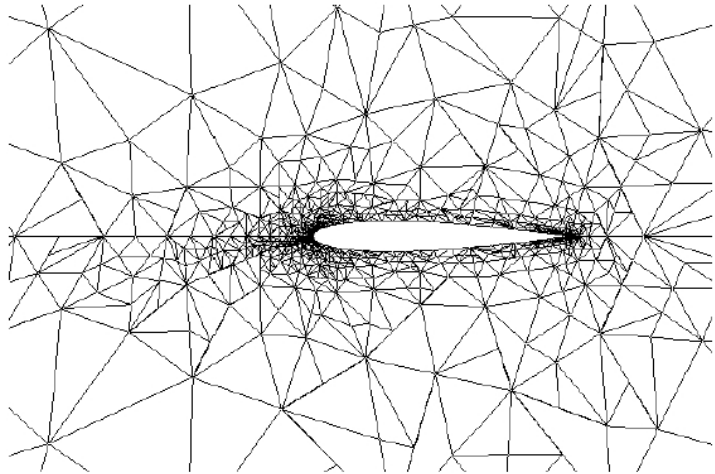
Subsonic Flow Over a NACA 0012 Airfoil



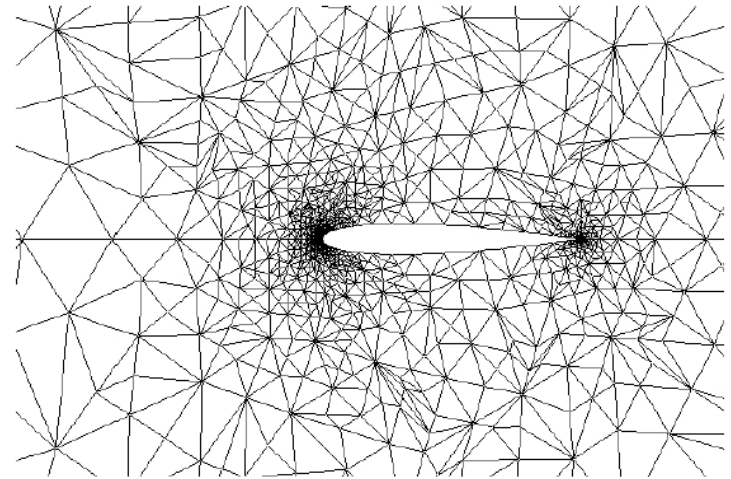


Subsonic Flow Over a NACA 0012 Airfoil

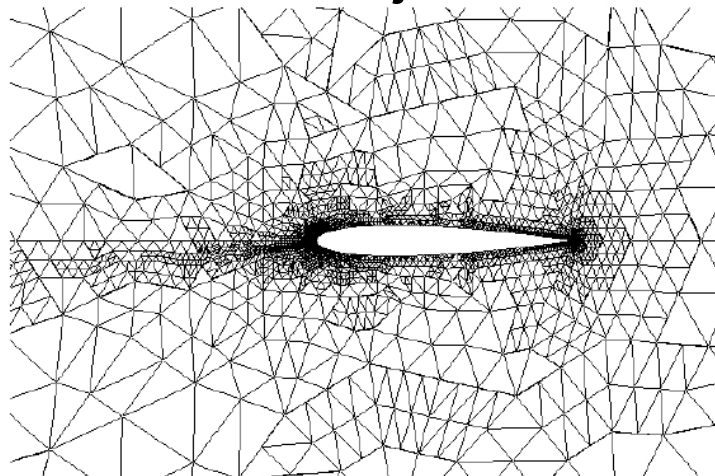




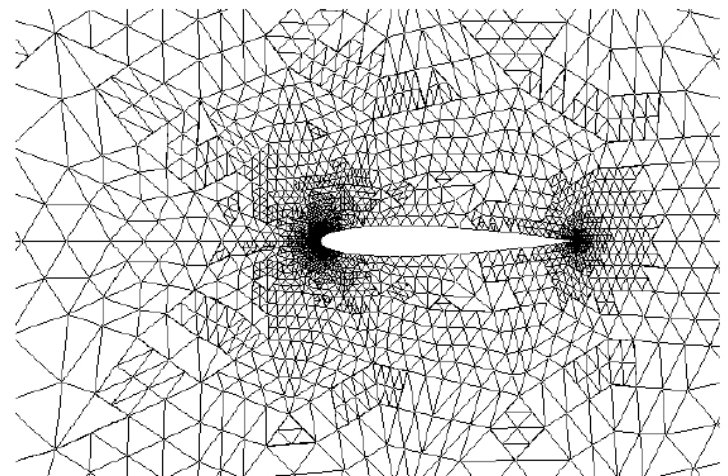
Aniso lift adjoint



Aniso drag adjoint



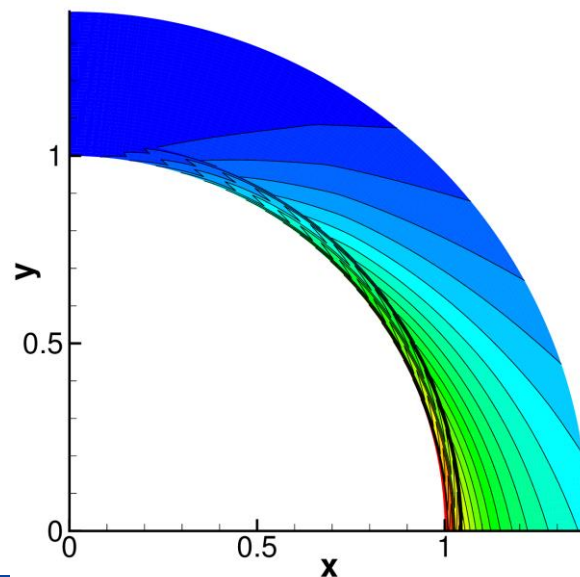
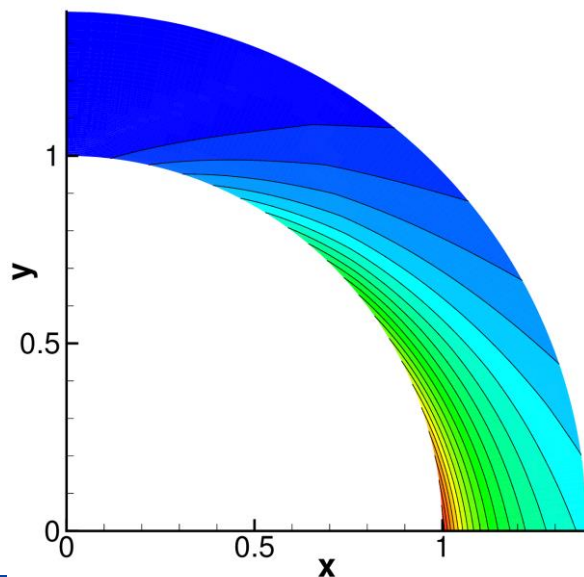
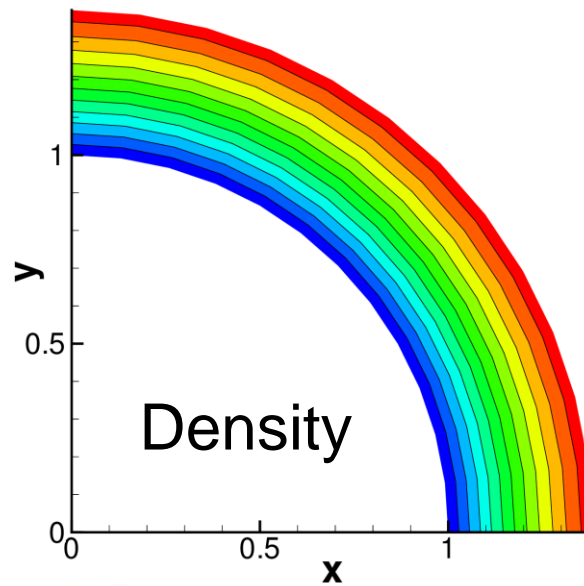
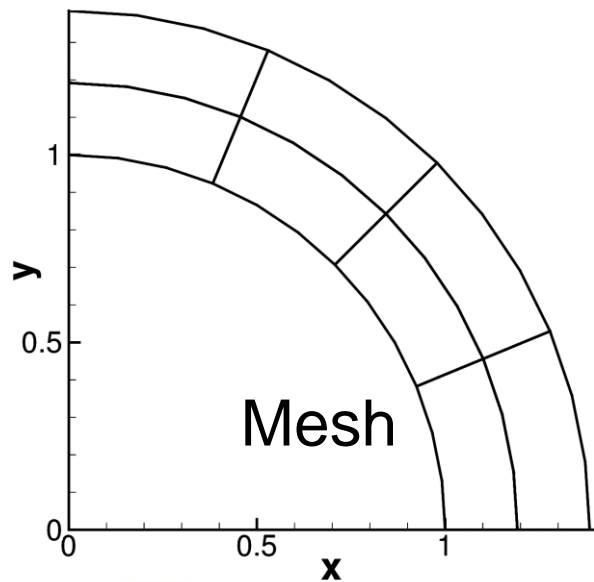
Iso lift adjoint



Iso drag adjoint



The Supersonic Vortex Transportation Problem

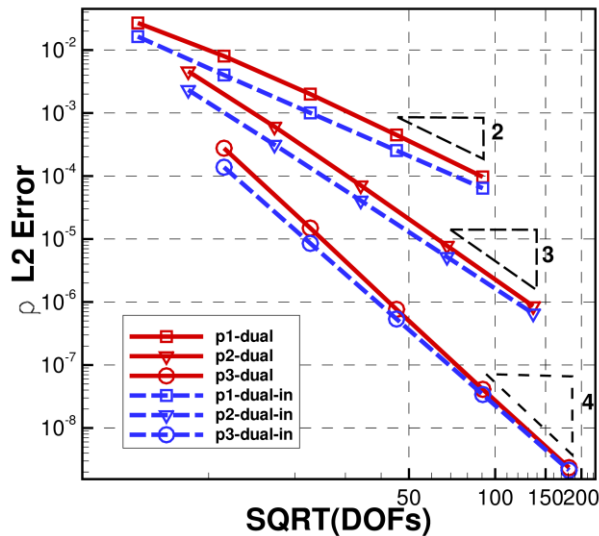


Dual-consistent adjoint

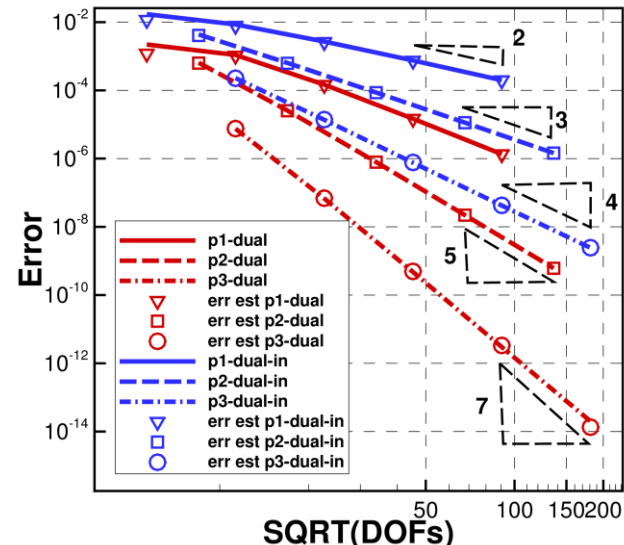
Dual-inconsistent adjoint



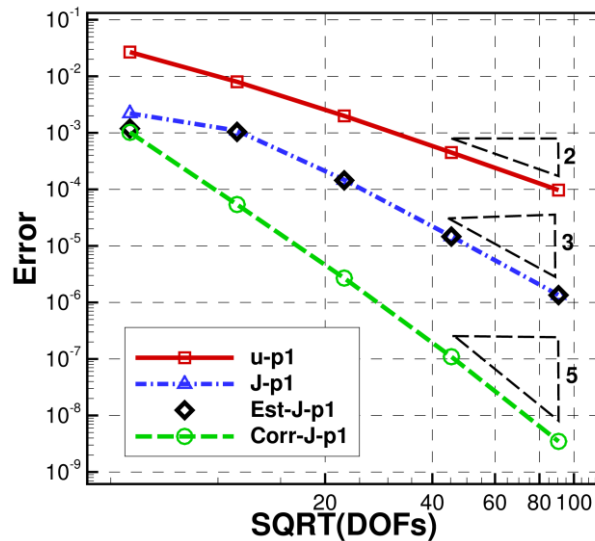
The Supersonic Vortex Transportation Problem



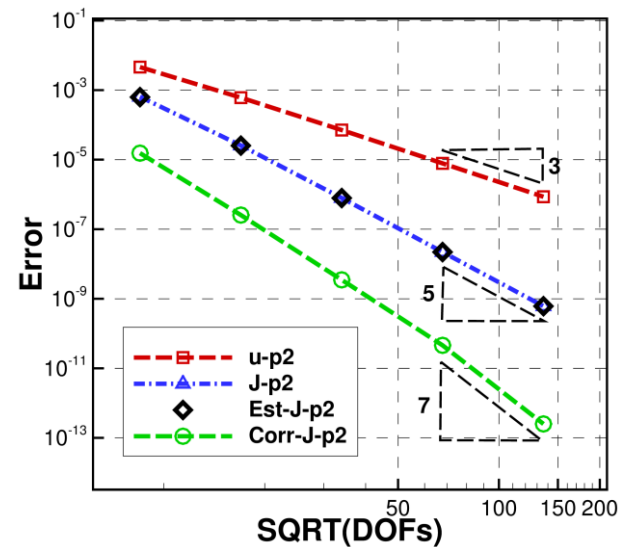
Primal sol error



Output error



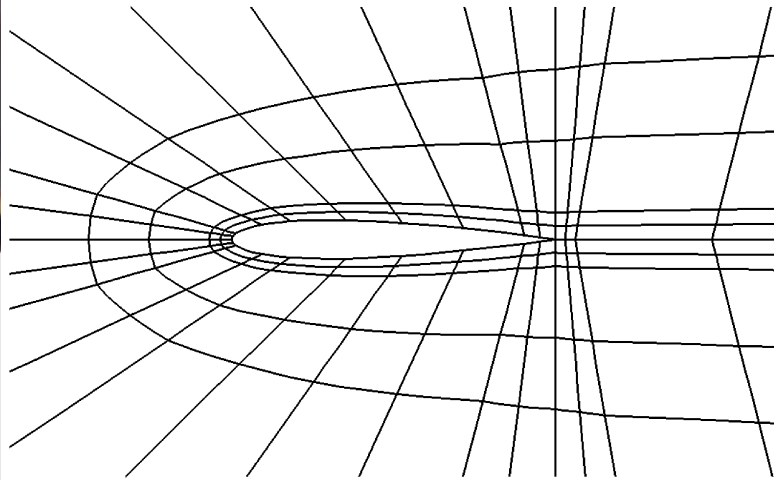
P1 error estimate



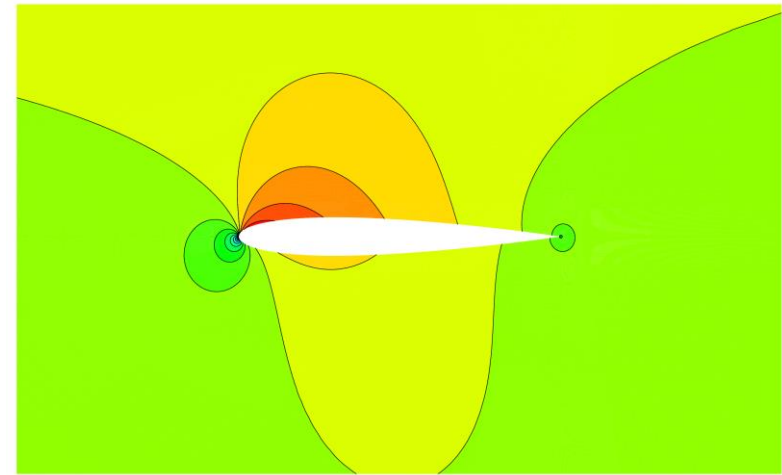
P2 error estimate



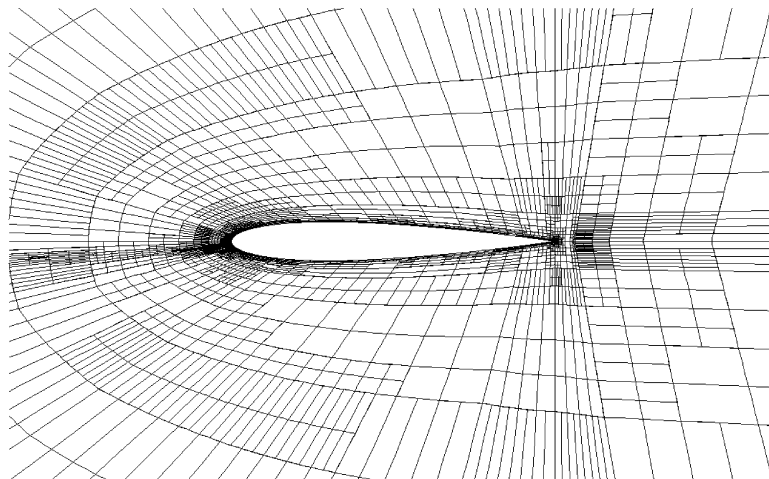
Inviscid Flow over the NACA-0012 Airfoil



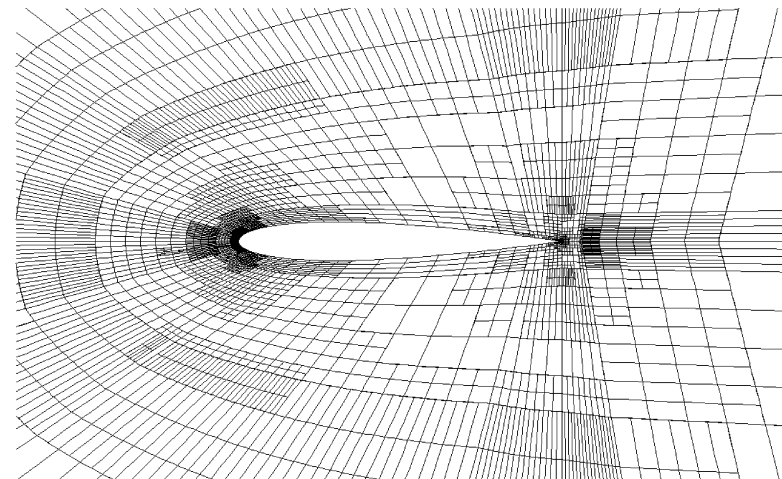
Initial mesh

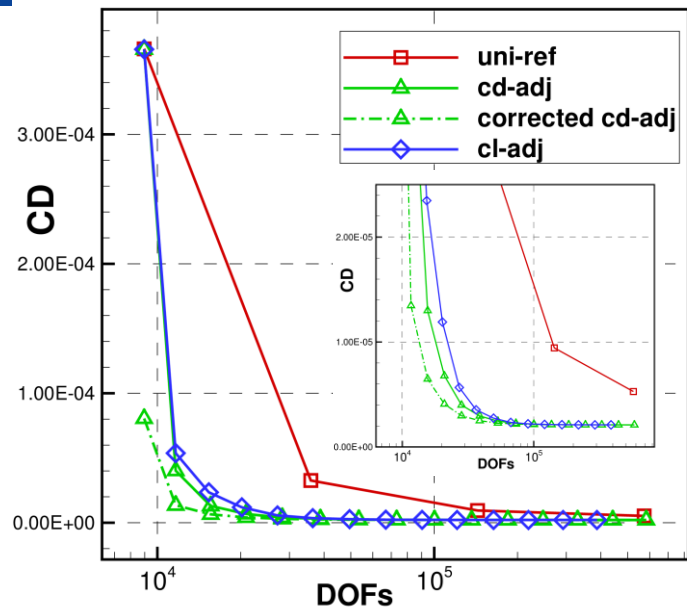
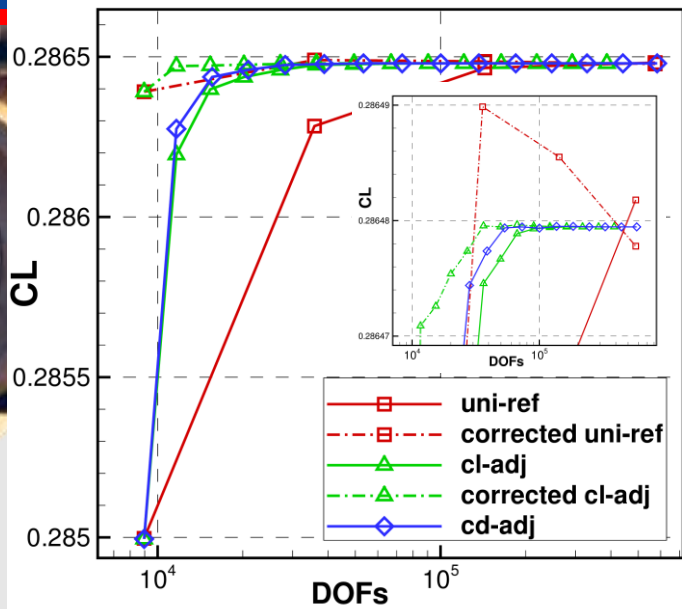


Adapted solution



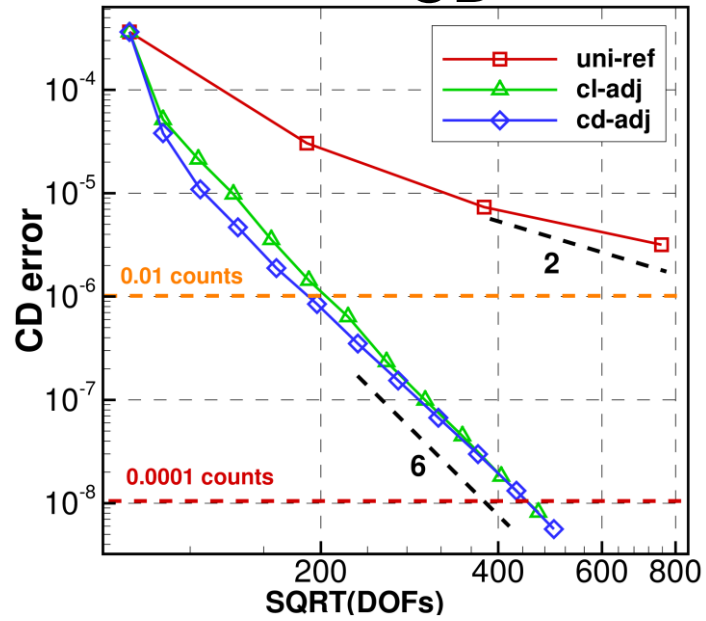
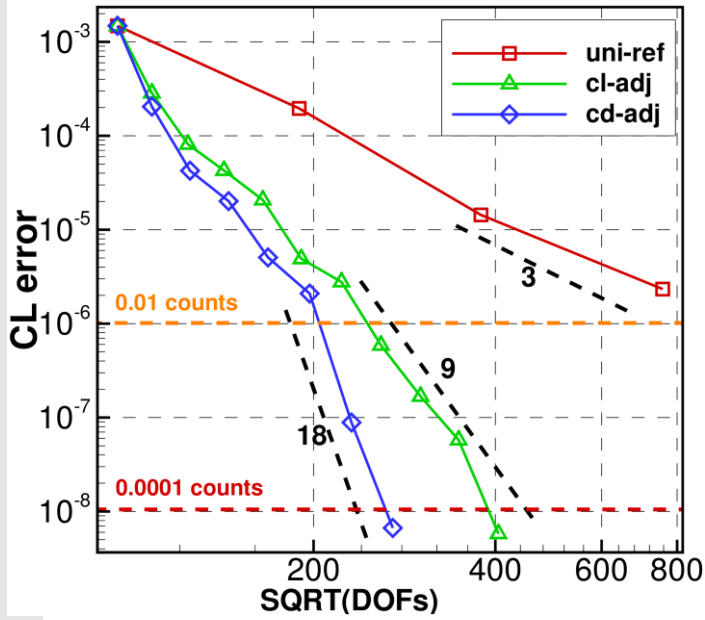
CL-adjoint





CL

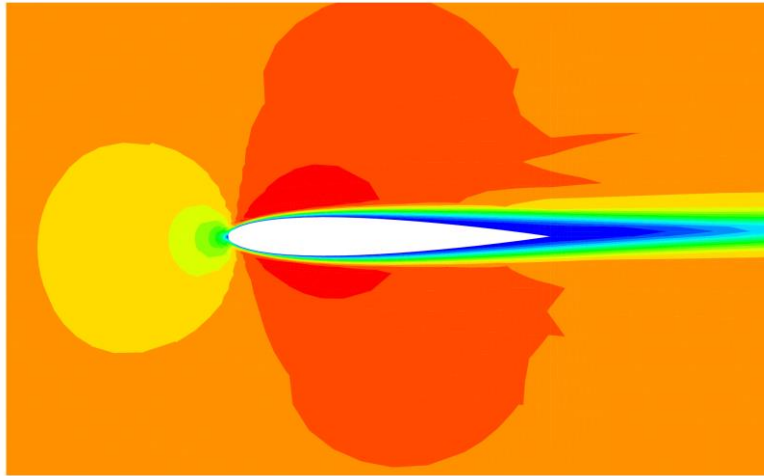
CD



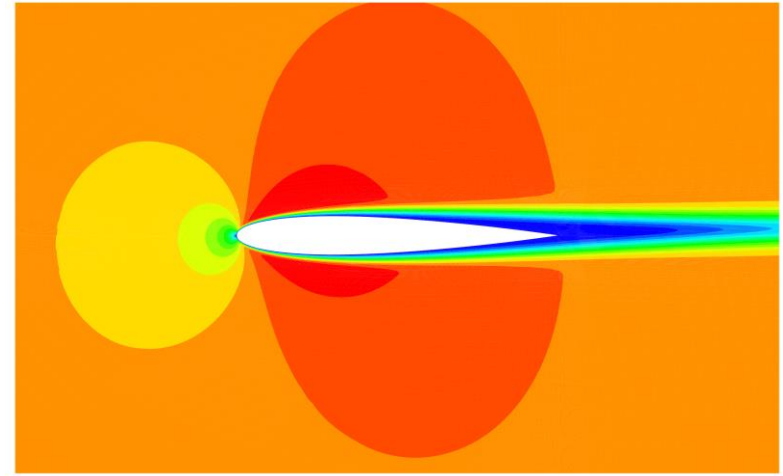
CL error

CD error **KU** THE UNIVERSITY OF KANSAS

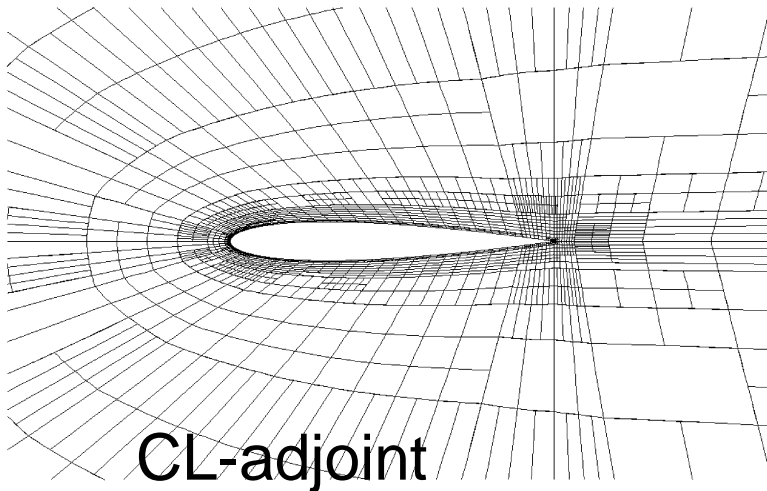
Laminar Flow over NACA-0012 ($\alpha=1^\circ$, $Re=5000$)



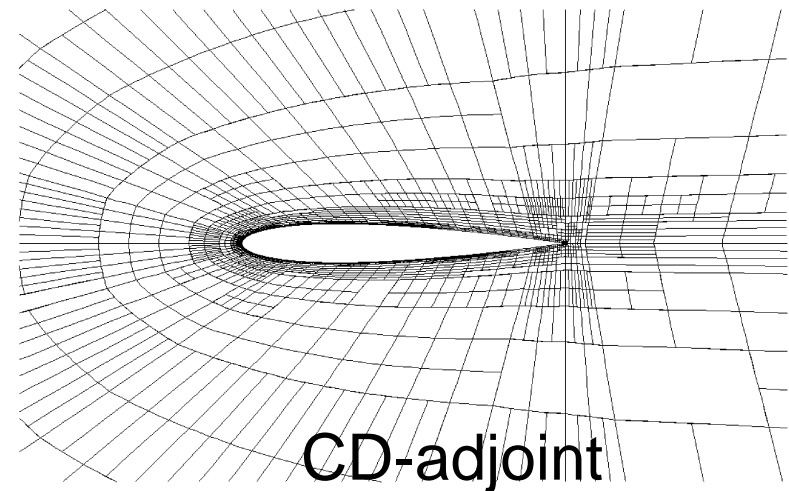
Initial solution



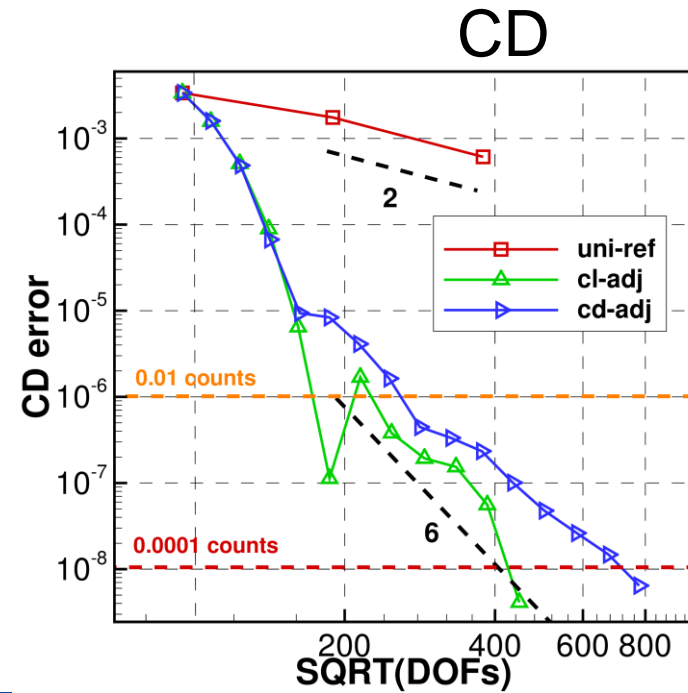
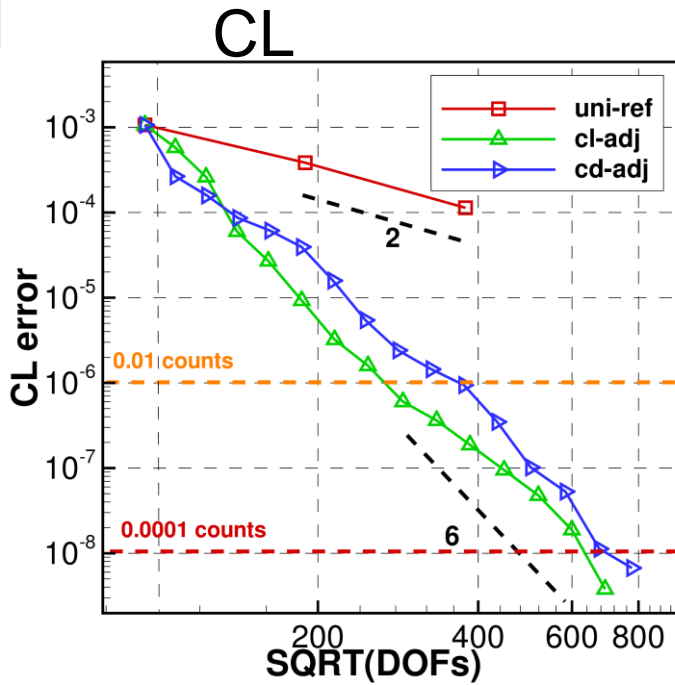
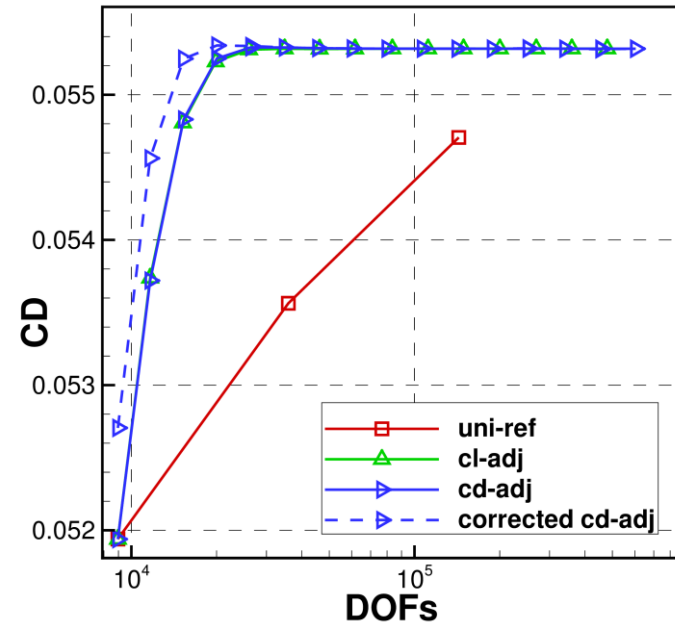
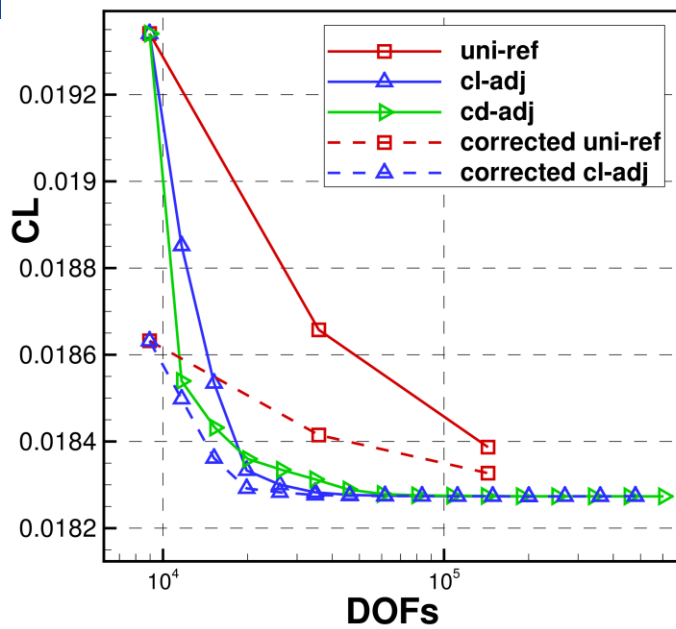
Adapted solution



CL-adjoint



CD-adjoint



CL error

CD error



Remaining Challenges in High-Order Methods

- High-order grid generation, highly clustered curved meshes near wall
- Error estimates and solution-based hp-adaptations
- Low memory efficient solver
- Shock capturing – to preserve accuracy in smooth regions, convergent and parameter-free